ISTANBUL MEDENIYET UNIVERSITY
INSTITUTE OF GRADUATE STUDIES
DEPARTMENTS OF MOLECULAR BIOLOGY AND GENETICS

Investigation of The Potential Therapeutic Effect of Endoplasmic Reticulum Stress and Apoptotic Mechanism Triggered by Epibrassinolide in Combination with Tamoxifen in MCF-7 and MDA-MB-231 Breast Cancer Cells

Master's Thesis

Zeynep Demirel

June 2024

ISTANBUL MEDENIYET UNIVERSITY
INSTITUTE OF GRADUATE STUDIES
DEPARTMENTS OF MOLECULAR BIOLOGY AND GENETICS

Investigation of The Potential Therapeutic Effect of Endoplasmic Reticulum Stress and Apoptotic Mechanism Triggered by Epibrassinolide in Combination with Tamoxifen in MCF-7 and MDA-MB-231 Breast Cancer Cells

Master's Thesis

Zeynep Demirel

Supervisor

Prof. Dr. Pınar Obakan Yerlikaya

June 2024

THESIS JURY APPROVAL

This master thesis titled "Investigation of The Potential Therapeutic Effect of Endoplasmic Reticulum Stress and Apoptotic Mechanism Triggered by Epibrassinolide In Combination With Tamoxifen In MCF-7 And MDA-MB-231 Breast Cancer Cells" written by Zeynep Demirel at the Department of Molecular Biology and Genetics was accepted by our jury.

JURY MEMBERS **SIGNATURE**

Supervisor:

Prof. Dr. Pınar OBAKAN YERLİKAYA

İstanbul Medeniyet University

Other Jury Members:

Assoc. Prof. Ayşe KARATUĞ KAÇAR

İstanbul University

Assist. Prof. Ömer Faruk SARIOĞLU

İstanbul Medeniyet University

Date of Defense: 12/ 06 / 2024

STATEMENTS

Style and Reference Manual Statement

Having reviewed this thesis written under my supervision, I confirm that it has been written in accordance with APA Manual of Style and used its in text reference format consistently throughout the entire text.

Signature
Prof. Dr. Pınar OBAKAN YERLİKAYA

Declaration of Originality

I hereby declare that all information in this dissertation has been obtained and presented in accordance with academic rules and ethical conduct. I also declare that, as required by these rules and conducts, I have fully cited and referenced all material and results that are not original to this work.

Signature
Zeynep DEMİREL

ACKNOWLEDGEMENTS

I would like to express my deepest gratitude to my esteemed advisor Prof. Dr. Pınar OBAKAN YERLİKAYA, who helped and supported me throughout the dissertation. I wouldn't have been able to achieve all these without her guidance. I am extremely grateful to my colleagues Esranur KOPAL and Nilay DİNÇKURT for their endless support and for always being by my side in all the ups and downs. I am also grateful to Zainab AL-LAMI who motivated and supported me during my master's journey. I must also thank Ünal ARABACI, Recep GÜNDOĞDU, and Özlem RECİMOĞLU for making things easier and for their support. Many thanks to Dr. Gülşen GÜNEL for her practical suggestions and assistance. I cannot express my thanks to my father who has always believed in me and been there and never complained about being my private driver to take me from late night laboratory shifts. I am extremely grateful to my mother who made my life easier. I couldn't have done this without their unwavering support.

Special thanks to Prof. Dr. Elif Damla ARISAN who allowed me to access her laboratory at Gebze Technical University, and her practical assistance.

I would like to thank TUBITAK for their financial support throughout my dissertation as part of the BIDEB 2210-A scholarship program and TUBITAK 1002 Project No:121Z846.

Lastly, I would like to thank myself for believing in my abilities, persevering, and completing the project.

CONTENT

LIST OF SYMBOLS

α : Alpha

β : Beta

κ: Kappa

γ : Gamma

°C: Degree Celsius

μ: Micro

LIST OF ABBREVIATIONS

BC: Breast cancer

COVID-19: Coronavirus disease 2019

BMI: Body mass index

HRT: Hormone replacement therapy

DCIS: Ductal carcinoma in situ

IDC: invasive (infiltrative) ductal carcinoma

ILC: Invasive lobular carcinoma

cm: centimeter

PR: Progesterone receptor

HER2: Human epidermal growth factor receptor 2

CNS: Central nervous system

TNBC: Triple-negative breast cancer

EGFR1: Epidermal growth factor receptor type 1

CK: Cytokeratins

CSC: Cancer stem cells

ERE: Estrogen response element

E2: Estradiol

NF-γ: Nuclear transcription factor γ

AP-1: Activator protein-1

IGF1: Insulin-like growth factor 1

CDK: Cyclin-dependent kinase

PI3K: 4-5 biphosphate 3-kinase

MAPK: Mitogen-activated protein kinase

RTK: Receptor tyrosine kinase

GPCR: G-protein coupled receptor

Grb2: Growth factor receptor bound protein 2

SOS: Son of sevenless

GAP: GTPase-activating protein

RT: Radiation therapy

BCS: Breast-conserving surgery

SERD: Selective estrogen receptor degrader

Rb: Retinoblastoma-associated protein

DOX: Doxorubicin

NK: Natural killer

APC: Antigen-presenting cell

PTX: Paclitaxel

HDAC: Histone deacetylase

DES: Diethylstilbestrol

TAM: Tamoxifen

SHBG: Sex hormone-binding globulin

MDR: Multidrug resistance

TME: Tumor microenvironment

ABC: ATP-binding cassette

P-gp: P-glycoprotein

DDR: DNA damage response

Hh: Hedgehog

BR: Brassinosteroid

BRI1: Brassinosteroids insensitive 1

BAK1: BRI1-associated receptor kinase

EBR: Epibrassinolide

NHR: Nuclear hormone receptor

UPR: Unfolded protein response

SILAC: Stable isotope labeling by amino acids in cell culture

ER: Endoplasmic reticulum

NE: Nuclear envelope

CALNX: Calnexin

CALR: Calreticulin

HSP47: Heat shock protein 47

PDI: Protein disulfide isomerase

ERAD: ER-associated protein degradation

PERK: PRKR-like ER kinase

IRE1α: Inositol-requiring enzyme 1 α

ATF6: Activating transcription factor 6

GRP78: Glucose-regulated protein 78

eIF2α: Eukaryotic initiation factor 2 α

ATF4: Activating transcription factor 4

ATG5: Autophagy-related gene 5

CHOP: C/EBP homologous protein

bZIP: Basic-leucine zipper

NRF2: Nuclear factor erythroid 2-related factor 2

KEAP1: Kelch-like ECH-associated protein 1

AKT: Protein kinase B

MHC: Major histocompatibility complex

LD: Luminal domain

SBD: Substrate-binding domain

NBD: Nucleotide-binding domain

RIDD: IRE1-dependent decay

TRAF2: Tumor necrosis factor receptor-associated factor 2

ASK1: Apoptosis signaling regulating kinase 1

JNK: c-JUN NH2-terminal kinase

MAMP: Mitochondrial outer membrane permeabilization

Cyt c: Cytochrome c

S1P: Site-1 protease

S2P: Site-2 protease

PCD: Programmed cell death

Caspase: Cysteine-dependent aspartate-specific peptidase

CARD: Caspase recruitment domain

DED: Death effector domain

FADD: Fas-associated molecules with death domain

DR: Death receptor

Bcl-2: B cell lymphoma 2

IMS: Mitochondrial intermembrane space

IAP: Inhibitor of apoptosis protein

ROCK1: Rho kinase 1

TNF: Tumor necrosis factor

TRAIL: TNF-related apoptosis inducing

DISC: Death inducing signal complex

LIST OF FIGURES

LIST OF TABLES

ABSTRACT

Investigation Of The Potential Therapeutic Effect of Endoplasmic Reticulum Stress and Apoptotic Mechanism Triggered by Epibrassinolide In Combination With Tamoxifen In MCF-7 And MDA-MB-231 Breast Cancer Cells

Demirel, Zeynep

Master's Thesis, Department of Molecular Biology and Genetics

Supervisor: Prof.Dr. Pınar Obakan Yerlikaya

June 2024, 120 pages

Breast cancer (BC) remains the primary cause of death globally, with 2.3 million cases reported in 2020 alone, marking it as an escalating global health issue. BCs are classified according to the presence or absence of hormone receptors. One of the subtypes includes estrogen-receptor-positive tumors. For instance, MCF-7 cell line exhibits the expression of estrogen receptor, progesterone receptor (PR), and HER2. Tamoxifen (TAM) is frequently used as a chemotherapy drug in the treatment of patients with estrogen receptor-positive tumors. It competes with estrogen to bind the estrogen receptors, thereby hindering proliferation and tumor growth through estrogen receptor signaling. Nevertheless, prolonged exposure to TAM leads to the development of resistance, representing a significant drawback in cancer treatment. MDA-MB-231 cell line represents triple negative BC, characterized by the absence of estrogen receptor, PR, and HER2 expression, resulting in a resistant profile for the cell line. This resistance can be de novo existed before treatment or acquired resulted from prolonged exposure to the drug. The development of chemoresistance encompasses the involvement of three distinct branches of endoplasmic reticulum (ER) stress signaling pathways. ER stress occurs when misfolded or unfolded proteins accumulate in the lumen of the ER, prompting the unfolded protein response (UPR). The UPR initiates the changes in the activities of key regulators, ultimately determining the fate of the cells. Epibrassinolide, a member of brassinosteroids, which is a plant growth regulator, is a naturally occurring plant steroid hormone. It has anti-cancer properties in several types of cancer. Our purpose was to evaluate the potential therapeutic effects of the ER stress-mediated apoptosis triggered by the combination of EBR with TAM in BC cell lines. To achieve this purpose, the combined treatment of TAM with EBR synergistically reduced the viability of BC cell lines in both a dose- and time-dependent manner. Then, the colony-forming capacity was hindered dramatically in 2D and 3D by administering the TAM and EBR. After exposure to the combination of TAM with EBR, DNA fragmentation increased, and mitochondrial membrane potential decreased. According to the cell cycle analysis, the subG1 ratio which indicates dead cells was remarkably enhanced by the combined treatment. Immunoblotting results revealed that the combination of TAM with EBR led to an

increase in the expression of ER stress and apoptosis biomarkers. Conversely, the expression of drug resistance markers was reduced. Moreover, tauroursodeoxycholic acid (TUDCA), which is an ER stress inhibitor, was used to prove the effect of the combination treatment caused by ER stress. Lastly, our immunoblotting results showed that the alterations in the expression of ER stress, apoptosis and drug resistance markers were reversed in the presence of TUDCA. In conclusion, our findings indicate that co-administration of EBR enhances the sensitivity to TAM in both hormone-sensitive and insensitive BC cell lines.

Keywords: Apoptosis, Drug Resistance, Endoplasmic Reticulum Stress, Epibrassinolide, Tamoxifen.

ÖZET

MCF-7 ve MDA-MB-231 Meme Kanseri Hücrelerinde Epibrasinolid ile Tamoksifenin Kombinasyonu Tarafından Tetiklenen Endoplazmik Retikulum Stresi ve Apoptotik Mekanizmanın Potansiyel Terapötik Etkisinin İncelenmesi

Demirel, Zeynep

Yüksek Lisans Tezi, Moleküler Biyoloji ve Genetik Bölümü

Danışman: Prof.Dr. Pınar Obakan Yerlikaya

Haziran 2024, 120 sayfa

Meme kanseri, dünya genelinde başlıca ölüm nedenidir ve 2020'de 2,3 milyon vaka bildirilmiştir. Dolayısıyla, bu artan bir küresel sağlık sorunudur. Meme kanseri hormon reseptörlerinin varlığına göre kategorize edilir. Östrojen reseptör pozitif alt tiplerinden biridir. Örneğin, MCF-7 hücre hattı östrojen, progesteron ve HER2 reseptörlerini içerir. Tamoksifen (TAM) östrojen reseptörü pozitif hastaların tedavisinde sıkça kullanılan bir kemoterapi ilacıdır. Çalışma mekanizması östrojen reseptörüne bağlanarak östrojen reseptörü sinyal yolağı aracılığıyla gerçekleşen proliferasyonu ve tümör büyümesini engeller. TAM'a uzun süre maruz kalan hücrelerde direnç gelişir. Üçlü negatif meme kanseri olarak bilinen MDA-MB-231 hücre hattında östrojen, progesteron ve HER2 reseptörleri bulunmamaktadır. Direnç tedaviden önce var olabilir (*de novo*) veya ilaca uzun süre maruz kalmanın sonucu olarak kazanılabilir. Üç farklı sinyal iletim yolu bulunan endoplazmik retikulum (ER) stresi ilaç direnci gelişiminde rol oynar. ER stres, yanlış katlanmış ya da katlanmamış proteinlerin ER lümeninde birikmesi durumunda ortaya çıkar ve bu da katlanmamış protein yanıtını tetikler. Katlanmamış protein yanıtı, anahtar düzenleyicilerin aktivitelerinde değişikliklere neden olarak sonunda hücrelerin kaderini belirler. Epibrasinolid (EBR) bitki büyüme düzenleyicisi olan brassinosteroidlerin bir üyesi olup doğal olarak meydana gelen bir bitki steroid hormonudur. EBR'nin birçok kanser türünde anti-kanser özellikleri bulunmaktır. Bu çalışmada amacımız EBR'nin TAM ile kombine tarafından tetiklenen ER stresi aracılığıyla apoptozun potansiyel terapötik etkilerinin meme kanseri hücre hatlarında değerlendirmekti. Bu amaçla EBR ve TAM'ın hücre canlılığı üzerindeki etkisi doz ve zamana bağlı olarak incelendi ve meme kanseri hücre hatlarının canlılığını sinerjistik olarak azalttı. Sonrasında, TAM ve EBR'nin uygulanmasıyla 2D ve 3D 'de koloni oluşturma kapasitesini ciddi bir şekilde engelledi. TAM ile EBR'nin kombinasyonuna maruz kaldıktan sonra DNA parçalanması arttı ve mitokondriyal membran potansiyeli azaldı. Hücre döngüsü analizine göre ölü hücreleri gösteren subG1 oranı kombine tedavi ile önemli ölçüde arttı. İmmünoblotlama sonuçları, TAM ve EBR kombine olarak verildiğinde ER stres ve apoptoz belirteçlerinin anlatım ifadelerinin arttığını gösterdi. İlaç direnci belirteçlerinin ifadeleri ise azaldı. Endoplazmik retikulum stres inhibitörü olan

tauroursodeoksikolik asit (TUDCA) kombinasyon tedavisinin ER stres tarafından oluşturulduğunu kanıtlamak için kullanıldı. Sonuç olarak, bulgularımız EBR'nin hem hormon duyarlı hem de hormon duyarsız meme kanseri hücre hatlarında TAM'a karşı duyarlılığını arttırdığını göstermektedir.

Anahtar kelimeler: Apoptoz, Endoplazmik Retikulum Stres, Epibrasinolid, İlaç Direnci, Tamoksifen.

1. INTRODUCTION

1.1. BREAST CANCER

Cancer is a major global health concern, and nearly 19.3 million new cases and almost 10 million deaths have been recorded in 2020 (Sung et al. 2021). The number of women who have been diagnosed with breast cancer (BC) increases day by day. In 2020, nearly 2.3 million cases were recorded, and the greatest cause of death around the world after colorectum and lung cancer in incidence and vice versa in mortality (Sung et al. 2021; Wilkinson et al. 2022). Diagnosis and treatment of cancer have been postponed since the Coronavirus disease 2019 (COVID-19) pandemic arose in 2019, which resulted in closures of healthcare settings, and fear of COVID-19 exposure (Siegel et al. 2023). The postponements in diagnosis and treatments may bring an increase in advanced-stage disease and mortality. The cancer incidence and mortality data may need some time to be quantified at the population level due to these and other secondary outcomes of the pandemic whose effects will be revealed gradually (Siegel et al. 2023).

The breast is made up of two types of tissues which are glandular and stromal supporting tissues. Glandular tissues contain lobules and ducts that are milk-producing and milk channels, respectively. Additionally, there is lymphatic tissue-immune system tissue in the breast to eliminate cellular fluids and waste. Several types of tumors may develop within different parts of the breast. For example, most of them are ductal cancers which are initiated in the cells that cover the ducts, and some are lobular cancers that begin in the lobules, and few may start in the other tissues (Sharma et al. 2010).

1.1.1. Risk Factors of Breast Cancer

Women demonstrate a tendency to the disease if any first-degree relatives get the disease. Almost 1 in 4 cases of BC is associated with the family background (Sun et

al. 2017). An affected first-degree relative which is a mother, sister, and daughter increases the chance of BC dramatically (Feng et al. 2018; International variation, effects of migration, and time trends n.d.). Having a first-degree relative who has been diagnosed with BC nearly doubles your risk of developing the disease (Barnard, Boeke, and Tamimi 2015). However, if you have two affected first-degree relatives, the risk approximately changes 3-fold, as shown in the cohort study conducted in the UK (Feng et al. 2018; International variation, effects of migration, and time trends n.d.; Mayrovitz (Ed.) 2022; Sun et al. 2017). Even though many genetic factors can increase the incidence of BC, mutations in *BRCA1* and *BRCA2* genes inherited as autosomal dominant account for around 40% of hereditary BC (Momenimovahed and Salehiniya 2019). Gene mutations inherited from a parent account for 5-10% of BCs. According to the statistics, women bearing a BRCA1 mutation have a 55-65% probability of developing BC during their lifetime. The risk decreases to 45% for women who carry the *BRCA2* mutation. A woman with a BRCA1 or BRCA2 gene mutation generally faces a 70% chance of developing BC by the time she reaches 80 years old (Feng et al. 2018).

One of the most important non-genetic risk factors is sex, which is beyond the individual's control. Being a woman increases the getting BC 100 times compared to men (Feng et al. 2018; Mayrovitz (Ed.)., 2022). At the age of 50 and above, most of the BC is diagnosed; therefore, aging unavoidably raises the development of BC (Feng et al. 2018; Sun et al. 2017). Additionally, the risk goes up rapidly during reproductive years, but it becomes slower after menopause that is around the age of 50 (Key et al. 2001). BC incidence shows a parallel increase with age which is since the age-related rise in carcinogenesis and the accumulation of cellular alterations during lifetime. Besides, there is a negative correlation between age and the resulting prognosis, which means that a lower survival rate is seen in women having cancer at the age of less than 50 compared to those diagnosed between 50 and 70. One possible explanation is the increased prevalence of highly aggressive triple-negative BC among patients aged 40 or younger (Mayrovitz (Ed.)., (2022). Consequently, mammography scanning is of great importance in women who are 40 or older (Sun et al. 2017).

The incidence of BC is high across all ethnic groups despite differences (Al-Shami et al. 2023). When compared to African American women who have a high chance of

developing BC under age 45, Caucasian women usually develop BC more than African American women (Al-Shami et al. 2023; Feng et al. 2018). Moreover, African American women lose their lives more because of cancer regardless of their age. The occurrence and death of BC are seen as lower in other races such as Hispanic, Asian, and Native American women (Feng et al. 2018). While Caucasian women generally face higher overall risks, it is important to note that black women exhibit the highest likelihood of developing BC before the age of 45. Besides, advanced-stage BC and high mortality rates are seen more in black women (Mayrovitz (Ed.)., 2022).

According to the existing evidence, smoking before menopause enhances the risk of BC. Conversely, some studies have found that women who began smoking after menopause had a significantly lower chance of developing BC because of the antiestrogenic effects of tobacco. Therefore, there is no conclusive study about smoking and developing BC (Winters et al. 2017). Alcohol consumption increases the risk of BC. Some studies revealed a dose-dependent relationship, while others showed an association with cumulative alcohol intake for over long periods. For example, a 10% increase in the risk is related to the consumption of 5-9.9 g/day. The underlying mechanism might be associated with alcohol's tendency to boost estrogen levels in the blood (Sun et al. 2017). As a result, the majority of alcohol-related breast malignancies are estrogen receptor +.

BC risk is lower in women who engage in physical activity and eat a lot of fruits and vegetables. The Mediterranean diet that contains high consumption of fruits and vegetables provides significant amounts of polyphenols and fiber which have been linked to reduced carcinogenesis. Polyphenols can suppress the enzymes lipoxygenase (LOX) and cyclooxygenase (COX) as well as the transcription factor NF- κB. These proteins are overexpressed in tumor cells and regulate the expression of inflammatory cytokines including TNF-α and IL-1. Some polyphenols have been shown to decrease estrogen signaling by either blocking aromatase, the enzyme responsible for estrogen synthesis, or binding to estrogen receptors thereby limiting tumor cell growth (De Cicco et al. 2019). Additionally, women who exercise 7 hours a week have a 10-25% decreased risk of BC than women who are not active, this benefit increases even more in post-menopausal women (Sun et al. 2017).

Obesity is highly related to an enhanced risk of BC (Gershuni, et al. 2016; Mayrovitz (Ed.)., 2022). The Body Mass Index (BMI) greater than 30 (kg/m^2) as is classified as obese (Gershuni et al. 2016). This relationship between BMI and BC is especially observed in post-menopausal women. High BMI increases the occurrence of BC since high amounts of adipose tissues increase the rate of conversion of androgenic precursor to estrogens by aromatase enzymes (Al-Shami et al. 2023; Feng et al. 2018; Momenimovahed and Salehiniya 2019). Estrogens are produced by ovaries in pre-menopausal women; however, during post-menopause, they are produced by adipose tissue, if an individual is overweight or obese, the possibility of production of high amounts of estrogens is relatively high by fat tissue (Feng et al. 2018). Not only being obese but also being at a normal weight with a higher fat distribution increases the risk. On the contrary, the risk goes down with higher BMI during premenopausal women especially Luminal A subtype of BC (Al-Shami et al. 2023b; Mayrovitz (Ed.)., 2022). However, triple-negative BC risk goes up in premenopausal women (Al-Shami et al. 2023; Momenimovahed and Salehiniya 2019). Furthermore, high blood insulin levels and insulin-like growth factors that induce the growth of cancer cells are detected in overweight people, which is related to specific cancers including BC. This contradiction is not fully understood, and the association between obesity and BC is complicated and yet to be entirely resolved (Feng et al. 2018; Mayrovitz (Ed.)., 2022; Momenimovahed and Salehiniya 2019).

An early onset of menstruation and a late onset of menopause lead to a higher number of menstrual cycles and longer exposure to endogenous estrogen throughout life, significantly raising the risk of BC (Houghton and Hankinson 2021). In this regard, it was found an immense risk of Luminal A subtype of BC due to menopause at late ages by studies of four non-case reference groups (Barnard et al. 2015). Also, the first pregnancy at an older age and low parity enhances the risk. Besides, the risk can be lowered by 5% to 10% if the menarche is delayed a year and per extra birth, respectively (Sun et al. 2017). The protective effects of both breastfeeding and multiparity have been demonstrated, and breastfeeding of at least 6 months has been found to have the most impact on reducing BC risk. Each year of breastfeeding diminishes the BC risk by 4.3% especially the aggressive subtypes (Beral et al. 2002; Fortner et al. 2019). Lastly, hormone replacement therapy (HRT) following

menopause presents another significant risk factor. Typically, HRT involves the combination of estrogen and progesterone. In most cases, combined hormone therapy is required because using estrogen alone increases the risk of uterus cancer. The use of combined hormone therapy after menopause elevates the risk of BC, enhances the chances of BC related mortality, and raises the likelihood of detecting cancer at an advanced stage. However, the risks associated with HRT are reversible (Feng et al. 2018). While HRT helps alleviate menopausal symptoms such as hot flashes, night sweats, mood swings, etc., it has been linked to serious adverse effects such as coronary heart disease, stroke, and increased risk of invasive BC (Perkins et al. 2018).

1.1.2. Classification and Stages of Breast Cancer

As aforementioned, BC is a highly heterogeneous disease. They are classified as ductal carcinoma in situ (DCIS), invasive (infiltrative) ductal carcinoma (IDC), invasive lobular carcinoma (ILC), and less common types of invasive BC.

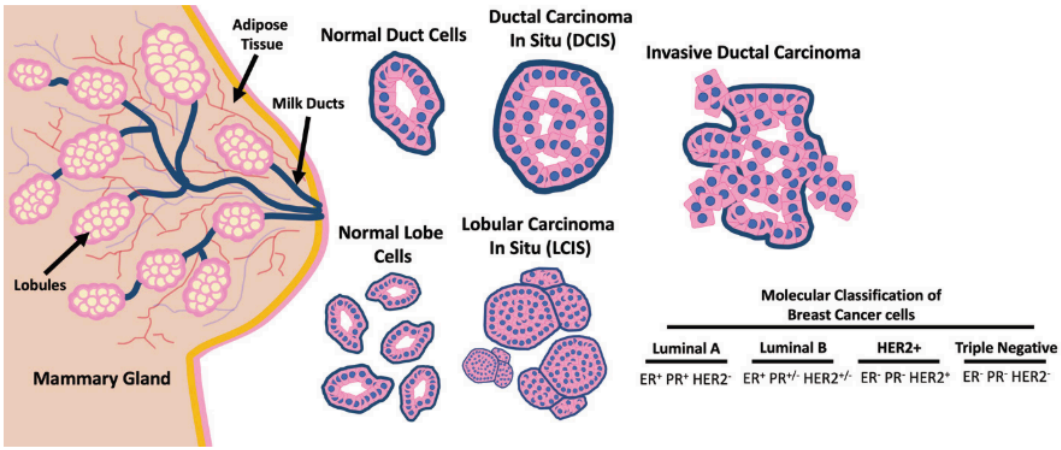

Figure 1. The figure illustrates the classification and subtypes of BC (Erzurumlu, Y., & Doğan, H. K. (2023).

Lobular carcinoma refers to cancer that develops in the breast gland; alternatively, it is known as ductal carcinoma. These two groups are further separated into two subgroups based on the site of the cancer cells meaning inside or outside of the mammary gland or milk duct. If it is found inside the mammary gland, it is termed lobular carcinoma in situ (LCIS), but if it is located outside, it is called invasive lobular carcinoma (Erzurumlu and Doğan 2023). Also, invasive, and infiltrative means that cancer cells migrate to further the ducts of the mammary gland. Understanding the

stages of BC is crucial for determining the rate of growth and spread of cancerous cells. Thus, cancerous tissues obtained from the patients are processed and staged from 0 (zero) to 4 based on some specific parameters with the help of laboratory studies. The stage is determined by the degree to which cancer cells resemble normal ones. Stage 0 is not described even as BC. The tumor is less than 2 cm in size at stage 1 and does not spread to another place. In stage 3, the tumor can be larger than 5 cm or smaller than 5 cm, it can extend to lymph nodes in the neck. Lastly, in stage 4, extensive metastasis to different tissues and organs is found (Erzurumlu and Doğan 2023).There are also molecular subtypes of BC. To get the best and most appropriate treatment, which subtype of BC should be determined. The detailed information of these subtypes is mentioned below.

1.1.2.1. Hormone receptor-positive groups

Hormone receptor-positive BC is a sort of BC that has the expression of estrogen receptor and/or progesterone receptor (PR). If tumor cells express estrogen receptors or PRs, it is termed estrogen receptor-positive or PR-positive, respectively. This type of BC is developed during any age; however, it is frequently seen in the period of post-menopausal. The estrogen receptor + subtype is divided into two types: Luminal A and Luminal B (Sarhangi et al. 2022). The expression of estrogen receptors serves as a vital diagnostic marker, given that 70-75% of invasive breast carcinomas exhibit significantly increased levels of ER. Over half of patients with estrogen receptor-positive BC also show PR expression, while it is rare in those with ER-negative BC. Estrogen receptor regulates PR expression. Hence, physiological PR levels provide information about functional estrogen receptor pathways. BC cells often exhibit abundant expression of estrogen receptor and PR which could be used as valuable diagnostic and prognostic markers for the disease. High levels of PR expression correlate with better overall survival, longer time to relapse, and delayed time to treatment failure or disease progression while reduced expression is linked to a more aggressive disease course, increased risk of relapse, and poorer prognosis (Mayrovitz (Ed.)., 2022). The most common subtype of BC is Luminal A, which has estrogen receptor-positive, PR-positive, low proliferation index, and low expression of Ki-67 (< 20%) which is a proliferation marker of cancer cells. Prognosis is better in Luminal

A than Luminal B, which has estrogen receptor-positive, PR-positive and/or negative, HER2 (human epidermal growth factor receptor 2)-positive and/or negative, low and/or high Ki-67. Therefore, Luminal B is also classified into two groups; the first is HER2-negative, and the second is HER2-positive.

Moreover, Luminal A shows better response to endocrine therapy such as anti-estrogen (tamoxifen) or aromatase inhibitors but shows poor response to chemotherapy. In addition, the most prevalent mutations seen in Luminal A are *PIK3CA* (45%), *MAP3K1*, *GATA3*, *TP53*, *CDH1*, and *MAP2K4*. Low grade means growing slowly, the best prognosis with less tumor recurrence, non-invasiveness, and higher survival rate are also important features of tumors in this group. In the case of relapse, it occurs more frequently at the bone level, while visceral and central nervous system (CNS) relapses are less common (Mayrovitz (Ed.)., 2022).

Luminal B is seen in nearly 20% of all BC cases, less than Luminal A, and has a worse prognosis. As stated before, Ki-67 expression which is a proliferation marker shows fluctuating levels means sometimes high (higher than 20%) and sometimes low. This makes them higher grades which means growing fast. It is a more aggressive form of BC type than Luminal A (Sarhangi et al. 2022). Besides, Luminal B cancers have different genetic alterations, which frequently arise in the *TP53* and *PIK3CA* genes. Furthermore, they take advantage of hormone therapy and chemotherapy more than Luminal A. Even if bone recurrence is common, a greater rate of visceral relapse is seen, and the survival rate is lower (Mayrovitz (Ed.)., 2022).

1.1.2.2. HER2 subtype

HER2-positive BC represents another subtype of hormone receptor-positive BC, comprising roughly 20% of all BC cases (Mayrovitz (Ed.)., 2022). This group is described as having high HER2 expression and lacking estrogen receptor and PR. Since HER2 is overexpressed, there are a lot of HER2 proteins in the tumors, which increases growth signaling molecules thereby promoting tumor growth swiftly. For this reason, they are growing readily when compared to the luminal ones. Therefore, the HER2 positive subtype is more aggressive. HER2 mutations provoke other cancers such as gastric, uterine, ovarian so on (Sarhangi et al. 2022). Furthermore, they had a

worse prognosis, but they have improved thanks to the administration of HER2-targeted therapies. This subtype is also subcategorized into Luminal HER2 and HER2-enriched. Luminal HER2 has estrogen receptor, PR, and HER2 expressions, and Ki-67 is between 15 to 30%. In HER2-enriched, there is no estrogen receptor and PR expression, only HER2 overexpressed. In addition, Ki-67 is greater than 30%. Thus, HER2-enriched has a poor prognosis when compared to luminal ones. They need particular medications that target HER2/neu protein such as trastuzumab, pertuzumab, and tyrosine kinase receptor inhibitors like lapatinib and neratinib, as well as surgery and precision chemotherapy (Mayrovitz (Ed.)., 2022). HER2-positive BCs, unlike luminal subtypes, bear a high prevalence of 72% of *TP53*, and 39% of *PI3K* mutations, as well as elevated expression of Ki-67 protein. HER2-positive BC is a greatly aggressive type of cancer that has a high recurrence rate. Recurrence can happen at any time, it is usually seen in five years following treatment. The risk of recurrence is much lower today than in the past thanks to the development of targeted medicines (Sarhangi et al. 2022).

1.1.2.3. Triple-negative breast cancer

Triple-negative breast cancer (TNBC) is deprived of estrogen receptor, PR, and HER2 expressions. They account for nearly 20% of all BCs, which changes among different ethnicities (Mayrovitz (Ed.)., 2022). There are notable features such as unusual metastatic patterns, poor prognosis, and aggressive biological behavior. TNBC is most commonly seen in women who are in the period of premenopausal. Characterized by its aggressive nature, TNBC encompasses around 80% of breast tumors linked to *BRCA1* and *BRCA2* mutations. In addition to the aggressiveness, it is distinguished by early recurrence, and increased likelihood of being diagnosed at advanced stages (Sarhangi et al. 2022). It shows a fast proliferation rate (with high Ki-67 expression), DNA repair gene mutations, and augmented genomic instability. In the aspect of histology, it is not easy to differentiate, rapidly proliferating, and heterogeneous tumors with an uncertain prognosis. Moreover, they are immunohistochemically subcategorized into basal and non-basal TNBC. Basal-TNBC has expressions of cytokeratins (CK) 5/6, and human epidermal growth factor receptor type 1 (EGFR1), but non-basal one doesn't have the expression of CK 5/6 (Mayrovitz (Ed.)., 2022).

They can metastasize to distant places such as the visceral and brain, bone metastasis is not seen, and tumor relapse is usually seen in three years. As said before, TNBC has aggressive clinical behaviors, develops faster, spreads to neighboring tissues, is unfortunately less curable, and has a poor prognosis (Sarhangi et al. 2022).

1.1.3. Molecular Mechanisms in Breast Cancer Development and Progression

Many signaling pathways provide cellular communications that are important for normal human development. Cancer cells and cancer stem cells (CSCs) expectedly impair or invade a couple of signaling pathways. Cancer is brought about by genetic and epigenetic alterations, enabling cells to employ mechanisms which check their growth, survival, differentiation, fate, and migration. Therefore, alterations in proto-oncogenes result in the overactivation of these signaling mechanisms; however, changes in tumor suppressors cause inactivation which ends up with the elimination of negative regulators of signaling. In this part, the signaling mechanisms that override the regulation of mammary gland development and breast CSC functions will be explained such as estrogen receptor signaling, HER2 signaling, RAS signaling, MAPK, mTOR, and Notch signaling (Feng et al. 2018).

Firstly, the estrogen receptor signaling mechanism will be mentioned. Estrogen receptors are composed of membrane estrogen receptors (G protein-coupled receptors) and nuclear estrogen receptors which are estrogen receptor α and estrogen receptor β. Estrogen receptor α and β are transcription factors that stimulate or suppress the expression of target genes when the ligand binds. Estrogen receptor α encoded by *ESR1* and estrogen receptor β encoded by *ESR2* have similar structural properties which assist their primary roles. In BC, estrogen receptor α expression is much higher than estrogen receptor β. Estrogen-mediated signaling can be classified as genomic and non-genomic based on the variations in the cellular and molecular mechanisms that lead to the regulation of gene expression with estrogen-receptor complexes binding directly or indirectly to the DNA. In direct signaling, estrogen response elements (EREs) are the specific DNA regions where estrogen receptor complexes move to the nucleus and directly bind to it (Schuur and DeAndrade 2015). ERE sequence elements have been found in ample gene promoters and regulatory regions,

but over one-third of estrogen receptor-regulated genes lack them. Estrogen receptor α and estrogen receptor β function as transcription factors activated by ligands during the process. When estradiol (E2) binds to these two types of nuclear hormone receptors in the cytoplasm, their conformation changes, and they can form homo or heterodimers, and they move to the nucleus in which it connects to the chromatin at ERE sequences, enhancer regions within or near promoters of target genes to regulate transcription. As previously described, E2 can impact on the transcription of genes lacking ERE in their promoter regions. In this process, the mechanism is known as "indirect genomic signaling", and it is based on estrogen receptors regulating the gene expression without directly binding to the DNA. The interaction with other transcription factors and response elements allows the estrogen receptor complex to function indirectly. In this approach, the target gene expression is activated or inhibited by estrogen's indirect signaling. According to a few studies, estrogen receptor α can block NF-κB from attaching to the promoter of cytokine genes by interacting with its c-ReI component. In addition, estrogen receptor α can interact with several transcriptional modulators including ATF2, c-JUN, nuclear transcription factor γ (NF-γ), and ATF1/cAMP response element binding protein (ATF1/CREB) (Clusan et al. 2023). Moreover, nuclear hormone receptors can exploit the protein-protein interactions to stimulate the expression of genes including activator protein-1 (AP-1) sites. AP-1 is a transcription factor which controls several biological events including cell differentiation, proliferation, and apoptosis. There are some examples of genes stimulated through the AP-1 pathway, which are insulin-like growth factor-1 (IGF1), collagenase, IGF1-receptor, ovalbumin, and cyclin D1. Estrogen receptor α interaction with cyclin D1 is a well-studied mechanism that causes elevating BC cell proliferation. Cyclin D1 is a key activator of cyclin-dependent kinases (CDKs) 4 and 6 that regulates the cell cycle shifting between G1 and S phase in plenty of cancer cells. The synergy between the estrogen receptor α and cyclin D1 feedback loop may reveal anti-estrogen treatment resistance and suggest using targeted CDK4/6 inhibitors alongside hormonal therapy in ER-positive patients. Previous findings indicate that estrogen receptor α and β function distinctively with respect to the ligand and response elements at AP-1 sites. For instance, 17β-estradiol induces AP-1-dependent transcription through estrogen receptor α, while this mechanism is suppressed by estrogen receptor β. Additionally,

the binding of 17β-estradiol to estrogen receptor α provokes transcription when coupled to Sp-1 in GC-rich regions, whereas it doesn't activate the transcription when engaged to estrogen receptor β. There is a well-known example of this opposite activity of estrogen receptor α and β. When both receptors are available, estrogen-bound estrogen receptor β reduces cyclin D1 expression whereas estrogen receptor-mediated synthesis is hindered. The diversity of transcriptional regulatory processes in various cells by both estrogen receptors, as well as their communication with adjacent transcription factors, might account for the divergences reported in tissues-specific biological responses to estrogen. Apart from nuclear hormones' direct genomic signaling, as stated before, there is also membrane receptor non-genomic indirect signaling. In this process, membrane-bound receptor (GPER1) activates several cytoplasmic processes such as regulation of membrane-based ion channels, synthesis of secondary messengers, regulation of cAMP, and protein kinase activation of signaling cascades which lead to alterations in gene expression indirectly (Girgert et al. 2019). Moreover, adenylyl cyclase and EGFRs are activated depending on estrogen and enhanced by GPER1 bound to estrogens. Non-genomic activities of estrogens could comprise self-regulation of receptor expression, as both estrogen receptor α and β are candidates to be phosphorylated by protein kinases such as MAPKs (Fuentes and Silveyra 2019).

Another important signaling mechanism in BC is HER2 signaling. Human epidermal growth factor receptors (HERs or EGFRs) 1-2-3-4 are grouped as tyrosine kinase receptors found in both healthy tissues and several forms of cancers. HER2 (HER2/Neu, c-ERBB2) is one of the EGFR, which is a receptor tyrosine kinase that has also extracellular ligand binding domain, transmembrane, and intracellular domains like the others. When a ligand binds to HER2, it ignites the dimerization, and the tyrosine kinase domain is induced to be phosphorylated in the cytoplasm (Crusio edt. 2019). Therefore, several downstream signaling pathways (e.g. 4-5 biphosphate 3-kinase (PI3K), and mitogen-activated protein kinase (MAPK)) are activated. These signaling pathways are strongly linked to breast carcinoma. In a great number of human BC cell lines, overexpression of HER2 is observed, which results in the amplification of HER2 signaling that is relevant to tumor growth and cancer progression (Feng et al. 2018).

RAS takes an important place in supporting BC downstream of the disarranged oncogenic pathways, which acts as a hub for the primary intracellular signaling pathways that control cell growth, motility, angiogenesis, and immunological evasion. Therefore, oncogenic factors require the RAS function to disseminate their signals and execute their abnormal programs, inhibiting the RAS function may reduce upstream tumorigenic signals. N-RAS and K-RAS are shown to be overexpressed in basal-like and HER2 subtypes of BC (Galiè 2019). RAS signaling is triggered by a variety of receptors such as receptor tyrosine kinases (RTKs), G-protein coupled receptors (GPCRs), and the integrin family. RAS is activated by these signaling cascades via an assembly of several scaffolding proteins that lead the activation from GDP- to GTP-bound state (Gimple and Wang 2019). HER2, homologous of EGFR, is linked to RAS signaling through interactions with the adaptor proteins growth factor receptor bound protein 2 (Grb2), which brings in SOS1 as RAS GDP-GTP exchange factor thereby activating RAS protein via conformational changes (Gimple and Wang 2019). Overexpression of these receptors in BC cells enhances the RAS signaling pathway (Galiè 2019).

When transmembrane receptors (RTKs) are engaged, Grb2 and son of sevenless (SOS) complexes from the cytoplasm are attracted to the cell membrane's inner surface. SOS is a key guanine nucleotide exchange factor (GEF) which transmits the signal from RTK to RAS. Later, RAS-GDP is converted into RAS-GTP via SOS. In this mechanism, GRB2 serves as a link between RTK and SOS. RAS-GTPase catalyzes RAS-GTP to inactivate RAS-GDP via GTPase-activating proteins (GAPs) (Song et al. 2023).

1.2. TREATMENT OPTIONS

1.2.1. Chemotherapy and Hormone Therapy (Local and Systemic Treatments)

Surgery and radiation therapy (RT) are local treatment options in BC therapy. For surgery, there are two ways which are breast-conserving surgery (BCS) and mastectomy. Breast-conserving removes only the tumor and its surrounding normal tissue. Some lymph nodes behind the arm may be excised. If the tumor is located near the chest wall lining, a portion of it may be removed. This is also called a lumpectomy

or partial mastectomy. This can be performed in individuals dealing with early-onset BC. On the other hand, total mastectomy is a procedure that removes the entire cancerous breast. Before surgery, chemotherapy may be administered to shrink the tumor that will be removed, and this is called neoadjuvant therapy. Following surgery, some people might get radiation therapy, chemotherapy, targeted or hormone therapy to eliminate remaining cancer cells. This is called adjuvant therapy which reduces the likelihood of cancer recurrence (WEB1). For estrogen receptor +, HER2+ tumors, and TNBC, 10-year locoregional recurrence rates in BCS followed by RT are nearly 2%, 3%, and %5 respectively, comparable to those observed after mastectomy (Hong and Xu 2022). In RT, X-rays or other sorts of radiation are used to harm or avoid cancer cell development. RT is classified into two categories which are external and internal RT. External radiation therapy is given to BC patients. Internal radiation therapy with strontium-89 is utilized to reduce bone pain resulting from metastatic BC. It is given intravenously and transported to the bones.

Hormone therapy is the preferred one since two-thirds of BC cell growth is accounted for by estrogen activation of ERα. Reducing the estrogen receptor α activity or depriving the tumor of estrogen can prevent BC recurrence and improve patients' survival rates. Tamoxifen is one of the estrogen receptor α antagonists, a member of the SERM family, which is well-known and widely used in clinics (Clusan et al. 2023). It has been the only treatment option for advanced BC for over 20 years, but at the end of the 1990s, the introduction of aromatase inhibitors considerably impacted first- and second-line therapy. Those active compounds such as letrozole, anastrozole, or exemestane have therapeutic effects because they suppress the activity of the enzyme aromatase, which converts androgens to estrogen. In pre-menopausal women, the ovaries generate most of the estrogen. However, in post-menopausal women, instead of estrogens, aromatase found in adipocytes and breast tissues can produce estrogen and promote tumor progression. Fulvestrant, an estrogen receptor α antagonist, was the pioneer in the development of a novel class of therapeutically useful drugs in the early 2000s. This class comprises selective estrogen receptor degraders (SERDs) that attach to estrogen receptor α and deactivate it via degradation. As aforementioned, SERMs are chargeable for the conformational change of estrogen receptor α by recruiting co-repressors. Fulvestrant binds to estrogen receptor α with the same affinity

as E2 without agonist action. It is typically used to treat luminal metastatic BC or individuals who developed resistance to a 1st hormone therapy IAs or SERMs (Clusan et al. 2023).

CDK4/6 assumes a critical function in fostering the proliferation of cancer cells. Stimulation of CDK4/6 through D-type cyclins such as cyclin D1/CDK4 and cyclin D3/CDK6 facilitates the phosphorylation of the retinoblastoma-associated protein (Rb) (Y. Hu et al. 2021). Phospho-Rb facilitates the cell cycle progression and division by activating E2F transcription. Given the frequent occurrence of cyclin D upregulation and the consequent restoration of phospho-Rb expression in hormone receptor + BC cells, targeting the G1/S checkpoint emerges as a crucial therapeutic strategy to halt the proliferation of cancer cells (F. Ye et al. 2023). Recent studies indicate that CDK4/6 inhibitors not only hinder the cell cycle but also restrain tumor growth through various additional pathways. These include amplifying cytostasis induced by signaling pathway inhibitors, prompting senescence, regulating cellular metabolism, and even fostering anti-tumor immune responses (M. Zhang et al. 2021). Prescription drugs known as CDK4/6 inhibitors exhibit clinical efficacy when used in conjunction with hormonal therapies for the treatment of hormone-receptor + and HER2-progressive or metastatic BC. Palbociclib, abemaciclib, and ribociclib are among FDA-approved CDK4/6 antagonists used for treating various forms of BC (Łukasik et al. 2021). Palbociclib demonstrates efficacy against hormone-receptor + and HER2- BC or metastatic BC in both pre-and post-menopausal women. Its primary administration involves combining with hormonal therapies like aromatase inhibitors and estrogen receptor antagonists (F. Ye et al. 2023).

Doxorubicin (DOX), as a topoisomerase II inhibitor, induces DNA strand breaks, impeding the activity of topoisomerases crucial for DNA replication and transcription processes. It has exhibited substantial therapeutic potential and is acknowledged as one of the most effective chemotherapy agents approved by the FDA for treating a range of cancers including breast, carcinomas, sarcomas, and hematological malignancies (Kciuk et al. 2023). The anti-cancer efficacy of DOX is well-established, attributable to its ability to intercalate into DNA, inhibit topoisomerase II, disrupt mitochondrial function, and enhance free radical generation, consequently inducing oxidative damage (Thorn et al. 2011). Besides their cytotoxic impact, chemotherapy

medications might also enhance the infiltration of CD8+ T cells and natural killer (NK) cells into tumors, along with promoting the maturation of antigen-presenting cells (APCs) like tumor macrophages or dendritic cells to reinvigorate an immune-reactive tumor microenvironment thereby augmenting the tumor's susceptibility to immunotherapy (Kciuk et al. 2023). Paclitaxel (PTX) is another chemotherapeutic agent which is extensively utilized in advanced BC treatment. PTX disrupts the normal functioning of microtubule growth by inducing hyper-stabilization of their structure, leading to arrested function. This impairs the cell's ability to utilize its cytoskeleton flexibly (WEB2). Mitotic arrest induced by PTX arises from the activation of the mitotic checkpoint. This checkpoint serves as the primary cell cycle control mechanism during mitosis which is aimed at averting chromosome missegregation (Weaver 2014).

Advancements in genomics, proteomics, and computational biology have led to the discovery of innovative cancer therapy approaches, where previously established drugs are emerging as promising treatments in cancer therapy. A drug repurposing strategy can expedite pharmaceutical advancements and suggest safer, more efficient, and cost-effective options with reduced side effects (Barzaman et al. 2020). For breast cancer treatment through drug repurposing, various alternatives have been proposed including alkylating agents, anthracyclines, anti-metabolites, CDK4/6 inhibitors, aromatase inhibitors, mTOR inhibitors, and mitotic inhibitors (Shim and Liu 2014). Combining CDK4/6 inhibitors with fulvestrant has been demonstrated to prolong the survival of BC patients compared to those treated with fulvestrant alone. The concurrent administration of aromatase inhibitors like exemestane and tamoxifen with histone deacetylase (HDAC) inhibitors, such as entinostat and vorinostat, has displayed the most favorable anti-cancer clinical results. In roughly 70% of BC cases, resistance to hormonal therapy is observed, largely linked to the PI3K/AKT/mTOR pathways, and this pathway serves as a crucial target for intervention in both HER2-positive and HER2-negative BC cases (Barzaman et al. 2020). Another notable signaling pathway inhibitor is everolimus, an mTOR inhibitor that has received FDA approval. Combining everolimus with exemestane or trastuzumab has demonstrated promising clinical outcomes in HER2-positive and HER2-negative BC cases (Nagarajan and McArdle 2018).

1.2.2. Tamoxifen

In the 1930s, it was discovered that tumor-initiating compounds have properties of inhibiting the growth of healthy and malignant tissues under certain circumstances. At that time, estrogens were known to promote the growth of BC cells and could be utilized for the treatment of advanced BC. Diethylstilbestrol (DES) which is a synthetic estrogen showed benefit in clinical trials. Therefore, this triggered a surge of studies into high-dose and synthetic estrogens, which finally became the standard care in postmenopausal patients bearing advanced BCs during the initial years of the 1960s. In the meantime, exploration into anti-estrogenic composites for contraceptive purposes resulted in the identification of MER-25, a breakthrough that paved the way for the discovery of TAM (Patel and Bihani 2018). TAM was initially on the markets as a fertility regulator in the UK. However, it also demonstrated the impacts in clinical studies of advanced BC in the 1970s. These factors resulted in its initial acceptance in the UK, followed by approval and adoption in the US and other parts of the world. Tamoxifen was equally effective as high-dose estrogens such as DES but had fewer adverse effects. Walpole et al. developed tamoxifen whose original name is ICI 46,474 that is a member of the triphenylethylene class of SERMs (Patel and Bihani 2018). TAM acts as an antagonist to estrogen receptor in breast tissue yet behaves as an agonist in bone tissue. It competitively binds to estrogen receptors, hindering estrogen-dependent gene transcription, cell proliferation, and the progression of the tumors (Akram et al. 2017).

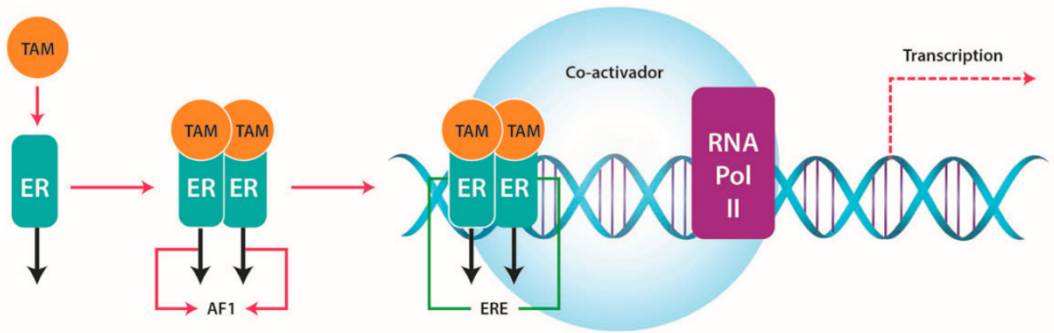

Figure 2. The mode of action of TAM is shown (Rondón-Lagos, M. et al (2016).

SERMs interact with either one of two subunits of estrogen receptor (α and β) resulting in target-site and tissue-specific activity (An et al. 2016). TAM which is different from estrogen targets ERα and recruits corepressors thereby inhibiting BC cell proliferation. It blocks estrogen connecting with its receptor, required for its activation in BC cells. It decreases tumor growth factor-α and insulin-like growth factor 1 whilst enhancing sex hormone-binding globulin (SHBG) levels. The rise in SHBG reduces the extent of accessible estradiol. These alterations limit the levels of substances that promote tumor growth. It leads to apoptosis in estrogen receptor + cells. This activity is assumed as the consequence of inhibiting protein kinase C that hinders the synthesis of DNA. Another theory of the apoptotic impact of TAM may result from the 3-fold rise in intracellular and mitochondrial Ca^{2+} levels or inducing the tumor growth factor β. Other investigations have found TAM suppresses cell proliferation through causing cell cycle arrest in the G0/G1 state. Furthermore, TAM has been shown to enhance cellular proliferation via a variety of signaling pathways including MAPKs. This mitogenic impact could be the result of altered estrogen metabolism (Rondón-Lagos et al. 2016). Therefore, it has been the preferred treatment for pre-and post-menopausal women having estrogen receptor + BC for five years. After around ten years of follow-up, recurrence rates were reduced by 21%, 29%, and 47% for 1, 2, and 5 years of treatment separately. The decreases in mortality were 12%, 17%, and 26% sequentially. According to the result obtained from ATLAS randomized trial including nearly 13.000 patients to terminate TAM treatment after 5 years or complete to 10 years of therapy, longer treatment results in a considerable reduction in recurrence and mortality compared to the shorter treatment (Howell and Howell 2023).

1.2.3. Drug Resistance in Breast Cancer

Drug resistance undertakes 90% of deaths from cancer. Multidrug resistance (MDR) reduces the potency of chemotherapeutic agents thereby resulting in relapse and metastasis. Resistance which is innate and acquired accounts for almost half of the drug-resistant patients. Intrinsic resistance is seen before the treatment is applied, and it can arise from genetic mutations, the expansion of CSCs, and the stimulation of innate pathways that protect against toxic exogenous substances. Nonetheless, acquired resistance can be developed from proto-oncogene activation, changes in gene

expression caused by epigenetic markers or mutations, and modifications in the tumor microenvironment (TME) following therapy (Kinnel et al. 2023).

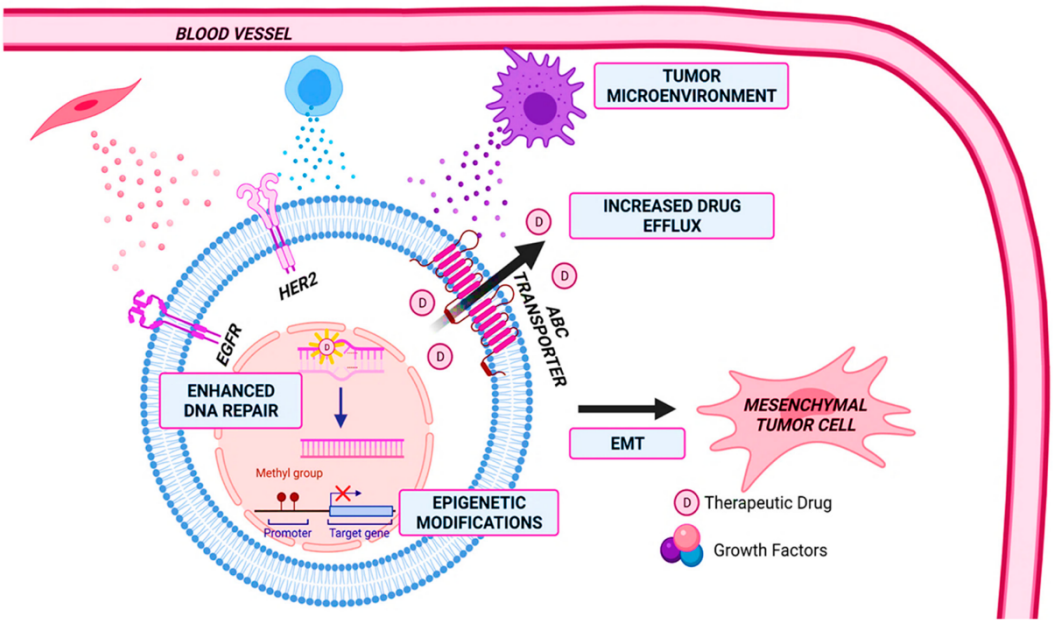

Figure 3. The drug resistance mechanisms are demonstrated (Kinnel, B. et al (2023).

One of the drug resistance mechanisms is the increased drug efflux that gives rise to a diminish in the stack of intracellular drugs. The ATP-binding cassette (ABC) transporter family takes a significant position in the drug efflux. There are 48 *ABC* genes that are categorized into 7 groups: ABCA, ABCB, ABCC, ABCD, ABCE, ABCF, and ABCG. ABCB1, ABCC1 and ABCG2 are directly associated to MDR. ABCB1, known as MDR1 or p-glycoprotein (P-gp) can be produced in healthy tissue as well, but it is overexpressed in several cancers (He et al. 2021). Highly expressed ABCB1 has already been related to chemoresistance in numerous cancer types such as breast, kidney, colon, pancreas, and liver (Martin et al. 2014). ABCG2 has a significant role in BC therapy resistance and an important marker of CSCs. ABCG2 can transport drugs that are both positively and negatively charged. TNBC has a higher level of ABCC1 and ABCG2 expression than the other BC subtypes (Nedeljković et al. 2019). Another mechanism is DNA damage repair of cancerous cells. Normally, chemotherapeutic drugs target to damage DNA such as cisplatin, gemcitabine, 5-fluorouracil. However, DNA damage can be repaired by DNA damage response (DDR), which leads to resistance via repairing DNA lesions (Bukowski et al. 2020). Therefore, targeting prominent players in the DDR is one strategy to combat

resistance. Chemotherapeutic drugs are known to cause senescence as well. Senescence is a state in which cell proliferation is permanently stopped. Telomere shortening, surplus mitogenic signaling through oncogenes, and non-telomeric DNA damage are three primary senescence triggers. Therapy that triggers senescence in cancer cells can develop CSC-like traits over time, allowing them to escape senescence and lead to progression (Gordon et al. 2012).

Chemotherapy drug tolerance also can be influenced by gene silencing through CpG sites hypermethylation, oncogene overexpression through hypomethylation, histone modifications, and non-coding RNA expression variations (Bukowski et al. 2020). TAM is commonly used in estrogen receptor + BC patients, which is one of the examples of a targeted drug that results in developing resistance. TAM resistance differs by case. Nevertheless, decreased estrogen receptor expression can be attributed to familiar factors such as epigenetic changes and mutation. BC is highly heterogeneous, which means that it contains numerous subpopulations of cancer cells with distinct gene expressions that influence the extent of sensitivity to cancer treatments. The self-renewal properties of CSCs make them important in tumor heterogeneity, recurrence, and metastasis (Nedeljković et al. 2019). Deregulation of the signaling pathways such as Wnt/β-catenin, Hedgehog (Hh), Notch, and JAK/STAT pathways, which take important roles in development, can lead to the development of CSC and resistance to therapy (Kinnel et al. 2023).

Another important thing is the TME which is made up of blood vessels, fibroblasts, immune cells, signaling molecules, and extracellular matrix. These are also significant in contributing to innate and acquired resistance. Hypoxia is a critical feature of the TME that influences cancer progression. Hypoxia has been shown to activate a variety of processes related to the CSC phenotype including angiogenesis, drug efflux via enhanced ABCC1 and ABCG2 expression, regulation of senescence and apoptosis, metastasis, and genomic instability (Wang et al. 2019). Hypoxia-induced factors (HIFs) are produced under hypoxic conditions, and it is a transcription factor that occurs during low oxygen levels for interceding the effects of hypoxia. HIF-1 stimulates epithelial-mesenchymal transition (EMT) which is a characteristic of TNBC (Nedeljković et al. 2019). HIF-1α is also thought to promote drug resistance in estrogen receptor + BC cell lines (Lima et al. 2016).

EMT is a process that occurs in normal cells and is required for embryonic development and wound healing. However, this can be exploited by several pathways and resulting in tumorigenesis. EMT is involved in treatment resistance, tumor invasion, and metastasis in cancer. In the time of EMT, E-cadherin function is decreased, resulting in diminished cell-cell adhesion and apoptosis resistance (Lima et al. 2016).

In 30% of estrogen receptor-α + breast tumors, tumor cells might evade hormonal regulation and proliferate without triggering estrogen. Hormonal escape is usually followed by the loss of the epithelial phenotype and the acquisition of more migratory and invasive abilities. At this point, hormone therapy is not useful for resisting malignant development (Clusan et al. 2023).

1.3. EPIBRASSINOLIDE

Epibrassinolide is a member of brassinosteroids (BRs), which are plant hormones derived from steroids (Liu et al. 2014). They have essential functions in growth, root and stem elongation, differentiation, and stress tolerance in plants. Fruits, seeds, leaves, and pollens are the sources of the BRs (Coskun et al. 2015). BRs regulate gene expression via interacting with metabolic pathways, activating cell division and differentiation processes in plants. Their functions are well described in plants. Also, the signaling mechanism is well-known in plants, which occurs via transmembrane heterodimer BR receptor consisting of *brassinosteroids insensitive 1 (BRI1)* which encodes BRI1-associated receptor kinase (BAK1), but the exact mechanism of EBR in mammalian cells was unknown (Lei Wang et al. 2006). While BRs promote plant development and differentiation, epibrassinolide (EBR), which is one of the BR derivatives, structurally resembles mammalian steroids and has been found to trigger cell cycle arrest in G1/M, leading to death in hormone-dependent breast and prostate cancer cell lines (Steigerová et al. 2010, 2012). In this regard, it was proposed that EBR could trigger apoptosis by engaging with nuclear hormone receptors (NHRs) that bind to steroid mammalian glands such as estrogen or androgens. Based on the results obtained by Obakan et al. EBR causes caspase-dependent apoptosis in both NHR-expressing and non-NHR cells (Obakan et al. 2014a, 2014b). The apoptosis induced by EBR was triggered by elevated unfolded protein response (UPR) because of severe

endoplasmic reticulum stress. This mechanism was elucidated by the SILAC (stable isotope labeling by amino acids in cell culture) approach (Obakan et al. 2015). As a result, they found that EBR-mediated apoptotic response targets primarily ER-stress chaperone Calreticulin in cancer cells (Obakan-Yerlikaya et al. 2017).

1.4. ENDOPLASMIC RETICULUM STRESS AND UNFOLDED PROTEIN RESPONSE

The endoplasmic reticulum (ER) is an enormous, continuous membrane-embedded organelle composed of unique domains in terms of structure and function such as the nuclear envelope (NE), peripheral tubular ER, peripheral cisternae, and numerous membrane contact spots at the plasma membrane, mitochondria, Golgi, endosomes, and peroxisomes. These domains are necessary for a variety of cellular functions encompassing protein and lipid production, regulation of calcium levels, and macromolecule exchange at ER-membrane contact sites (English and Voeltz 2013). The ER is made up of a continuous membrane system that contains the NE, and the peripheral ER, which are delineated by flat sheets and branched tubules. The shape and positioning of these ER domains are influenced by multiple integral membrane proteins as well as engagement with other organelles and the cytoskeleton. These connections are dynamic and reflect alterations inside the cell, whether through the cell cycle or developmental stage, intracellular signals, cell differentiation, or protein interactions (Schwarz and Blower 2016).

The structural organization of the ER is exceedingly diverse. The ER has a great degree of plasticity which allows it to take a variety of configurations to suit its various roles. The ER might be observed as flattened sacks, as it frequently does in protein production, or as an interconnected network of tubules. This tubular network is continuously reconstructed by mechanisms such as "tubule sliding," "tubule branching," and "ring closure" (Berridge 2002). The most prominent structural diversity within the ER is evident in its division into rough ER, smooth ER, and nuclear membrane. The rough ER associated with ribosomes is engaged in protein generation; however, might be involved in Ca^{2+} signaling. The smooth ER is primarily in charge of Ca^{2+} signaling in neurons and muscle cells (Berridge 2002).

The ER is a highly dynamic and complex cellular organelle that is in charge of synthesizing, modifying, and folding both secreted and transmembrane proteins (Chen and Cubillos-Ruiz 2021; McGrath et al. 2018). Also, it is responsible for quality checks and degradation of defective or misfolded proteins and thereby ensures that only appropriately folded proteins can arrive at their cell compartments (Sisinni et al. 2019). The nascent polypeptides undergo active folding and modification through a sequential process involving ER-resident enzymes, such as chaperones, foldases, glycosylating enzymes, and oxidoreductases, following co-translational translocation into the ER lumen (Oakes 2020).

Particular chaperones of the reticular compartment modulate the maturation process which can be brought together into 3 groups; GRP78 (BiP) and GRP94 simplify the assembly and folding of unspecific proteins; Calnexin (CALNX), Calreticulin (CALR), and lectin implicated in the glycoprotein maturation process; and Heat shock protein 47 (HSP47) particularly for collagen (Sisinni et al. 2019). Besides, another group of enzymes, known as protein disulfide isomerases (PDIs), play a role in either generating or breaking disulfide bonds. In healthy situations, damaged or misfolded proteins are eradicated via the ER-associated protein degradation (ERAD) process (Chen et al. 2021).

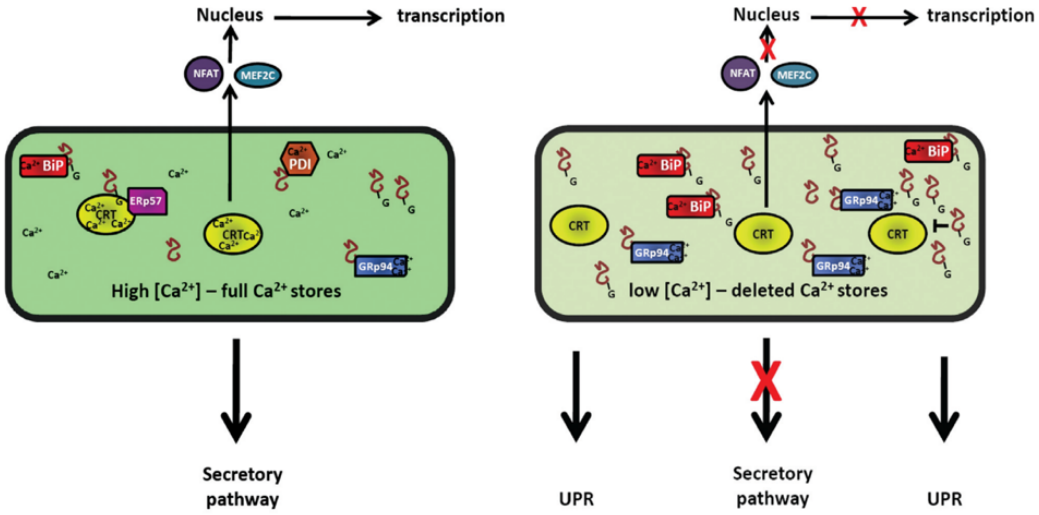

Figure 4. The response against Ca^{2+} imbalance is exhibited (Michalak, M. et al (2002).

Ca^{2+} has prominent functions since the changes in the concentration of the calcium ions determine the activity of reticular chaperons. For instance, CALR is one of the calcium-binding/buffering chaperones in the ER, which has a pivotal role in calcium

signaling in the ER lumen, and this has substantial effects on Ca^{2+}-dependent pathways including control of transcription during embryonic development (Coe and Michalak 2009). As aforementioned, GRP78 (BiP), GRP94, PDI, and oxidoreductase ERp57 also bind to misfolded proteins, and the secretory pathway and calcium-dependent transcription are fully active (Figure 4).

GRP78 is crucial for the quality checks of proteins within the ER and the modulation of estrogen receptor signaling in response to ER stress. The complete depletion of GRP78 causes fatality in 3.5-day-old embryos owing to the failure of embryo peri-implantation uncovered by gene knockout technologies ending up with GRP78 is prominent during embryonic development and pathogenesis (Bánhegyi et al. 2007). When proteostasis, the regulation of the functional proteome including from synthesizing to the degradation, is broken meaning that misfolded or unfolded proteins are accumulated in the lumen of the ER, this causes ER stress, and the cell responds to this through the process termed unfolded protein response (UPR) (Chen and Cubillos-Ruiz 2021). These perturbations include imbalances in Ca^{2+} levels, suppression of protein glycosylation or disulfide bond formation, hypoxia, as well as bacterial and viral infection (Bánhegyi et al. 2007).

The mammalian cells have three sensors of the ER stress that are PRKR-like ER kinase (PERK), inositol-requiring enzyme 1α (IRE1α), and activating transcription factor 6 (ATF6). In normal circumstances, these sensors are kept in an inactive form by binding to the most delineated ER-resident protein BiP/GRP78 (glucose-regulated protein, 78 kDa) (Chen and Cubillos-Ruiz 2021). When misfolded and/or unfolded proteins are accumulated in the ER lumen, the ER is overwhelmed, and the responses are initiated. Therefore, they become activated since GRP78 shows higher binding affinity to the mis/unfolded proteins by leaving the sensors. In this way, downstream signaling pathways of these sensors are activated (Sisinni et al. 2019).

The process known as homeostatic UPR is the earliest output of the UPR that aims to sustain cell function by restoring ER homeostasis by diminishing needs and boosting the capability of the protein-folding machinery (Oakes et al. 2020). In addition to these, global translational attenuation, mRNA decay, eradication of misfolded proteins via the ERAD machine that canalizes them to the cytoplasm for ubiquitination and

subsequent degradation by 26S proteasome, and recycling of misfolded proteins and cellular resources via autophagy stimulation can all help to maintain ER homeostasis (Chen and Cubillos-Ruiz et al. 2021; Oakes et al. 2020). Productive or non-lethal ER stress reestablishes ER homeostasis and assists cells in adapting to stress and survival. On the contrary, unresolved, or extreme ER stress can result in cell death. This cellular fate is determined by the magnitude and duration of the ER stress (Chen and Cubillos-Ruiz et al. 2021).

1.4.1. PERK/eIF2α/CHOP Signaling

PERK-(EIF2AK3) is a type I ER transmembrane protein whose N terminus is sited in the ER cavity that maintains its connection with GRP78 and gets involved in the modulation of GRP78 dimerization. The C-terminus which has a phosphorylation site and kinase activity with serine/threonine kinase activity is placed in the cytoplasm (Lin et al. 2019). Once PERK is activated through ER stress, firstly it undergoes oligomerization and autophosphorylation. Then, it phosphorylates the eukaryotic initiation factor 2 (eIF2α) at serine 51 (Ser51) residue. Afterward, phosphorylated eIF2α has been reported to accelerate the disassembly of odd 80S ribosomes, resulting in the global reduction of protein synthesis (Patra et al. 2023). This causes the 5'cap-dependent translation of many mRNAs to be temporarily hindered while enhancing the 5'cap-independent translation of others such as activating transcription factor 4 (ATF4) (Corazzari et al. 2017). Later on, ATF4 goes to the nucleus and connects to the promoter regions of the genes, and it increases cell longevity via triggering the activation of genes related to amino acid metabolism, redox processes, stress response, and protein production (Szegezdi et al. 2006). Autophagy-related gene 5 (ATG5) is one of the ATF4 targets, which encodes proteins required for autophagy, a self-eating process that degrades and recycles cellular contents (Corazzari et al. 2017). However, ATF4 induces not only the anti-apoptotic genes (Szegezdi et al. 2006). C/EBP Homologous Protein (CHOP) is another target of ATF4 that promotes cell death. This can be achieved by highly expressing pro-apoptotic proteins, and global protein production is reestablished via the upregulation of GADD34 which dephosphorylates eIF2α (McGrath et al. 2018). CHOP is a member of the CCAAT/enhancer binding proteins (C/EBPs) family which regulates genes involved in proliferation,

differentiation, and energy consumption (H. Hu et al. 2019). CHOP (29 kDa) is made up of 169 in humans and 168 in rodent amino acid residues and has two functional domains which are an N-terminal transcriptional activation domain and a C-terminal basic-leucine zipper (bZIP) domain (Ubeda et al. 1996). Deletion mutant studies unveiled the bZIP domain is essential for apoptosis mediated by CHOP. Cells lacking CHOP expression were discovered to exhibit resistance to apoptosis induced by ER stress (H. Hu et al. 2019).

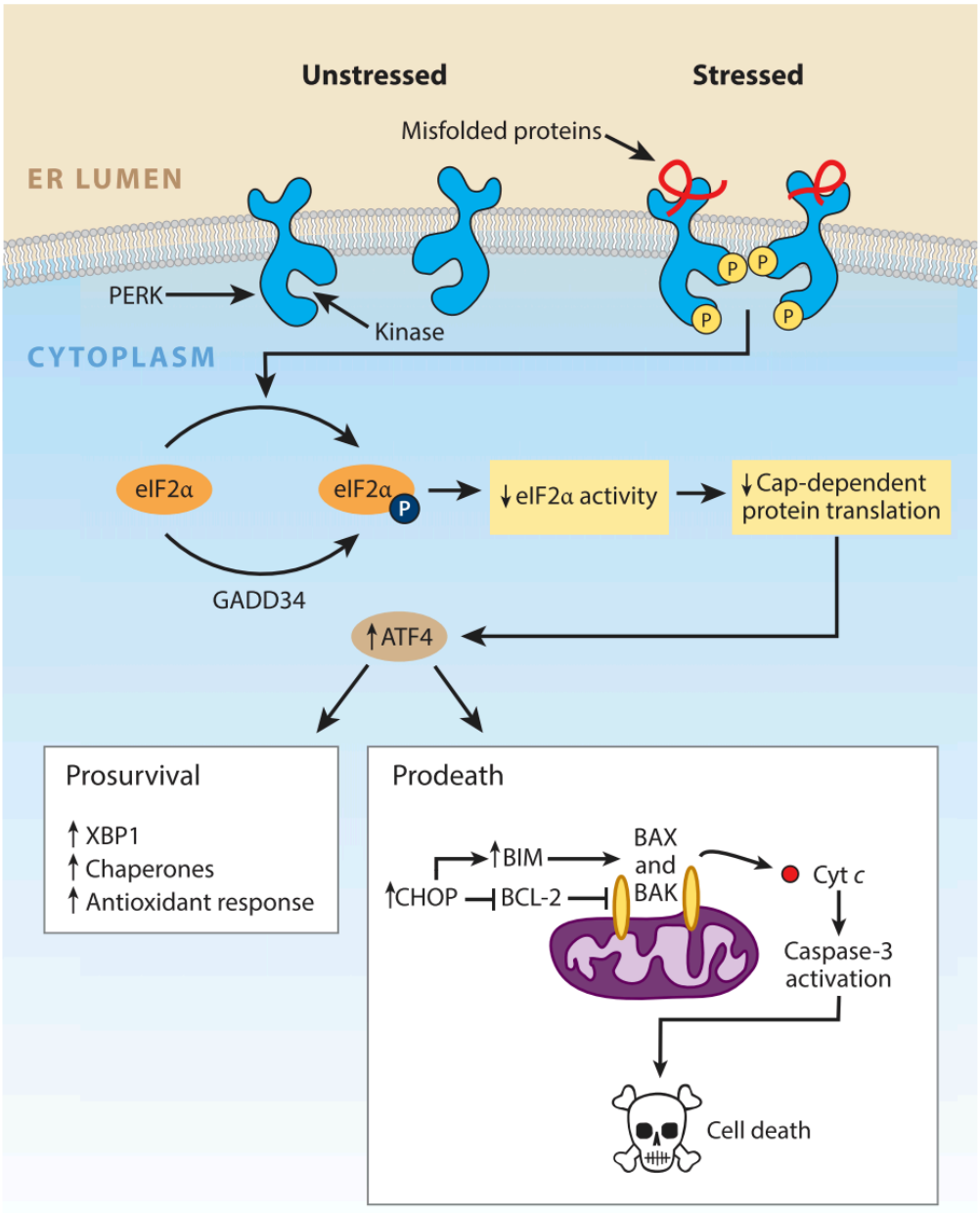

Figure 5. Under unstressed/stressed conditions, PERK signaling is demonstrated in detail (Oakes, S. A., & Papa, F. R. (2015).

Nuclear factor erythroid 2-related factor 2 (NRF2), the major regulator of the cellular antioxidant response, is another target directly phosphorylated by PERK thereby dissociating the NRF2/Kelch-like ECH-associated protein 1 (KEAP1) complex, stabilizing and activating the NRF2. Moreover, NRF2 is also activated by IRE1 and causes oxidative stress showing that the molecular mechanisms determining NRF2 activity in response to ER stress are multifaceted (Sarcinelli et al. 2020). According to the study, PERK is inhibited through phosphorylation by Protein kinase B (AKT).

The suppression of PERK signaling by AKT could block the downstream phosphorylation of eIF2α, hence inhibiting the cytoprotective action of eIF2α. Therefore, this results in greater cell death in tumor cell response formed by PI3K and AKT inhibitors, showing a role for PERK/eIF2α signaling in PI3K/AKT inhibitor resistance (Mounir et al. 2011). Altogether, these findings suggest that the PERK/eIF2α signaling pathway plays a crucial role in promoting cell survival during UPR (Clarke et al. 2012).

The response to acute and chronic ER stress is regulated by distinct PERK-dependent pathways. During prolonged stress, PERK enables a partial recovery of protein production while facilitating the translation of genes targeted by the UPR. This transition enables cells to deal with persistent stress while escaping from cell death (Guan et al. 2017). Similar to IRE1, there are limitations to examining PERK activity in large-scale datasets. The levels of PERK mRNA and protein do not provide insight into PERK activity.

1.4.2. The IRE1α Pathway

IRE1α is a type I transmembrane protein like PERK, and it has two domains which are endoribonuclease and serine/threonine kinase domains (Hetz 2012). When stress conditions occur and lead to aggregation of mis/unfolded proteins in turn BiP leaves from the luminal domain (LD) of IRE1α and binds to them, causing the activation of IRE1α (Read and Schröder 2021). When IRE1α is activated, it undergoes homodimerization and autophosphorylation. 3 main ways can be followed. Firstly, its endoribonuclease domain starts splicing of the mRNA encoding the bZIP transcription factor XBP-1 in mammals and Hac1 which is cleaved by orthologue IRE1 in the yeast, independent of the spliceosome (Bashir et al. 2021).

UPR is different a bit in the yeast compared to mammalians since they lack both PERK and ATF6. However, IRE1α is the most conserved branch of the UPR (Aragón et al. 2009). In yeast, there is only one available pathway IRE1 which is an orthologue of IRE1α that can respond to the accumulated unfolded proteins in the ER (Credle et al. 2005). Two models are put forward for triggering UPR by IRE1. One model proposes that unfolded proteins directly attach to the IRE1 resulting in the IRE1

oligomerization. According to studies about the core of IRE1's luminal domain, it is made up of two interfaces (Credle et al. 2005). The first interface forms a deep groove, and oligomerization is achieved by the second one. The grooves created by IRE1 are similar to those created by the major histocompatibility complex (MHC), which can bind to peptides with great specificity. It is also suggested that because of the depth of the groove, fully folded proteins cannot reach the groove thereby allowing only Ire1 to the unfolded proteins. The specificity of IRE1 to the unfolded proteins can be explained by this. In the other proposed model, the resident ER chaperon Kar2, which is known as BiP in mammalian cells, is coupled to deactivate IRE1 in favor of binding to unfolded proteins when they aggregate. This causes Kar2 to be released from IRE1, starting to oligomerize, which increases trans autophosphorylation of IRE1 in its activation sites at Serine 837, 840, 841, 850, and threonine 844 as well as the induction of endoribonuclease activity (Lee et al. 2008; Shamu1 and Walter 1996). Following this, the splicing of Hac1 in yeast (removing 252 nucleotides and forming Hac1*i*) or XBP-1 mRNA in mammalian cells is done. After the cleavage of Hac1 mRNA by IRE1, two exons are ligated by tRNA ligase. Further, newly ligated mRNA is translated into an active protein which actions as a transcription factor which can attach to the promoter regions of the target genes involved in UPR (Gonzalez et al. 1999; Hampton 2000).

For the IRE1 pathway in mammalians, it is proposed three models which are a direct association, competition, and allosteric models (Adams et al. 2019). In the direct association model, it is postulated that UPR signaling is stimulated by the direct binding of misfolded proteins to the LD of IRE1α. This mediates conformational changes which end up with the oligomerization of IRE1 LD (Credle et al. 2005; Kay et al. 2017; Promlek et al. 2011).

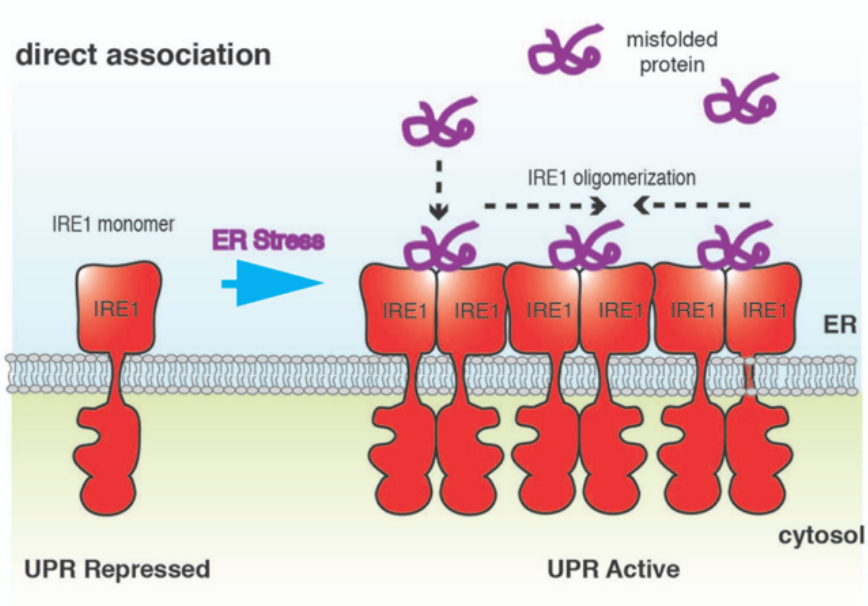

Figure 6. The direct association activation model of IRE1 is displayed (Adams, C. J. et al (2019).

In this scenario, BiP isn't responsible for uncovering ER stress yet it has an important role in the binding and sequestering inactivation of monomeric IRE1 (Figure 6). In the competition model, IRE1 LD binds to the substrate-binding domain (SBD) of BiP, this is the location where misfolded proteins compete with BiP for attaching (Preissler and Ron 2019). This interaction forms a repressive complex. As shown in the Figure 7, BiP interfaces with IRE1 through ERdj4 which suppresses UPR signaling through alleviating the production of IRE1 LD monomers. Therefore, BiP works as a regulator of UPR signaling via hindering the formation of dimerization of IRE1; however, it doesn't directly function as a sensor of ER stress (Preissler and Ron 2019).

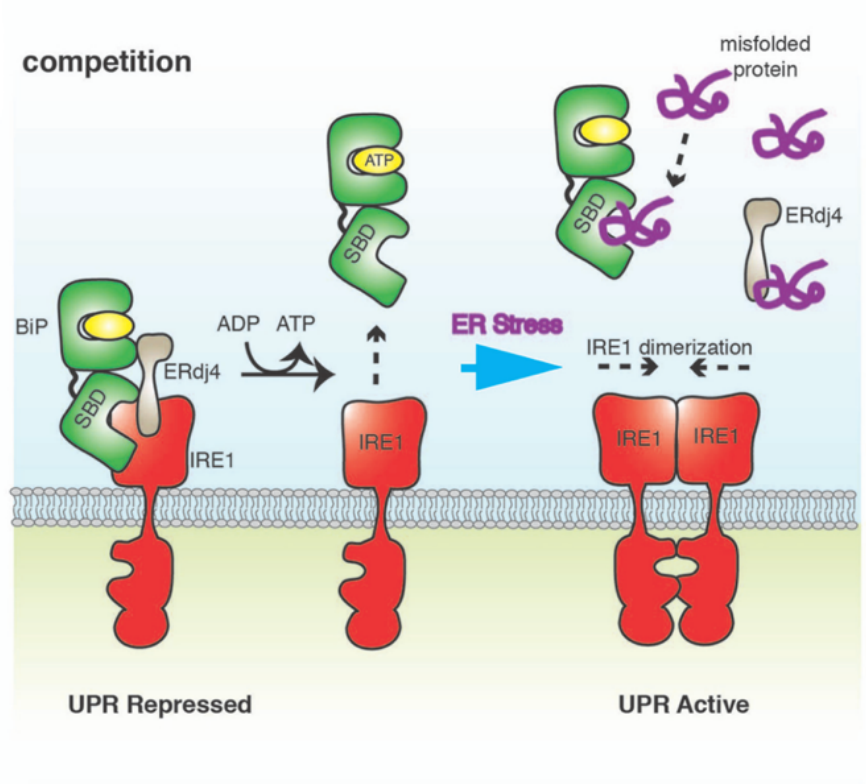

Figure 7. The competition model of IRE1 is demonstrated (Adams, C. J. et al (2019).

During the interaction of BiP with chaperone-substrate, its activity is precisely acquired from the tenet of nucleotide-dependent regulation of Hsp70. The prominent aspect of this mechanism is that ATP results in the dissociation of BiP from IRE1, not because of the misfolded proteins (Adams et al. 2019). NEF promotes the conversion of ADP to ATP leading BiP to separate from the IRE1 LD. At this point, misfolded proteins agonize for binding to free BiP and ERdj4 via IRE1 LD. During high ER stress, misfolded proteins occupy BiP and ERdj4, which hinders the association of BiP with IRE1 LD, and this provides the formation of the IRE1 dimerization thereby activating UPR signaling (Amin-Wetzel et al. 2017).

The last but not least model is the allosteric model which implies an interaction between the nucleotide-binding domain (NBD) of BiP and LD of IRE1 (Hartl et al. 2018). As seen in the Figure 8, misfolded proteins attach to the canonical SBD of BiP causing BiP NBD to dissociate from IRE1 LD through a structural alteration to initiate UPR signaling.

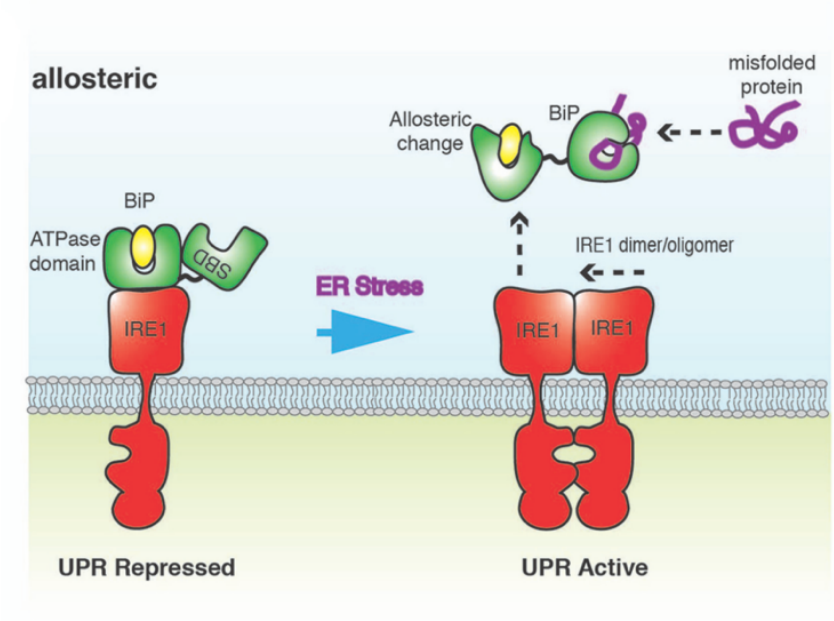

Figure 8. The allosteric activation model of IRE1 is depicted (Adams, C. J. et al (2019).

Since distinct domains of BiP are occupied by misfolded proteins and IRE1 LD, this process does not need to be competitive (Carrara et al. n.d.; Hartl et al. n.d.). In this scenario, BiP operates as a direct sensor of the ER stress. IRE1 has two isoforms: IRE1α and IRE1β. Both can splice and activate RIDD; however, IRE1α has more splicing activity while IRE1β has stronger RIDD activation (Imagawa et al. 2008). Once IRE1α is activated, XBP-1s (s stands for spliced) is formed when 26 intronic nucleotides are excised from XBP-1u (unspliced) and that contains 267 amino acids, forming 371 amino acids because of translational frameshift, which comprises a new carboxy-terminal (calfon2002 n.d.). As a result of this processing event, XBP-1s which works as a transcription factor can go to the nucleus and attach to the promoter regions of the genes which have roles in the ER protein translocation, folding, secretion, and misfolded protein destruction (Kaufman 2002).

One of the consequences of this is regulated IRE1-dependent decay which is abbreviated as RIDD is the process in which the numbers of the mRNAs and certain pre-miRNAs are degraded by the endonuclease activity of IRE1α (Huang et al. 2019). In the back of time, it was thought that only select ER-localized mRNAs were degraded (Hoekstra et al. 2006). This mechanism is active even under basal conditions, but in the case of ER stress, it starts augmenting. During this period, both splicing and RIDD can alleviate the unfolded protein burden in the ER, and homeostasis is reoccurred (Read and Schröder 2021). Nevertheless, if the XBP1 splicing and RIDD

are not enough to return the homeostasis to the equilibrium level, contrary to the splicing that is diminished during the stress prolonged, RIDD persists and degrades the mRNAs which encode prosurvival proteins as well (Upton et al. 2012). This eventually results in the death of the cell through apoptosis.

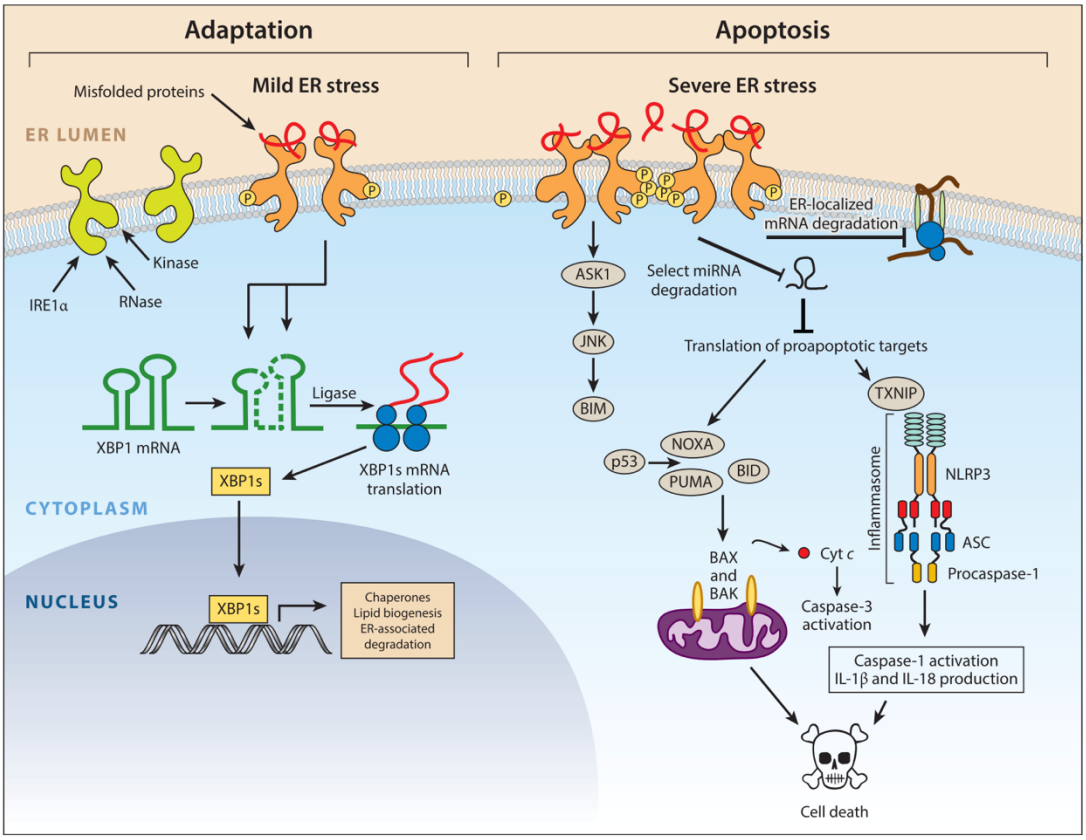

Figure 9. IRE1a signaling pathways is illustrated under mild and severe ER stress (Oakes, S. A., & Papa, F. R. (2015).

In the case of prolonged ER stress, IRE1α interacts with adaptor proteins such as TRAF2 (tumor necrosis factor receptor-associated factor 2), and ASK1 (apoptosis signaling regulating kinase 1) is activated that further triggers the c-Jun NH_2-terminal kinase (JNK) pathway and p38 to boost apoptosis (Bhattarai et al. 2020; Oakes and Papa 2015). The JNK-mediated phosphorylation has been shown to activate pro-apoptotic BIM while inhibiting anti-apoptotic BCL-2. When it is stimulated, BH3-only proteins such as BIM and BID prohibit mitochondrial-protecting proteins such as BCL-2, BCL-XL, and MCL-1. In certain instances, multidomain proapoptotic BAX and BAK proteins are directly stimulated, resulting in the mitochondrial outer membrane permeabilization (MAMP), and thereby mitochondrial toxic proteins such

as Cytochrome c (Cyt c) can be released into the cytoplasm. This drives the activation of downstream effector caspases (e.g. Caspase 3) and cell death (Oakes and Papa 2015). This shows that the apoptotic pathway regulates the cell fate during ER stress.

1.4.3. The ATF6 Pathway

ATF6 (90 kDa) is a type II transmembrane protein and a member of the bZIP transcription family, which is different from both PERK and IRE1α (Haze et al. 1999). It is the third branch that has a prominent function in UPR signaling (Read and Schröder 2021). The regulation mechanism of ATF6 differs significantly from both PERK and IRE1α, and the reason behind this can be explained by it has no sequence similarity with those (Le and Kimata 2021).

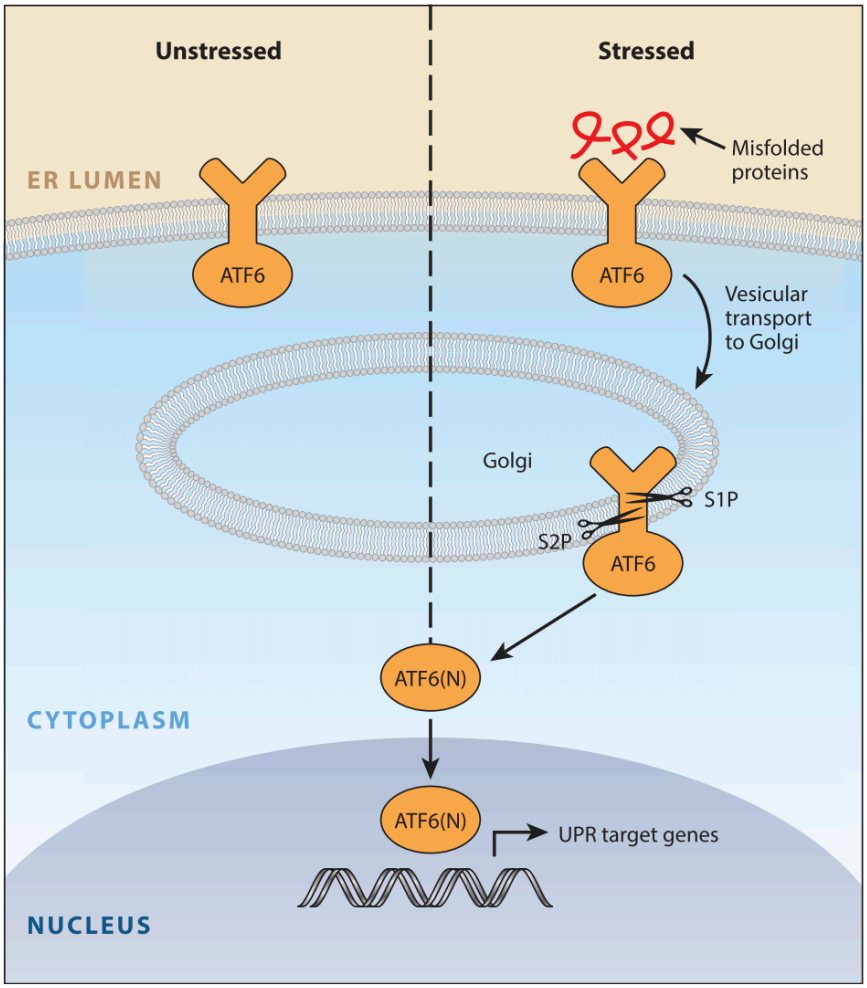

Figure 10. ATF6 signaling is exhibited both under unstressed and stressed conditions (Oakes, S. A., & Papa, F. R. (2015).

Nonetheless, BiP (GRP78) has the same role in the retaining of ATF6 in the ER during unstressed conditions which means it is a negative regulator of ATF6 as in both PERK and IRE1α (Le and Kimata 2021). In the mammalian cells, ATF6 is comprised of both ATF6α and ATF6β which is synthesized as pATF6α/β(P) (Adachi et al. 2008). It has two domains, one is the bZIP domain in the cytosol, and the other is the ER stress-sensing domain in the ER lumen (So 2018). As aforementioned, the sensor is retained in the ER via binding with BiP under normal conditions. When unfolded proteins are aggregated in the ER lumen, BiP leaves the sensor and ATF6 becomes activated. Once activated, it relocates to Golgi where it undergoes cleavage by site-1 (S1P) and site-2 (S2P) proteases, this is different from the other two sensors (J. Ye et al. 2000). During this process, the luminal domain and transmembrane anchor are eliminated by S1P and S2P respectively. This causes the formation of mobilization of a 50 kDa ATF6f which is an amino-terminal cytoplasmic fragment (Hillary and Fitzgerald 2018). After the regulated intramembrane proteolysis (RIP), the free ATF6f which functions as a transcription factor goes into the nucleus and attaches to the ER stress-response element (Read and Schröder 2021). In this way, it triggers the expression of chaperones and UPR mediators including BiP and XBP1 which aid in proteostasis and enhance the output of the IRE1 branch (Hillary and Fitzgerald 2018). Yamamoto *et al.* produced ATF6α- and ATF6β knockout mice, which developed normally, but they figured out that this double-knockout resulted in embryonic lethality (Yamamoto et al. 2007).

1.5. APOPTOSIS

Apoptosis, a form of programmed cell death (PCD), is necessary for normal development and tissue maintenance, ensuring proper cellular turnover. There are several types of cell death pathways based on their morphologic appearance including apoptosis, autophagy, and cytoplasmic cell death which are type I, type II, and type III, respectively (Galluzzi et al. 2018). Damaged or toxic cells are eliminated by PCD to preserve cellular homeostasis. There is increased resistance to PCD during aging, which is related to decreased immune activity, but the rate of malignancy increases with aging (Tower 2015). In its early stages, apoptosis exhibits cell shrinkage, chromatin condensation, nuclear fragmentation, and plasma membrane blebbing as

seen in light microscope examinations. Also, they show a deficiency in inflammatory reactions. Phagocytosis rapidly occurs, and anti-inflammatory cytokines and other cellular contents aren't spread into the neighboring tissues (Hanson et al. 2023). In this process, a group of enzymes known as caspases (cysteine-dependent aspartate-specific peptidases) takes a major role and accomplishes the death. They have significant roles in survival, inflammation, differentiation, and proliferation. Caspases are cysteine proteases that detect a specific four amino acid sequence in protein and cut through aspartate residue (Savitskaya and Onishchenko 2015).

In the human genome, twelve genes express twelve caspases, these are caspase-1 to caspase-10, and caspase-12 and caspase-14. Caspases are synthesized as inactive zymogens and classified into two groups: apoptotic caspases and inflammatory caspases (Savitskaya and Onishchenko 2015). This classification is based on the amino acid sequence. Caspases 1, 4, 5, 11, and 12 are pro-inflammatory which have a role in cytokine maturation in case of inflammation (Li and Yuan 2008). Apoptotic caspases are further subcategorized into initiators which are caspase-8 and caspase-9, and executioners which are caspase-3, caspase-6, and caspase-7 that lead to death (Li and Yuan 2008). The characterization of caspases is dependent on the N-terminal prodomain which contains a proteolysis site that varies in length depending on the types of caspases. A short prodomain that includes 25 amino acids is observed in executioner ones, whereas a longer prodomain that compromises 100-200 amino acids is seen in initiator ones (Savitskaya and Onishchenko 2015). The initiator caspases also have motifs caspase recruitment domains (CARDs) and death effector domains (DEDs) which are also found in molecules such as Fas-associated molecules with death domain (FADD), Apaf-1, and RIP-associated Ich-1/CED homologous protein with death domain (RAIDD), which enhance their accumulation (Slee et al. 2001). Besides, initiators and inflammatory caspases are typically found as monomers in cells and become activated upon dimerization. However, executioner caspases are found in the form of dimers that are activated by intramolecular proteolysis typically performed by an initiator caspase. Consequently, the active form of caspase is composed of two small and two large subunits (Asadi et al. 2022).

The caspases exist in the cytoplasm of the cell, most of which are dormant, procaspases. Under proper conditions, they get activated by autocatalytic cleavage and

cut and activate other caspases by that means resulting in a self-amplifying cascade. Initiator caspases such as caspase-8 and caspase-9 cleave and trigger downstream executioner caspases such as caspase-3, caspase-6, and caspase-7, which then cleave a variety of cellular proteins including cytoskeleton proteins (Tower 2015). Apoptosis can occur through two pathways: intrinsic and extrinsic. The intrinsic pathway is alternatively referred to as the mitochondria-mediated pathway. The proteins in the mitochondria perceive numerous stress signals such as radiation-induced DNA damage, lack of growth factors, and toxins. The extrinsic pathway is called the death receptor pathway (Igney and Krammer 2002). It is stimulated through surveilling NK cells or macrophages which generates death ligands. When death ligands bind to death receptors (DRs) found in the target cell membrane, it results in activation of procaspase 8 to caspase 8 (D'Arcy 2019). Both intrinsic and extrinsic pathways lead to the activation of executioner caspases. These caspases also activate endonucleases, which degrade DNA, and proteases which degrade nuclear and cytoskeletal proteins. In this way, the cell collapses (Slee et al. 2001).

1.5.1. Intrinsic Pathway of Apoptosis

One way of apoptosis is the intrinsic pathway. The mitochondria have a significant role in this process; therefore, it is also termed a mitochondrial pathway. There are pro-apoptotic and anti-apoptotic B cell lymphoma 2 (Bcl-2) family proteins in the cells, and if the balance is disturbed enough, they can drive through the apoptotic pathway (Tower 2015). They are categorized into three classes, one prevents apoptosis which is BCL-2, BCL-XL, MCL-1, BCL-W, and BCL-B; and the other promotes apoptosis which contains BAX, BAK, and BOK. The third class of BH3-only proteins is a bit different since it includes only one of four BH (Bcl-2 homology) motifs that promote apoptosis by binding and regulating anti-apoptotic BCL-2 proteins (Youle and Strasser 2008). BH motifs that are numbered according to the order of discovery contain 10-20 amino acid regions of the highest amino acid sequence resemblance among family members. Most BCL-2 homologs do not have at least one BH motif (Marie Hardwick and Soane 2013). There are some examples for BH3-only; BAD, BIK, BID, BIM, NOXA, and PUMA (Youle and Strasser 2008). BAK and BAX which, are in the pro-apoptotic family, are critical for initiating permeabilization of the

outer membrane of mitochondria (OMM), and subsequent release of apoptotic molecules like Cytochrome c, and DIABLO (SMAC), ultimately leading to caspase activation (D'Arcy 2019). The intrinsic apoptotic pathway is stimulated by cellular stresses such as DNA damage, ER stress, activated oncogenes, hypoxia, oxidative stress, and irradiation (Cavalcante et al. 2019; Tower 2015). This activates BH3-only proteins (e.g. BID, NOXA, PUMA), and they engage in interactions that activate BH3 pro-survival or pro-apoptotic proteins, potentially halting cell death or facilitating its progression (Cavalcante et al. 2019).

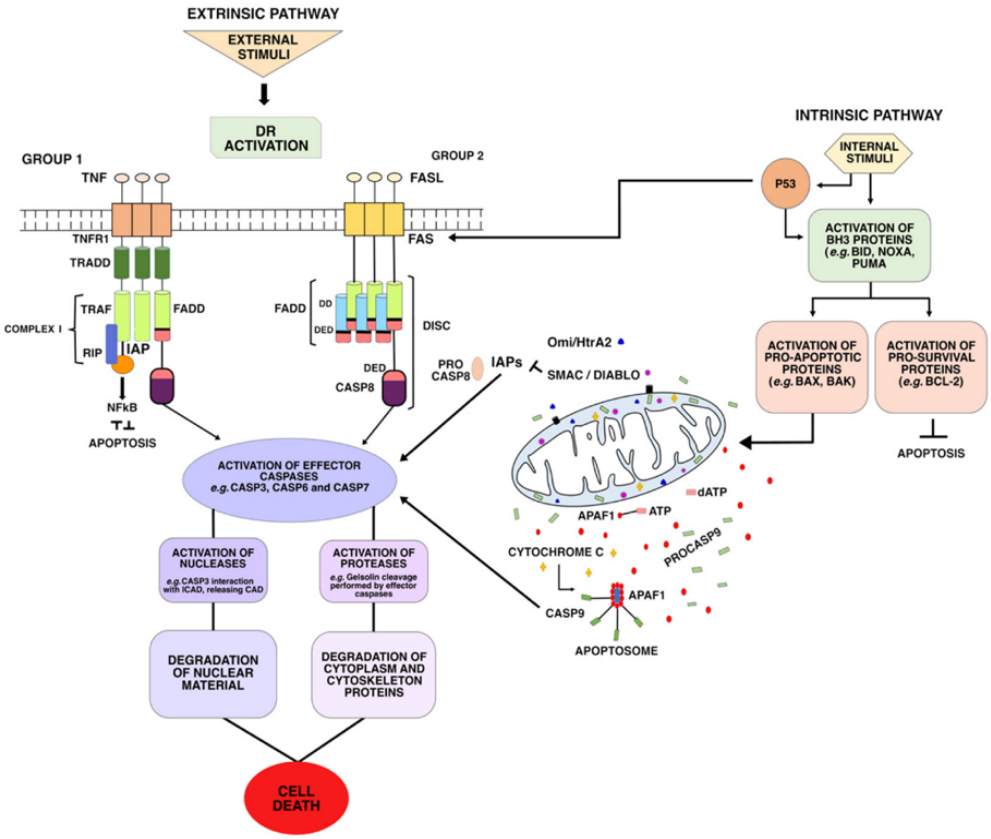

Figure 11. The intrinsic and extrinsic pathways of apoptosis are demonstrated elaborately (Cavalcante, G. C. et al (2019).

In the first case, pro-survival proteins (e.g. BCL-2, BCL-XL, MCL-1) dominate and inhibit apoptosis. In the second case, if the balance between prosurvival and proapoptotic proteins shifts towards the pro-apoptotic ones, BAX and BAK cause mitochondrial outer membrane permeabilization (MOMP), where there is an irreversible point since apoptogenic proteins are released from mitochondrial intermembrane space (IMS) and result in the activation of caspases in the cytoplasm

(Tait and Green 2010). One of the proteins released through MOMP is cytochrome c (Cyt-c) forms a heptameric complex with Apaf-1 called apoptosome which activates procaspase 9 to caspase 9. Besides, pro-apoptotic proteins such as SMAC/DIABLO and Omi/HtrA2 interact with inhibitors of apoptosis proteins (IAP) thereby activating executioners (effectors) caspases such as procaspase 3 and procaspase 7 (Yuan and Akey 2013).

The activation of procaspase 9 is achieved by binding to the caspase recruitment domain (CARD) of Apaf-1, and when it is activated (caspase 9), it should be bound to the apoptosome to retain the catalytical activity. Caspase 9, the initiator one, cleaves and activates executioner caspases such as caspase 3 and caspase 7 via proteolysis, which rearranges vital protein loops in the creation of active sites (Yuan et al. 2011).

This initiates an amplified caspase activation cascade. Further, cellular substrates known as death substrates are cleaved by activated executioner caspases, which end up with changes in characteristic biochemical and morphology. Chromatin condensation and nuclear shrinkage are the results of the cleavage of nuclear LAMINs. The inhibitors of DNase CAD (caspase-activated deoxyribonuclease) and ICAD, DNA fragmentation factor, are cleaved, which results in the liberation of endonuclease that translocates to the nucleus to fragment the DNA. Moreover, cytoskeletal proteins such as actin, plectin, Rho kinase 1 (ROCK1), and gelsolin are chopped up which gives rise to cell fragmentation, blebbing, and the production of apoptotic bodies. At the end of the eat me signals, phagocytes devour the dead cells (Cavalcante et al. 2019; Igney and Krammer 2002).

1.5.2. Extrinsic Pathways of Apoptosis

In the extrinsic pathway, the signaling that comes from external stimuli is conveyed through transmembrane receptors of the tumor necrosis factor (TNF) receptor family as defined by cysteine-rich extracellular domains and cytoplasmic death domains. Therefore, it is also known as a receptor-mediated death pathway. These receptors are called death receptors since they have an internal protein domain incorporating signaling recognized as the death domain (Tower 2015). Well-known members of this family are Fas, TNFR1, DR3, DR4, DR5, and DR6 (Elrod and Sun 2008). Fas and DR5 can be stimulated by other proteins like p53 and MYC.

Natural ligands produced by NK cells or macrophages such as the TNF family bind to the DRs embedded in the target cell membrane. In this way, the extrinsic pathway is stimulated causing the activation of procaspase 8 to caspase 8 (D'Arcy 2019). For the activation of caspase 8, a death ligand such as CD95, TRAIL-R1 (TNF-related apoptosis-inducing ligand-R1) and TRAIL-R2 binds to a DR and recruits monomeric procaspase 8 to a death-inducing signal complex (DISC) placed on the cytoplasmic domain of the ligand-bound DR (death and antideath article). The DISC contains an adaptor protein called FAS-associated death domain (FADD, also known as MORT1) or TNF receptor-associated death domain (TRADD), which helps procaspase 8 to engage with the DISC (Kim et al. 2004). When procaspase 8 monomers are recruited to the DISC, they dimerize and activate. Then, caspase 8 triggers apoptosis through one of two separate sub-pathways. The sub-pathway induced is determined by the type of cells which can be type I or type II. Type I cells have enough active caspase 8 on the DISC to induce apoptosis directly. However, the amount of active caspase 8 is insufficient in type II cells, and mitochondria act as amplifiers of the signal (Tait and Green 2010).

The crosstalk between extrinsic and intrinsic pathways is accomplished via the cleavage of BH3-only protein (e.g. BID) by caspase 8, resulting in the activation of BID and augmenting the signal through mitochondria that leads to more effective apoptosis. P53 positively regulates BID at the transcriptional level (Carneiro and El-Deiry 2020). There are decoy receptors that are highly associated with death receptors (DRs), but they do not have a death domain. The signaling conveying from death receptors can be alleviated thanks to the decoy receptors that attach to death ligands and fight with them for the cell surface. In this way, they inhibit the activation of proapoptotic DRs. For instance, DcR3, FasL decoy receptor, is overexpressed in primary lung, colon, and BC, while two TRAIL receptor decoys (DcR1 and DcR2) are highly expressed in non-malignant cells, potentially limiting TRAIL toxicity (LeBlanc and Ashkenazi 2003). In this study, our objective was to assess the possible therapeutic impact of ER stress and apoptotic pathways triggered by the combination of EBR and TAM in both MCF-7 and MDA-MB-231 cell lines.

2. MATERIALS AND METHODS

2.1. CELL LINES

MCF-7 is a human BC cell line obtained from adenocarcinoma, which has estrogen receptor, PR, and HER2, and MDA-MB-231 is a TNBC cell line obtained from metastatic adenocarcinoma which means that it doesn't have estrogen receptor, PR, and HER2. Unlike MCF-7, It is hormone hormone-independent and a more aggressive form of BC. These two cell lines were purchased from the American Type Culture Collection (ATCC) (https://www.atcc.org/).

2.2. CELL CULTURE

MCF-7 and MDA-MB-231 BC cell lines were grown in T25 flasks (NEST) that contain the complete medium which is composed of Gibco Dulbecco's Modified Eagle Medium (DMEM), 10% Fetal Bovine Serum (Gibco) and 1% Penicillin streptomycin (Gibco) additive antibiotics and incubated at incubator at 37°C and 5% CO_2.

2.2.1. Passage

MCF-7 and MDA-MB-231 cell lines were passaged when they were reached to 80% confluency. Firstly, the medium in the T25 flasks was discarded. Then, the cells were washed off with 1 mL 1X Phosphate Buffered Saline (PBS) (EcoTech) at least twice. After the washing step, 1 mL 0.25% Trypsin-EDTA (1X) (Gibco) was added to each flask, and they were incubated for 2-3 minutes at incubator 37°C and 5% CO_2. When incubation time was over, they were checked to be sure of their detachment from the surface under the light microscope (Nikon, Eclipse TS100). Mechanical disaggregation was applied to each flask if the detachment was not achieved completely. After the detachment was accomplished, the enzymatic activity of trypsin

was terminated by adding the same amount of complete DMEM (1:1 ratio). Later, the detached cells were collected within a 15 mL conical tube and centrifuged at 2500 rpm for 5 min (Eppendorf, Centrifuge 5424 R). Following centrifugation, the supernatant was discarded, the pellet formed was resuspended with a complete medium, and the amount of DMEM was changed depending on the pellet formed. Upon resuspension, 10 µL cell suspension was put on the improved Neubauer hemocytometer, and the cells were counted under the light microscope. According to the experiment conducted, the cells were seeded to both the main stock (T25) and the plates/petri.

2.2.2 Freezing and Thawing Cells

MCF-7 and MDA-MB-231 cells were frozen to maintain the cell stocks at -80°C. The cells were frozen at the density $4x10^5$ within a freezing medium composed of 90% FBS and 10% Dimethyl sulfoxide (DMSO) (Riedel-De-Haën) in a 1.5 mL cryovial tube (Biosigma, SentezLab), and they were kept at -80°C (Haier). Which type of cells, at which passage number, and when and by whom were frozen should be written on the cryovial.

When we need new cells because of too high passage numbers and/or unexpected situations like contamination or insufficient growth, we use the cells from our stocks. At that time, the thawing process was performed. The cells were taken from -80°C and thawed a little bit so as not to get heat shocked. After that, 1 mL complete medium was added to the cells and pipetted to defrost completely. Later, they were transferred to the 15 mL conical tube and centrifuged at 2500 rpm for 5 min to remove the freezing medium. Upon centrifugation, the pellet formed was resuspended with a complete medium whose amount was changed based on the pellet. At this point, cells were ready to seed into T25 flasks.

2.2. CELL VIABILITY ASSAY

$1x10^4$ cells were seeded in each well of 96 wells. After 24 hours, they were treated with the drugs which are (E/Z) 4-hydroxy Tamoxifen (TAM) (Sigma-Aldrich), Epibrassinolide (EBR) (Apollo Scientific), Tunicamycin (ER stress inducer) (CAYMAN CHEMICAL), and Tauroursodeoxycholate (TUDCA, ER stress inhibitor)

(SIGMA) according to the required volume. After 24 hours of incubation, 10 µL MTT (3-(4,5-Dimethylthiazol-2-yl)-2,5-Diphenyltetrazolium Bromide) reagent (Bio Basic) was given to each well and incubated for 4 to 6 hours in the incubator at 37°C and 5%CO_2. Following incubation, 100 µL dimethyl sulfoxide (DMSO) (Riedel-De-Haën) was given to each well to solubilize the formed insoluble formazan crystals and incubated at dark for 5 minutes. Lastly, the density of the formazan was read at 570 nm with the help of a spectrophotometer (Thermo Scientific, Multiskan FC 357).

2.3. TRYPAN BLUE DYE EXCLUSION ASSAY

$3x10^4$ cells were seeded in each well of 6 wells. Following 24 hours, the TAM and EBR drugs were given to the cells and incubated for 24 hours in the incubator. After incubation, cells were washed with 1X PBS (EcoTech) and centrifuged at 13200 rpm for 1 min. Then, they were trypsinized and detached from the surface by trypsin (Gibco), and enzymatic activity was halted by a complete medium (1:1 ratio). Again, the cells were centrifuged at 13200 rpm for 1 min. After that, the cells were harvested. According to the pellet obtained, they were resuspended with a 1:1 ratio of complete DMEM and 0.4% Trypan blue stain (EcoTech). Then, 10 µL cell suspension was put on the improved Neubauer hemocytometer, and the cells were counted for each condition under the inverted light microscope (Hermle, Centrifuge Z 206 A). The result was repeated at least twice.

2.4. COLONY FORMATION ASSAY

The cells were seeded at the density of $2x10^4$ cells in each well of 6 wells. After 24 hours, they were treated with the TAM and EBR drugs and incubated in the incubator for 24 hours. Then, the medium was discarded, and the cells were washed with 1X PBS once. Upon, a fresh complete medium was given to each well, and cells were left for 10-12 days to grow and be colonized. Additionally, the medium was changed once every 2-3 days. When the control condition became confluent, the experiment was halted. Each well was rinsed with 1 mL 1X PBS twice. Then, the cells were fixed with a 3:1 ratio of 1 mL methanol: acetic acid for 45 min RT on the shaker. After fixation,

they were stained with 500 µL 0.5% crystal violet (Merck) for 2 hours RT on the shaker. When the staining process was completed, the stain was removed and each well was washed off with ddH_2O, and they were left to dry off. The image of each well was taken. Lastly, Image J was used for the analysis of the number of colonies, and the graph of the number of colonies was plotted.

2.5. HANGING DROPS

The cells were sub-cultured. Before seeding, both BC cells and drugs (TAM and EBR) were prepared based on the calculation in 1.5 mL Eppendorf tubes. They were seeded at the density of $2x10^4$ cells in each drop on the cover of 60 mm petri dishes (NEST). To retain the environment as moisture, 2 mL 1X PBS was put in the Petri dishes. After seeding was done, the cover was flipped back carefully. In this way, the drops were hung. This experiment was conducted as time-dependent. Therefore, they were looked at under the inverted light microscope (Nikon, H600L) at 24, 48, and 72 hours. In the end, Image J was used for the analysis of the diameters of the spheres.

2.6. FLUORESCENCE STAININGS

2.6.1. 4'6-diamidino-2-phenylindole (DAPI)

$2x10^5$ cells were seeded in 6 well plates (NEST). After the cells gained their morphology, they were exposed to the drugs which are TAM, EBR, and their combination for 24 hours. Then, the medium containing the drugs was discarded. Later, the stain 5mg/mL DAPI (Thermo) was given to the cells with the complete medium at the ratio of 1:1000 (µL). They were incubated in the incubator at 37°C and 5% CO_2 for 20 minutes. Following incubation, the medium containing the stain was removed, and 1 mL of 1X PBS was added to each well. The cells were investigated under the fluorescence microscope (Carl Zeiss Microscopy, Axio Observer 5 Colibri7) (ex/em: 358/461nm).

2.6.2. 3,3'-Dihexyloxacarbocyanine Iodide (DiOC6)

The cells were seeded at the density of $2x10^5$ in 6 well plates. Then, they were treated for 24 hours with the drugs which were TAM, EBR, and their combination. When treatment time was over, the medium containing the drugs was removed. After that, the cells were stained with 4 nM DiOC6 (Thermo) which was given in the complete medium (1:1000 ratio) for 20 minutes in an incubator at 37°C and 5% CO_2. Upon staining, the medium containing the stain was discarded, and 1 mL 1X PBS was given to the cells, they were observed with the help of a fluorescence microscope (Carl Zeiss Microscopy, Axio Observer 5 Colibri7) (ex/em: 482/504 nm).

2.6.3. Propidium Iodide

$2x10^5$ cells were seeded in 6 well plates. Later, they were exposed to the TAM, EBR, and combinations of them for 24 hours. After incubation, the medium including the drugs was discarded. Afterward, cells were dyed via 5 mg/mL propidium iodide (PI) (Sigma-Aldrich, Saint Louis, UK) stain which was given in the complete medium at a 1:1000 ratio. They were incubated in an incubator at 37°C and 5% CO_2. Subsequently, the medium and stain mixture were eliminated, and 1mL of 1X PBS was added per well. They were examined under the favor of a fluorescence microscope at ex/em: 535/615 wavelength (Carl Zeiss Microscopy, Axio Observer 5 Colibri7).

2.7. FLUORESCENCE ACTIVATING CELL SORTING

$2x10^5$ cells were seeded for each condition. After 24 hours, they were exposed to the drugs mentioned for 24 hours. After the drug treatment time was out, the medium of each condition was collected in 1.5 mL Eppendorf tubes, and they were centrifuged at 13200 rpm for 1 minute. Then, the cells were washed off with 1 mL 1X PBS, and they were centrifuged at 13200 rpm for 1 minute. After that, 500 µL trypsin-EDTA (Gibco) was given to each well and incubated in the incubator for 2-3 minutes at 37°C and 5%CO_2. Following, they were checked to confirm their detachment under the light microscope, and the enzymatic activity was stopped with the same amount of complete medium. Again, they were centrifuged at 13200 rpm for 1 minute. At the end of the centrifuge, the pellet formed at the bottom of the tube contained whole cells. These

pellets were resuspended and fixed with 1 mL of 70% ethanol (ISOLAB) dropwise manner with some agitation. They were stored at +4°C (Flavel) for 4-6 months. When these samples were read at BD Accuri C6 flow cytometer device, firstly, they were centrifuged at 13200 rpm for 1 min to remove ethanol (TEKKİM). Then, 1 mL 1X PBS was added to each tube and centrifuged at 13200 rpm for 1 min. Lastly, the pellet was resuspended with 300 µL 1X PBS, and 3µL PI and 1µL RNase A (EcoTech, EcoZyme) were added to each tube. They were incubated on the ice for 15 minutes, and they were read at BD Accuri C6 flow cytometer device.

2.8. PROTEIN ISOLATION

The cells were seeded at the density of $4x10^5$ cells in 60 mm petri dishes (NEST). After they had gained morphology and become 80% confluent, they were treated with the selected doses of TAM and EBR. Following 24 hours, the medium of each condition was collected and centrifuged at 13200 rpm for 1 min (except for control). Then, the supernatant was discarded. Meanwhile, 1mL 1X ice-cold PBS was added to each Petri, and scrapped by the back of a pipette tip. Again, they were centrifuged at 13200 rpm for 1 min, and the step was repeated twice. According to the amount of the pellet formed, Mammalian Protein Extraction Reagent (MPER) (+) (Thermo) was added to each and resuspended the pellet and incubated for 20 min at RT on the shaker (DLAB, SKO180S). After, they were centrifuged at 13200 rpm for 15 min at +4°C (Eppendorf, Centrifuge 5418 R). Subsequently, total proteins were collected in supernatant, and they were kept as stock at -20°C (Flavel).

2.9. BRADFORD ASSAY

1X Bovine Serum Albumin (BSA) (Sigma-Aldrich) standard proteins were added into 96-well plates (NEST) at an increased volume (0, 2, 4, 6, and 8 µL) per well, and 1 µL protein sample was put into the wells, two repeats were done for each condition. 100 µL Bradford reagent (Sigma-Aldrich) was given to per well, and they were incubated at dark for 15 minutes in RT. Following incubation, the absorbance of the protein samples was analyzed at 595 nm by a spectrophotometer (Thermo Scientific,

Multiskan FC 357). By using absorbance values obtained from the Bradford assay, the absorbance versus concentration of the BSA standard proteins graph was plotted via Excel. By using this graph, the amounts of each protein sample were calculated.

2.10. WESTERN BLOTTING

Protein samples as 25 µg were prepared according to calculations obtained from the Bradford assay. 12% Tris-glycine gels were poured and polymerized. Then, before loading into wells, samples were heated at 95°C for 5 min and loaded per well for each condition. During the running process, the voltage was increased from 50 to 70 and 90 respectively. After the running was completed, the transfer of proteins from gel to a 0.45 µm polyvinyl-fluoride (PVDF) membrane (MERCK), which was activated by methanol (Sigma-Aldrich) in 1 min, in ddH_2O 5 min, and transfer buffer in 10 min, was achieved by using a semi-dry Trans-blot (Analytik Jena, Biometra Fastblot) device. For the transfer of proteins whose molecular weight was lower than 100 kDa, the transfer was done for 15 minutes at 200 mA. For the proteins higher than 100 kDa, the transfer was taken for 20 minutes at a constant current (200mA). After transfer, the membrane was incubated with 5% skim milk (Bioshop) dissolved with 1X TBS-T for 1 hour at RT on a shaker (DLAB, SKO180S). In addition, to confirm the running was completed properly, the gel was stained with Coomassie G-250 blue (B2025-1EA, MERCK) for 1 hour at RT. Right after, destaining was done to remove the excessive stain with destaining buffer and clear the background.

When the blocking step was completed, the membrane was put into a 50 mL falcon tube which contained the primary antibody (Calreticulin (1:1000) (CST), Calnexin (1:1000) (CST), PDI (1:500) (CST), BiP (1:1000) (Invitrogen), PERK (1:1000) (ABclonal), IRE1α (1:1000) (ABclonal), ATF6 (1:100) (Invitrogen), CHOP (1:1000) (CST), PARP (1:1000) (StJohn's Laboratory), Caspase 9 (1:250) (CST), Caspase 3 (1:1000) (CST), P-glycoprotein (1:1000) (ABclonal), MDR1 (1:250) (CST), MRP1 (1:250) (Invitrogen), β-actin (1:1000) (Boster) and GAPDH (1:1000) (Boster) in 3mL TBS-T and incubated at 4°C on a roller (DLAB, MX-T6-S) for overnight. After incubation, the membrane was washed off with 1X TBS-T buffer for 5 minutes three times. Then, it was put into another 50 mL falcon tube which contained the secondary

antibodies that are anti-rabbit (1:1000) (CST) or anti-mouse (1:1000) (Boster) in 3 mL TBS-T and incubated at 4°C on a roller overnight. Upon incubation, the membrane was rinsed with TBS-T buffer three times and 1X TBS once for 5 minutes in each. Next, the last step which is the visualization of bands was performed. For this purpose, solution A and solution B were prepared in 15 mL falcon tubes. Then, they were mixed in a container, and the membrane was sunk in this mixture and incubated for 1 minute at dark. Following incubation, the membrane was placed in the chemiDoc device (Azure, C300 Biosystems) and was visualized for 10 sec, 30 sec, 1 min, and 2 min 30 sec respectively.

2.11. STATISTICAL ANALYSIS

GraphPad Prism 9 software (https://www.graphpad.com) was used to analyze all the experiments statistically. Two-way ANOVA was used. Standard deviation values were utilized to create error bars in the graphs, and if p is lower than 0.5, it was considered statistically significant. ImageJ analysis was done for western blot. The experiments were conducted on a minimum of three occasions.

3. RESULTS

3.1. EPIBRASSINOLIDE AND TAMOXIFEN COMBINATION SIGNIFICANTLY REDUCED THE CELL VIABILITY OF MCF-7 AND MDA-MB-231 BREAST CANCER CELLS

To investigate the potential therapeutic effect of combining TAM with EBR, firstly MTT cell viability assay was performed to ascertain the cytotoxicity of TAM alone and in combination with EBR, and which dose should be used in both MCF-7 and MDA-MB-231 BC cell lines. As seen in the Figure 12, only 30 µM EBR was used since the dose is already known from previous studies (Coskun et al. 2015). For the selection of appropriate dose of TAM; 5, 10, and 20 µM concentrations were treated to the cells both alone and in combination with 30 µM EBR for 24 hours. 30 µM EBR and 20 µM TAM alone treatments decreased the cell viability of MCF-7 cells significantly, however; when cells were treated with the combination of 30 µM EBR and 20 µM TAM, the cell viability was drastically diminished by under 50%. When we compare the TAM and EBR alone conditions with the combined version, this is a highly statistically significant result; therefore, 20 µM TAM and 30 µM EBR were suitable doses for MCF-7.

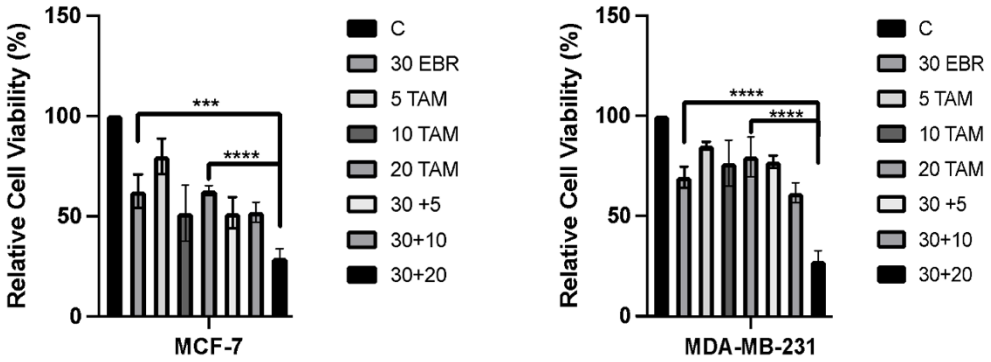

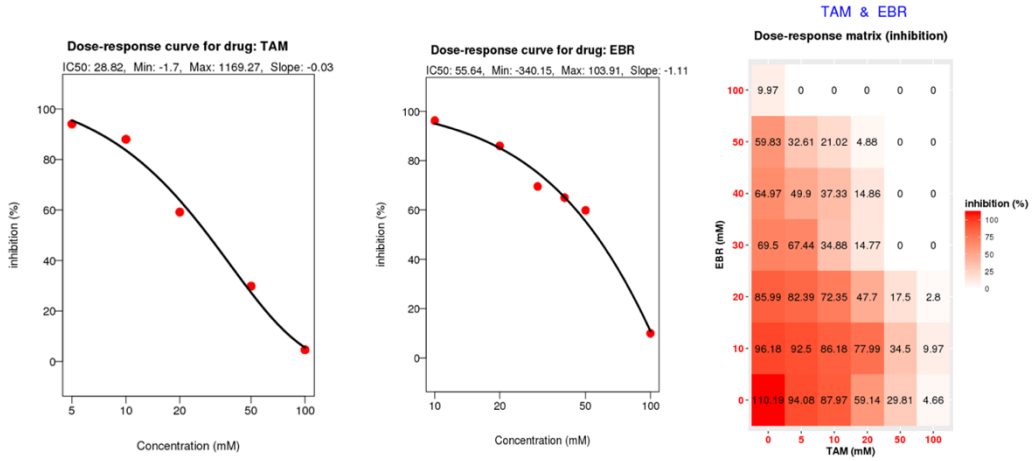

Figure 12. The combination of epibrassinolide and tamoxifen dramatically reduced the cell viability of MCF-7 and MDA-MB-231 Breast Cancer cells after 24 hours.
The results of cell viability assay of **A.** MCF-7 and **B.** MDA-MB-231 exposed to different doses of EBR and TAM for 24 h were demonstrated. The significant difference between only 30 µM EBR and the combination with 20 µM TAM, and only 20 µM TAM and the combination with 30 µM EBR were obtained. Synergistic effect was observed between 30 µM EBR and 20 µM TAM. Columns display the Mean ± St. Dev of eight replicates of three distinct culture conditions (***p<0.001, ****p<0.0001).

30 µM EBR alone decreased the cell viability when we compared to the control samples in MDA-MB-231 cell line. The response to 20 µM TAM was not the same as within the MCF-7 but to the combination of 20 µM TAM and 30 µM EBR, the response was nearly the same, and a statistically significant result was observed in MDA-MB-231. The curve was graphed by synergistic finder (WEB3), and according to the curve synergistic effect was obtained between 30 µM EBR and 20 µM TAM. Therefore, 30 µM EBR and 20 µM TAM were chosen for the upcoming experiments.

3.2. COMBINED TREATMENT OF EPIBRASSINOLIDE AND TAMOXIFEN DECREASED THE SURVIVAL OF MCF-7 AND MDA-MB-231 CELLS IN A TIME-DEPENDENT MANNER

After the MTT assay, the trypan blue dye exclusion assay (survival assay) was performed to determine the dose- and time-dependent effect of EBR to overcome TAM resistance in both MCF-7 and MDA-MB-231. Therefore, the doses selected from the result of the MTT assay that are 30 µM EBR and 20 µM TAM were administered to MCF-10A which is a breast epithelial cell line, MCF-7, and MDA-MB-231 cell lines

for 24, 48, and 72 hours. The graph in Figure 13 was plotted by using the numbers of live cells via GraphPad. In all cell lines, the control, 30 µM EBR, 20 µM TAM, and the combination of two drugs were designated by green, purple, blue, and red lines respectively.

The cell survival shown was further diminished by the combination treatment of TAM with EBR down after 24 hours in MCF-7 and MDA-MB-231 cell lines when we compare it with the control and other two drugs alone. There was no change after being exposed to drugs alone and in combination after 24 hours in MCF-10A cell line. Following 24 hours, the cell survival was increased in both MCF-7 and MDA-MB-231, however; the cell survival decreased slightly after 48 hours in MCF-10A. Therefore, the effective time for this combination was chosen as 24 hours.

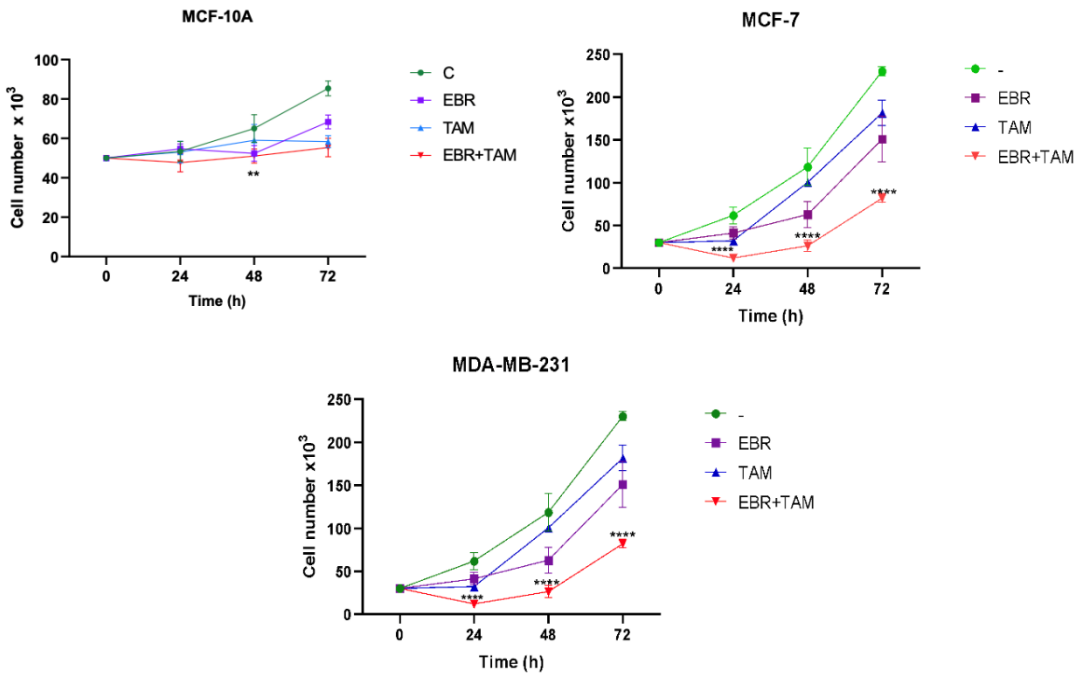

Figure 13. 30 µM EBR and 20 µM TAM combination has no effect in MCF-10A, but reduced cell survival in both MCF-7 and MDA-MB-231. A-C.
This figure shows the results of the trypan blue dye exclusion assay of MCF-10A, MCF-7, and MDA-MB-231 cells. When all three cell lines were exposed to the EBR and TAM alone and in combinations for 24, 48, and 72 h, no change was obtained in MCF-10A. However, the cell survival was further diminished after 24 h in both MCF-7 and MDA-MB-231 after being exposed to 30 µM EBR in combination with 20 µM TAM. After 24 h the cell survival was increased in all conditions (** $p<0.01$, **** $p<0.0001$).

3.3. THE COLONY FORMATION POTENTIAL OF BOTH MCF-7 AND MDA-MB-231 CELL LINES WAS DRASTICALLY REDUCED BY THE INCREASING DOSES AND COMBINATIONS OF BOTH TAMOXIFEN AND EPIBRASSINOLIDE

To observe how the colony formation potential was changed after the cells were exposed to the drugs alone and in combination, we carried out a colony formation assay. In this experiment, we used 6 conditions which are control untreated, 30 µM EBR, 10 µM TAM, 20 µM TAM, and their combinations with EBR. The graph was plotted via GraphPad as seen in Figure 14. The number of colonies was reduced following 30 µM EBR in both cell lines significantly when compared to control. When we compare the number of colonies exposed to 10 µM TAM with the combination of 30 µM EBR, and 30 µM EBR alone, the reduction is statistically significant in the MCF-7 cell line but not in MDA-MB-231. However, when we look at the 30 µM EBR alone and the combination with 20 µM TAM, we can see that the number of colonies was greatly diminished in both cell lines. Moreover, we can see the difference between 20 µM TAM alone and the combination with 30 µM EBR, and we have obtained extremely meaningful results in MDA-MB-231 cell line.

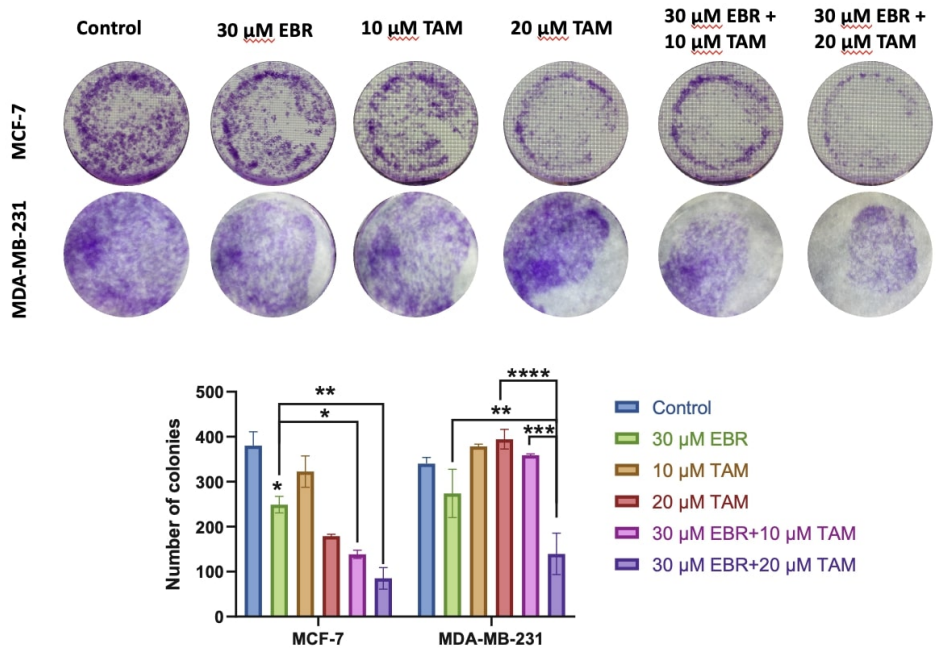

Figure 14. The colony-forming capability of both MCF-7 and MDA-MB-231 cell lines was significantly decreased when TAM and EBR dosages and combinations increased.

The figure shows the results of the colony formation assay in **A**, and **B.** The graph was plotted to display how the number of colonies is altered. The significant results were obtained between only EBR and the combination with 10 µM TAM and 20 µM TAM in both cell lines. In addition, we can see a significant decrease between 20 µM TAM and the combination with 30 µM EBR in MDA-MB-231 cells. (*p<0.05, **p<0.01, ***p<0.001, ****p<0.0001)

3.4. THE COLONY FORMATION POTENCY AND DIAMETERS OF MCF-7 AND MDA-MB-231 CELL LINES WERE DECLINED BY TREATMENT WITH BOTH TAMOXIFEN AND EPIBRASSINOLIDE

The hanging drop was another experiment to determine the changes in colony formation potency in the 3D aspect in both MCF-7 and MDA-MB-231 cell lines. This experiment was also performed in a time-dependent manner, and the same doses in the survival assay were used. The diameters of the sphere were measured with the help of ImageJ, and the graphs were plotted by using GraphPad. When we look at the 20 µM TAM with the combination of 30 µM EBR, we can see some cavities were formed after 24 hours in both MCF-7 and MDA-MB-231, and the diameters of the sphere were remarkably reduced (Figure 15). Especially when it was compared with the control and the drugs alone, the formation of cavities was significantly augmented. After 24 hours, the number of cells was enhanced in all conditions and both cell lines. Thus, we can conclude that all results were consistent about the effect of EBR and TAM combination in BC cell lines.

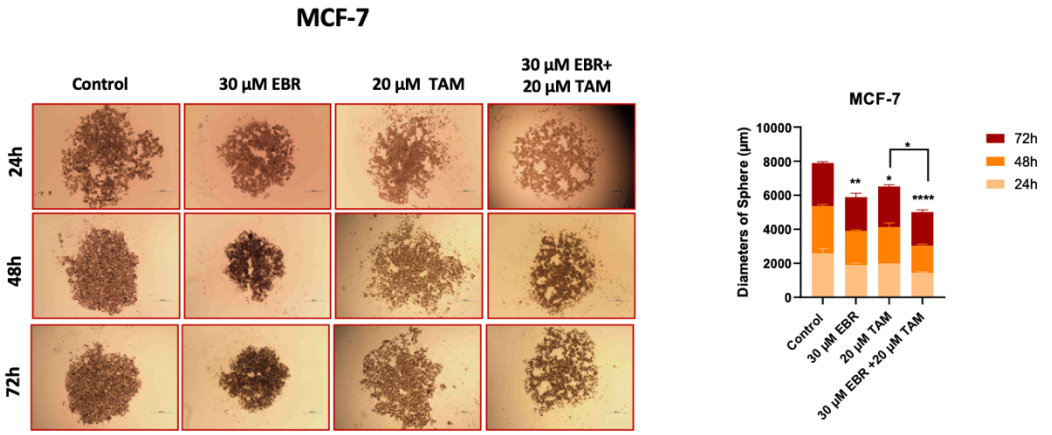

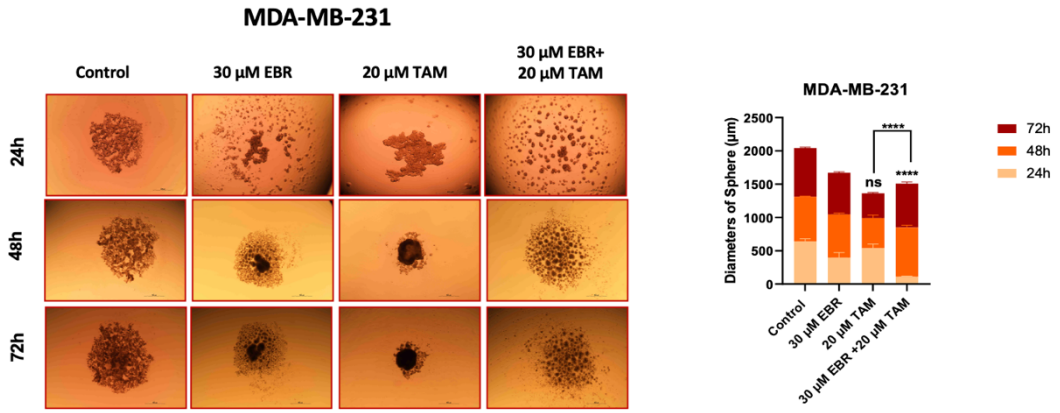

Figure 15. The combined treatment of tamoxifen and epibrassinolide reduced the colony formation potency and diameters of MCF-7 and MDA-MB-231 cell lines.
A. The result of hanging drop which designates 3D colony formation potency change in a time-dependent manner was seen in this figure. **B.** The graph was plotted by measuring three spots in each sphere in Image J. Observing the combination of 20 µM TAM with 30 µM EBR, cavities were observed after 24 h in both MCF-7 and MDA-MB-231, leading to a significant reduction in sphere diameters. After 24 h, the number of the cells augmented. (*p<0.05, **p<0.01, ****p<0.0001)

3.5. THE CELL VIABILITY WAS SIGNIFICANTLY DIMINISHED BY THE COMBINED TREATMENT OF EPIBRASSINOLIDE AND TAMOXIFEN IN BOTH CELL LINES

First, we performed fluorescence staining with PI which targets the dead cells and can be seen as red dots. As seen in Figure 16, light microscope (LM) and fluorescence microscope (PI) images are shown for both cell lines. When we look at the LM images, the number of live cells decreased, whereas the number of PI-positive cells increased following the combination of EBR and TAM in both MCF-7 and MDA-MB-231. The number of PI-positive cells significantly increased after 30 µM EBR and 20 µM TAM combination in both cell lines as seen in the graph that was plotted by GraphPad.

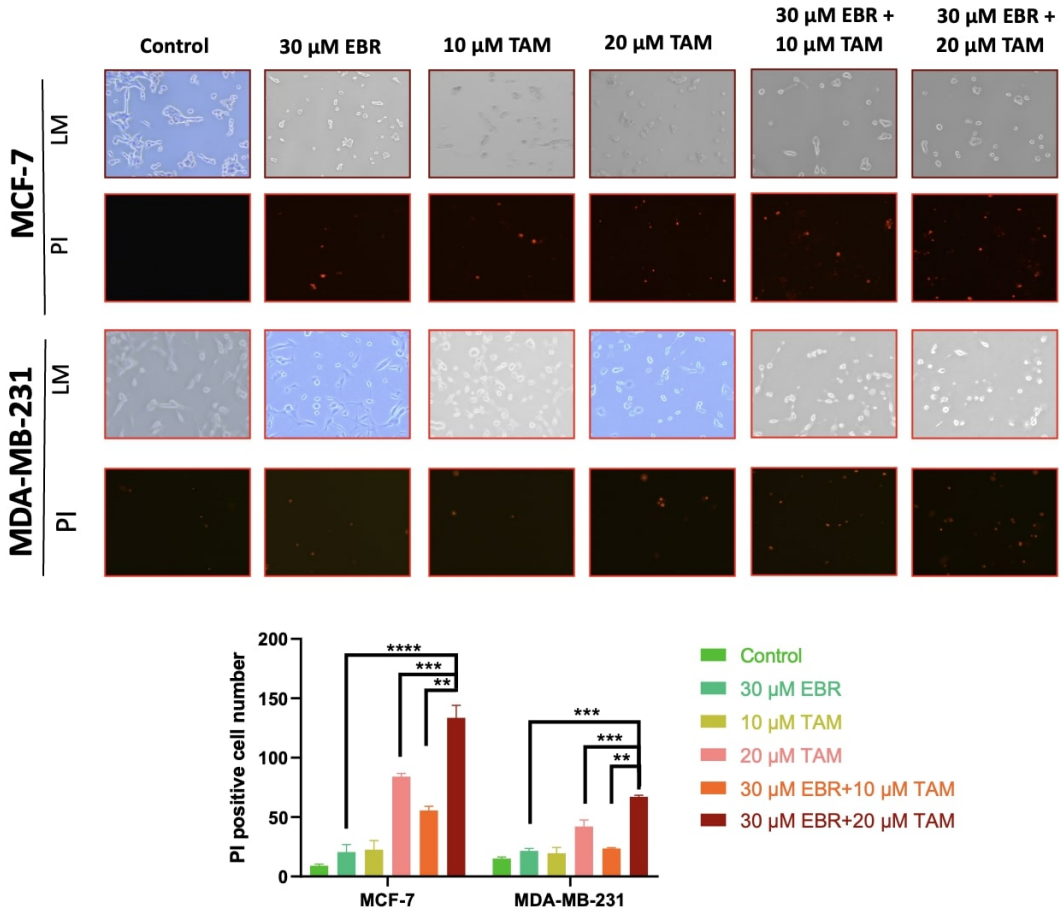

Figure 16. The combined treatment of 30 µM EBR and 20 µM TAM dramatically reduced the cell viability in both MCF-7 and MDA-MB-231 cell lines.
EBR and TAM treatment increased cell death rate in both MCF-7 and MDA-MB-231 cells which was determined by PI staining under fluorescence microscope (ex/em: 535/615 nm). As seen in both Figures A and B, the numbers of PI-positive cells were greatly increased by the combination treatment of 20 µM TAM and 30 µM EBR. (**p<0.01, ***p<0.001, ****p<0.0001)

3.6. COMBINED TREATMENT OF EPIBRASSINOLIDE AND TAMOXIFEN INCREASED THE FORMATION OF THE FRAGMENTED DNA AND DECREASED THE MITOCHONDRIAL MEMBRANE POTENTIAL

DAPI and DiOC6 were the other two fluorescence dyes that were used to stain fragmented DNA and mitochondria of live cells, respectively. We have carried out the fluorescence staining to see the effects of the drugs alone and in the combined version. The obtained results are shown in Figure 17. DiOC6 positive cells designate live cells with healthy mitochondria, stained as green, and DAPI positive cells which indicate dead cells are shown in bright blue dots. When we compare each condition with the control, the number of live cells was significantly diminished, which means the

mitochondrial membrane potential declined in both MCF-7 and MDA-MB-231 cell lines. This reduction is seen when comparing the 20 µM TAM alone and with 30 µM EBR. When we look at the DAPI results, we can see that the number of fragmented DNA was greatly enhanced as the doses increased, and the highest fragmented DNA numbers were obtained in the condition of 30 µM EBR and 20 µM TAM in both cell lines.

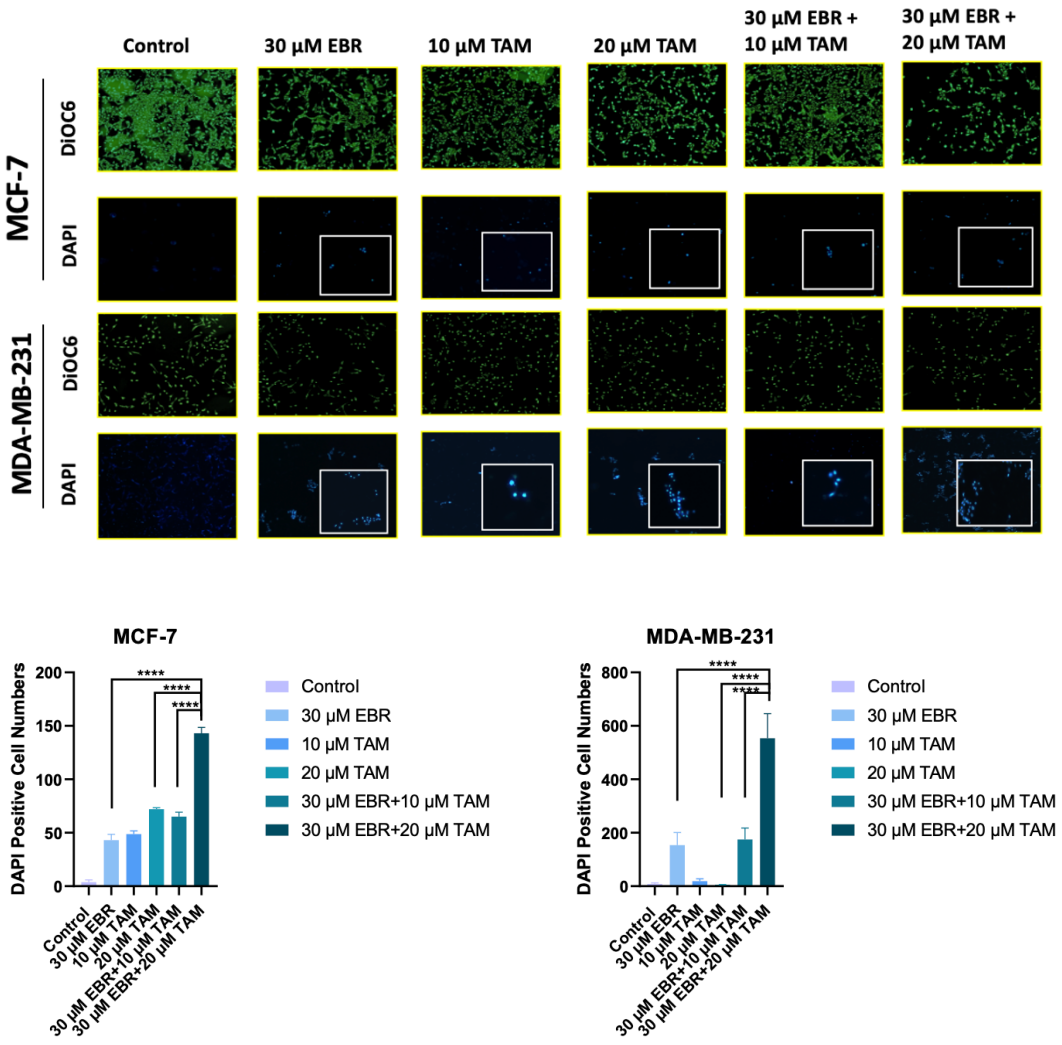

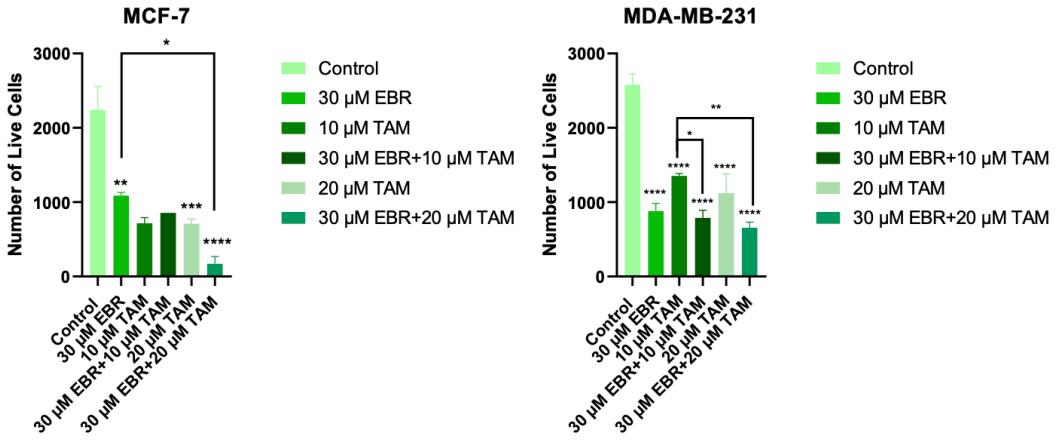

Figure 17. The combined treatment of 30 μM EBR and 20 μM TAM promoted fragmentation of DNA while decreasing mitochondrial membrane potential.
The figure displays the results of DAPI and DiOC6 fluorescent dyes of MCF-7 and MDA-MB-231. The graphs shown in B. and C. were drawn by GraphPad;however, firstly counting was done by Image J. DAPI-positive cell numbers shown in blue dots were enhanced as the doses increased and when comparing the combination of EBR and TAM with the drugs alone. Also, in B, the highest dead cell numbers were obtained in 30 μM EBR combination with 20 μM TAM in both cell lines. However, in the case of DiOC6, the opposite result means that the lowest number of live cells were obtained after being exposed to EBR and TAM combination for 24 h. (*p<0.05, **p<0.01, ***p<0.001, ****p<0.0001)

3.7. EPIBRASSINOLIDE TREATMENT IN COMBINATION WITH TAMOXIFEN INCREASED THE APOPTOTIC SUBG1 CELL POPULATION PERCENTAGE IN BOTH CELL LINES

Flow cytometer analysis was performed to detect how the subG1 ratio, which indicates the apoptotic dead cells, is changed, and the cell cycle is arrested. The results of this experiment are shown below. According to the data obtained, the graph demonstrated in Figure 18 was plotted through GraphPad. The stars depict the significance in the subG1 phase. When we look at the subG1 ratio of EBR, the increase in MCF-7 was three times higher than MDA-MB-231. When we compare 20 μM TAM alone and the combination with EBR, the subG1 phase was increased by half in MCF-7, however; the increase was doubled in MDA-MB-231. Besides, when we look at 20 μM TAM with EBR, the increase in the subG1 phase was three times higher than the combination of 10 μM TAM with EBR in MCF-7 cell line. Moreover, the subG1 ratio of 10 μM TAM with EBR was compared to 20 μM TAM with EBR, the increase was more than two times in MDA-MB-231.

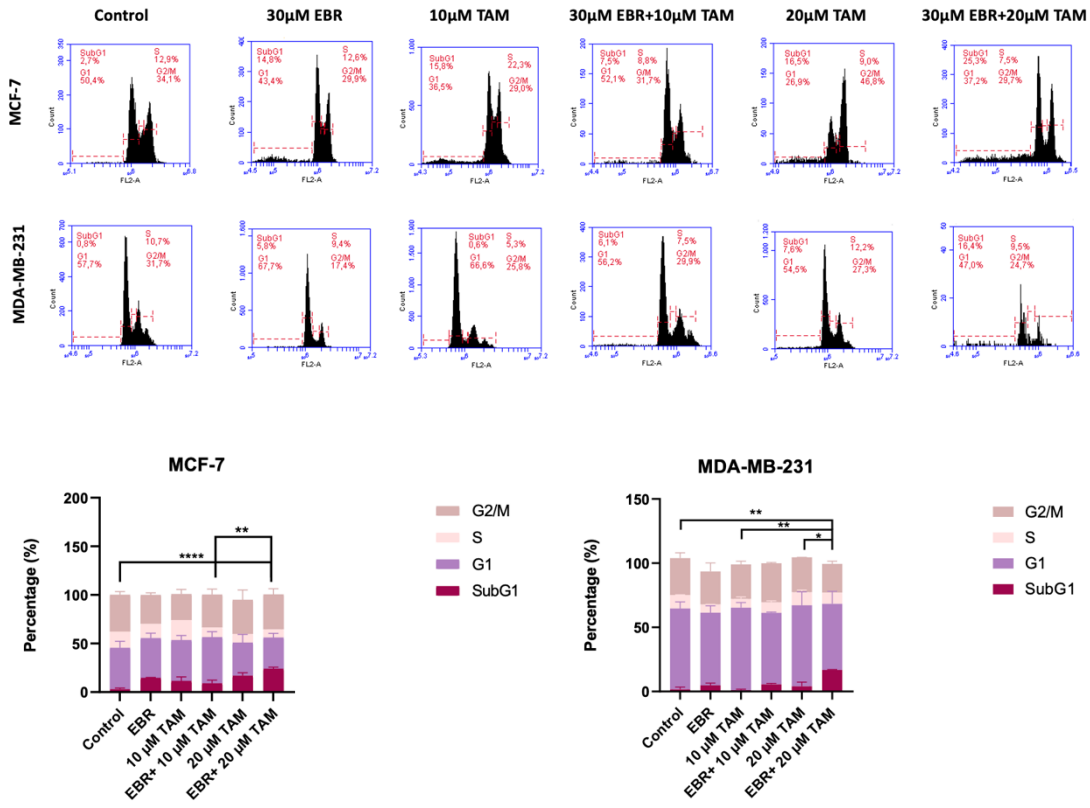

Figure 18. 30 μM EBR treatment along with 20 μM TAM enhanced the percentage of apoptotic subG1 cells in both MCF-7 and MDA-MB-231.
The results of the flow cytometer experiment are presented in this figure. In A, cell cycle phases can be seen in each condition for both cell lines. The graphs in B were plotted with the help of GraphPad. The significant stars are designated for the subG1 phase. In the analyzing the subG1 ratio of EBR, MCF-7 exhibited a threefold increase compared to MDA-MB-231. When comparing 20 μM TAM alone to its combination with EBR, the subG1 phase increased by half in MCF-7 while doubling in MDA-MB-231. Furthermore, the combination of 20 μM TAM with EBR resulted in a threefold higher increase in the subG1 phase compared to the combination of 10 μM TAM with EBR in MCF-7. Additionally, when comparing the subG1 ratio of 10 μM TAM with EBR to 20 μM TAM with EBR, the increase exceeded two times in MDA-MB-231. (*p<0.05, **p<0.01, ****p<0.0001)

3.8. THE EXPRESSION OF ER STRESS BIOMARKERS WAS INCREASED BY THE COMBINATION OF TAMOXIFEN AND EPIBRASSINOLIDE

The expression profiles of ER stress biomarkers were examined by immunoblotting. In this experiment, Tunicamycin (Tun) was used as a positive control, a well-known ER stress inducer. The MTT cell viability assay was performed to determine the dose of Tun, and the result is shown in Figure 19. 5 and 10 μg/mL concentrations were detected, and 5 μg/mL concentration reduced the viability significantly in both cell lines. What we have obtained is that expression levels of chaperone proteins which are

Calreticulin and PDI are significantly increased by TAM and EBR combination in both cell lines. The expression of BiP was also augmented through the combination of TAM and EBR in both cell lines. The expression of one of the ER stress sensors, IRE1a, was enhanced when MCF-7 cells were exposed to the combination of TAM and EBR. However, there was no change in MDA-MB-231 cell lines. The same result was also obtained for the expression of PERK which was increased in MDA-MB-231, and the expression was nearly unchanged in MCF-7. ATF6 expression was upregulated in drugs alone or in combination conditions in MCF-7 cells. Nevertheless, the expression of ATF6 was significantly upregulated when the cells were exposed to the combination of TAM with EBR in MDA-MB-231. The expression of an apoptotic biomarker CHOP triggered through ER stress was elevated when MCF-7 and MDA-MB-231 cell lines were exposed to the combination of TAM and EBR. GAPDH was used as a loading control in both cell lines, and the same bands were obtained in each condition and both cell lines.

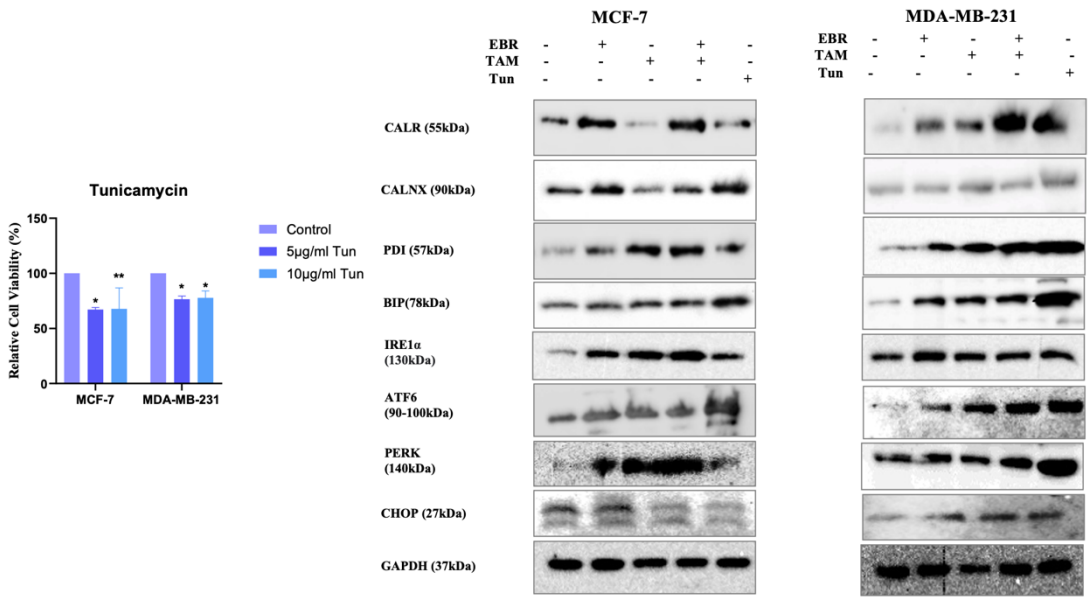

Figure 19. The combination of 30 μM EBR and 20 μM TAM boosted the expression of ER stress biomarkers.

The figure demonstrates the outcomes of the MTT assay of Tun and immunoblotting of ER stress biomarkers. The concentrations of 5 and 10 μg/mL were tested, with 5 μg/mL concentration notably decreasing the cell viability in both cell lines. The expression of CALR, CALNX, PDI, BiP, ATF6, PERK, and CHOP were augmented after exposure to the combination of 30 μM EBR with 20 μM TAM in both cell lines. Tunicamycin, an ER stress inducer, was used as a positive control. The expression of IRE1α was increased in MCF-7, but no change was observed in MDA-MB-231. GAPDH was used as a loading control. (*p<0.05, **p<0.01)

3.9. THE EXPRESSION OF APOPTOTIC BIOMARKERS WAS AUGMENTED THROUGH TREATMENT WITH TAMOXIFEN AND EPIBRASSINOLIDE

To see the effects of the combined treatment of TAM and EBR on the apoptotic biomarkers such as cleaved PARP (c-PARP), caspase 9, and caspase 3 their expression profiles were investigated in both MCF-7 and MDA-MB-231 cell lines via immunoblotting. The expression of the c-PARP after being exposed to the combination treatment was higher than the drugs alone conditions in both cell lines. The expression of Caspase 9 is one of the initiator caspases, which initiates the intrinsic pathway of apoptosis was further cleaved in both cell lines when they were treated with 20 µM TAM in combination with 30 µM EBR. The expression of Caspase 3 was diminished when the combination of TAM and EBR was administered to MDA-MB-231. Besides, there is no expression of Caspase 3 in MCF-7 cell lines (Jänicke et al. 1998). GAPDH was used as a loading control.

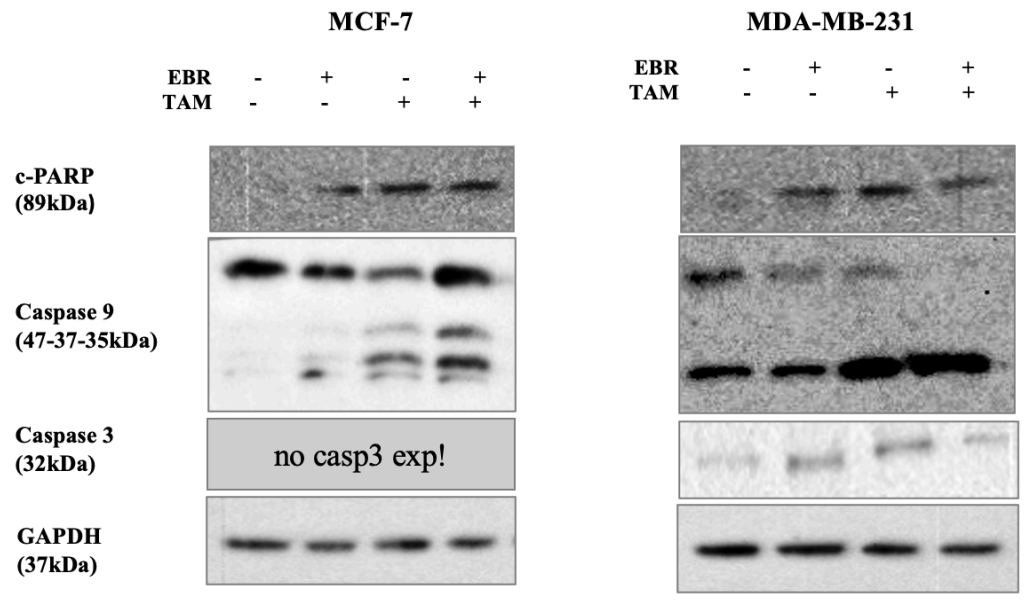

Figure 20. The changes of apoptotic biomarkers are shown after being exposed to 30 µM EBR and 20 µM TAM both alone and combination.

The results of apoptotic biomarkers of immunoblotting are shown in this figure. The change in expression profiles of c-PARP and Caspase 9 were enhanced after EBR and TAM combination in

both MCF-7 and MDA-MB-231. However, the expression of caspase 3 was declined by combined treatment of EBR and TAM. Also, the expression of Caspase 3 is not present in MCF-7. GAPDH was utilized as loading control.

3.10. EPIBRASSINOLIDE TREATMENT OVERCAME THE RESISTANCE TO TAMOXIFEN IN BOTH MCF-7 AND MDA-MB-231

To understand whether EBR overcomes TAM resistance, multi-drug resistance markers (MDRs), P-glycoprotein (ABCB1) (P-gp), and MRP1 (ABCC1) were analyzed by immunoblotting. As shown in Figure 21, there was no expression of P-gp in MCF-7 (David et al. 2004). Nevertheless, when we compare the expression of P-gp obtained after treatment with TAM alone and in combination with EBR, the expression was significantly decreased in MDA-MB-231. When we look at the expression of MRP1 firstly in the MCF-7 cells, we can see that the expression was drastically downregulated after combination therapy. The high expression of MRP1 that occurred after treatment with TAM, was significantly diminished when combined with EBR in MDA-MB-231. The expression of the MRP1 marker was significantly reduced in both cell lines.

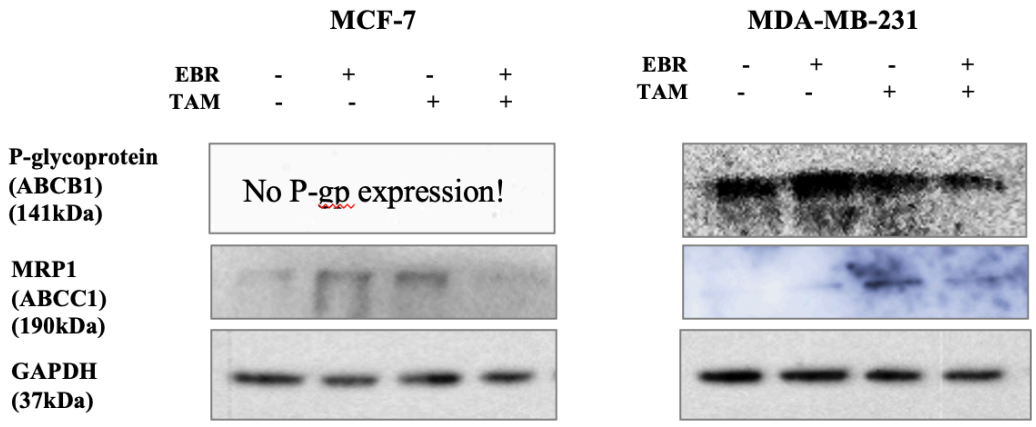

Figure 21. The resistance biomarkers' response to 30 µM EBR and 20 µM TAM combination is demonstrated.

The figure demonstrates the outcomes of resistance biomarker expression changes obtained by immunoblotting. In MDA-MB-231, the expression of P-gp was decreased in MDA-MB-231 when treated with the combination of EBR and TAM. There is no expression of P-gp in MCF-7. The expression of MRP1 significantly reduced in both cell lines after combination therapy. GAPDH was utilized as the loading control.

3.11. EPIBRASSINOLIDE REDUCED THE CELL VIABILITY THROUGH ENDOPLASMIC RETICULUM STRESS INDUCTION PROVEN BY PRETREATED TUDCA, AN ER STRESS INHIBITOR

To understand whether EBR induces ER stress, tauroursodeoxycholic acid (TUDCA) which is an ER stress inhibitor was used in concentrations of 5 and 10 µM as pretreatment for 30 min (F. Chen et al. 2022). The relative cell viability result was shown in Figure 22. The cell viability was greatly diminished after the combined treatment, however, when the cells were pretreated with 5 µM TUDCA for 30 min, the cell viability loss was significantly prevented in both cell lines (Figure 22). Nearly the same results were obtained in both cell lines. Besides, when the cells were pretreated with 10 µM TUDCA, the reduction in the cell viability was inhibited to approximately the same extent as 5 µM TUDCA. Therefore, we have chosen the 5 µM TUDCA for our next experiments. Our results indicated that the cell viability loss was hindered by pretreated 5 µM TUDCA in MCF-7 and MDA-MB-231 cell lines.

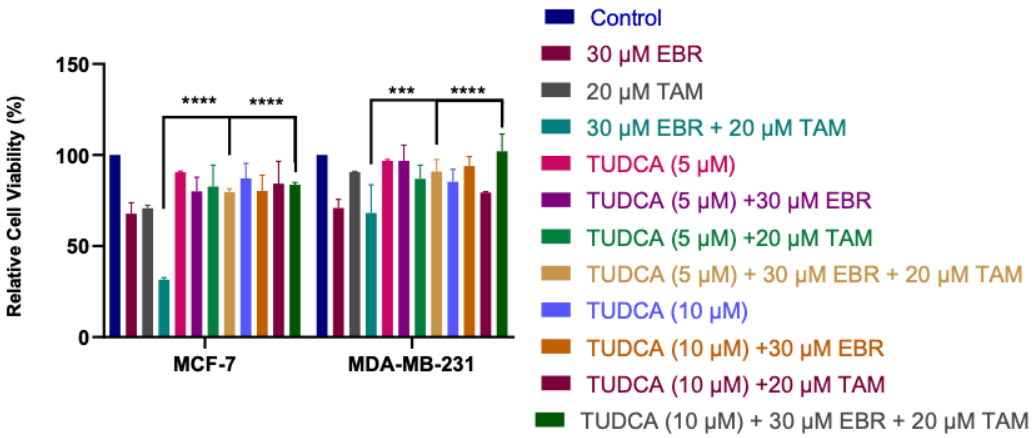

Figure 22. The effects of TUDCA, an ER stress inhibitor, on the cellular viability of MCF-7 and MDA-MB-231 were depicted.

The figure shows the cell viability results of MCF-7 and MDA-MB-231 cell lines after pretreated with both 5 µM and 10 µM TUDCA for 30 min. The decrease caused by 30 µM EBR, 20 µM TAM, and the combination of these two drugs was impeded by both pretreatment with 5 µM and 10 µM TUDCA in both cell lines. (***$p<0.001$, ****$p<0.0001$)

3.12. THE EXPRESSION PROFILES OF ER STRESS MARKERS WERE DECREASED WHEN COMBINED WITH THE TUDCA, AN ER STRESS INHIBITOR

To see whether EBR induced ER stress, an ER stress inhibitor TUDCA was utilized to prevent the activation of ER stress and its downstream pathways. For this purpose, the expression of ER stress biomarkers was checked in the presence of 5 µM TUDCA as a pretreatment for 30 min. Figure 23 demonstrated that chaperone proteins, CALR and PDI expressions were increased in both cell lines after the combined treatment of 20 µM TAM and 30 µM EBR; however, the expression was dramatically decreased in the presence of 5µM TUDCA. Moreover, the expression of BiP was upregulated when treated with the EBR and TAM combination, on the other hand its expression was remarkably downregulated in the presence of 5µM TUDCA. The expression of one of the sensors of ER stress, ATF6, was enhanced by the combination therapy of EBR and TAM, however its expression was highly diminished in the presence of TUDCA in both cell lines (Figure 23).

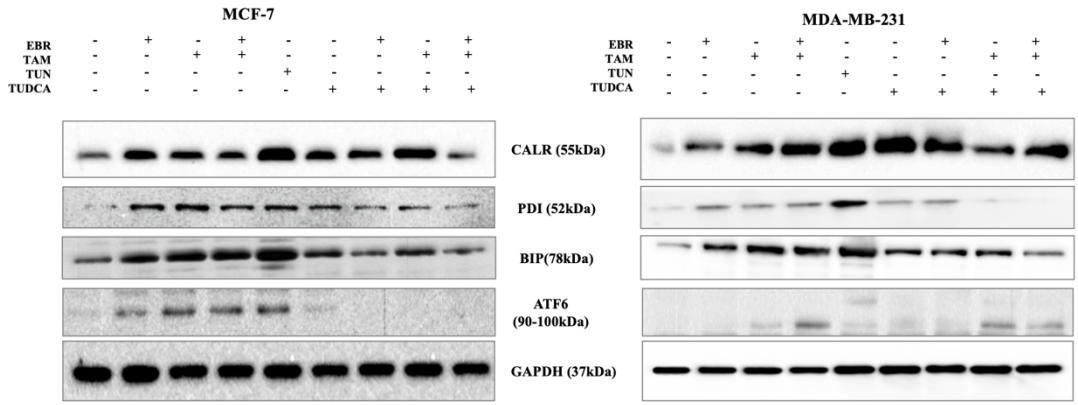

Figure 23. The expression profiles of ER stress markers were observed in the presence of 5 µM TUDCA.

The outcomes of immunoblotting of ER stress biomarkers in the presence of 5 µM TUDCA is displayed in this figure. The expression of all biomarkers was increased by the combined treatment of 30 µM EBR and 20 µM TAM in both cell lines. Nevertheless, the expression was significantly reduced in the presence of 5 µM TUDCA. GAPDH was utilized as a loading control.

3.13. TUDCA INHIBITED CELL DEATH SHOWN BY THE ALTERATION OF EXPRESSION PROFILE OF APOPTOTIC MARKERS

Apoptotic markers were investigated via immunoblotting to see how their expression changed after being treated with the combination of 20 μM TAM and 30 μM EBR, and in the presence of 5μM TUDCA. The expression of c-PARP (89 kDa) was checked in MCF-7, and full-length (116 kDa) PARP was examined in MDA-MB-231. The combination treatment of 20 μM TAM and 30 μM EBR caused an increase in the expression of c-PARP in MCF-7, however a decrease was observed in the presence of 5 μM TUDCA.

The expression of full-length PARP was reduced after being treated with the 20 μM TAM and 30 μM EBR in MDA-MB-231; however, the decrease in its expression was inhibited in the presence of TUDCA. Moreover, Caspase 9 expression declined; however, when the cells were pretreated with 5 μM TUDCA, caspase 9 expression was enhanced in both cell lines. As aforementioned, Caspase 3 is not expressed in the MCF-7 cell line. Nevertheless, the combination of 20 μM TAM and 30 μM EBR resulted in a decrease in the expression profile of Caspase 3, while its expression increased in the presence of TUDCA in MDA-MB-231. GAPDH and β-actin were loading controls in MCF-7 and MDA-MB-231, respectively.

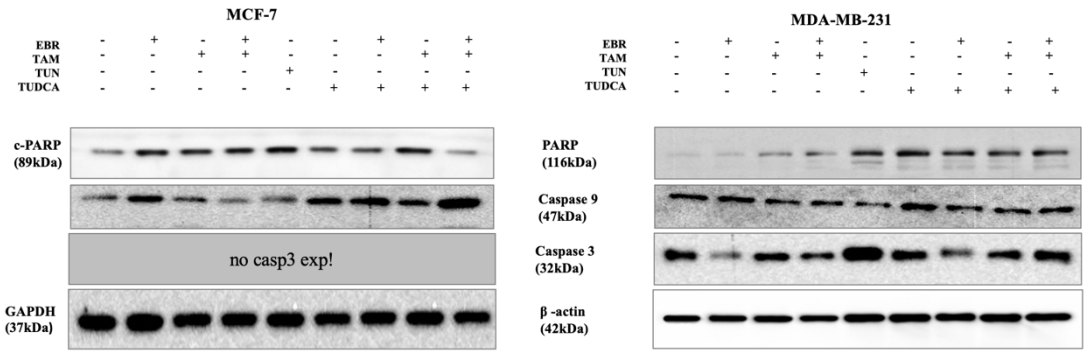

Figure 24. The alterations of apoptotic biomarkers when exposed to 30 μM EBR and 20 μM TAM were examined in the presence of 5 μM TUDCA.

The figure demonstrates the immunoblotting results of apoptotic biomarkers in the presence of 5 μM TUDCA in MCF-7 and MDA-MB-231. c-PARP expression was increased after combination therapy, but the expression was reduced in the presence of 5 μM TUDCA in MCF-7. PARP expression was

declined by the combination of 30 μM EBR and 20 μM TAM in MDA-MB-231. However, in the case of 5 μM TUDCA, the reduction was hindered. The expression of Caspase 9 was diminished by the 30 μM EBR and 20 μM TAM in both cell lines. However, the reduction is reversed by pretreating with 5 μM TUDCA. There is no expression of Caspase 3 in MCF-7, but the expression of Caspase 3 was reduced by 30 μM EBR and 20 μM TAM in MDA-MB-231. Later, the expression of Caspase 3 was increased in the presence of 5 μM TUDCA. GAPDH and B-actin were used as loading controls.

3.14. EPIBRASSINOLIDE TREATMENT IN THE PRESENCE OF TAMOXIFEN DECREASED THE MULTI-DRUG RESISTANCE MARKER EXPRESSION, AND TUDCA HINDERED THE DECREASE

Immunoblotting was carried out in the presence of TUDCA to understand if the resistance to TAM was overcome due to ER stress induction triggered by EBR. Tunicamycin was utilized as a positive control, a well-known ER stress inducer. The expressions of MDR1 and MRP1, which are multi-drug resistance (MDR) markers, were analyzed in MCF-7 and MDA-MB-231 cells. MDR1 is not expressed in MCF-7 cell line. The expression of MDR1 was significantly reduced after combination therapy in MDA-MB-231; however, the expression was increased in the presence of TUDCA. The expression of MRP1 decreased after being exposed to 30 μM EBR treatment in combination with 20 μM TAM, and TUDCA hindered the decrease in both cell lines.

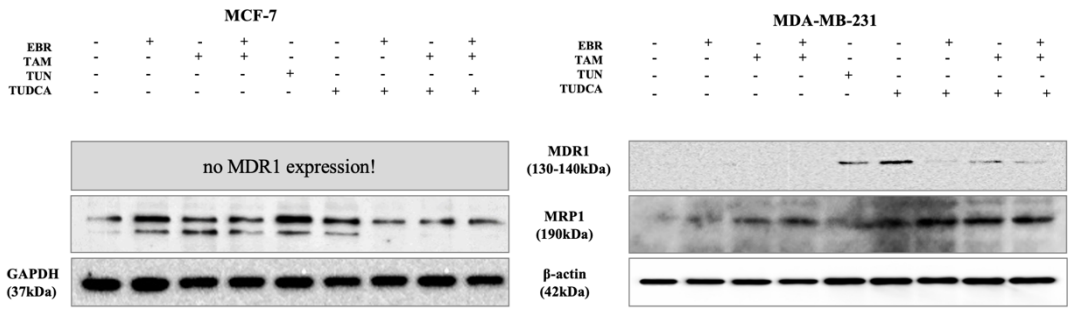

Figure 25. The changes in the drug resistance markers were evaluated in the presence of 5 μM TUDCA.

The results of immunoblotting for multi-drug resistance markers which are MDR1 and MRP1 are shown in this figure. The expression of resistance markers was diminished by treatment of 30 μM EBR with 20 μM TAM in both cell lines. However, the pretreatment of 5 μM TUDCA prevented the decrease in both cell lines. β-actin and GAPDH were used as loading controls.

4. DISCUSSION

Breast Cancer (BC) is the main cause of death around the world, and 2.3 million cases were reported in 2020. Therefore, it is a growing global health concern. BCs are categorized based on the presence or absence of hormone receptors. One of the subtypes is estrogen-receptor-positive ones. For example, MCF-7 cell line expresses estrogen receptor, progesterone receptor (PR), and HER2. To treat patients with estrogen receptor + tumors, TAM is a commonly used chemotherapeutic drug in clinics. Its mode of action is to target estrogen receptors thereby inhibiting proliferation and tumor growth via estrogen receptor signaling. However, after a long time of exposure to TAM, resistance occurs which is one of the drawbacks of cancer treatments. MDA-MB-231 BC cell line symbolizes triple negative BC, and the expression of estrogen receptor, PR, and HER2 are not present which brings a resistant profile to the cell line. The resistance might be *de novo*, which exists before treatment, or acquired which is caused by long-term exposure to the drug. The primary mechanism of de novo resistance to TAM involves the absence or reduction of estrogen receptor expression, while most BC patients who develop acquired resistance to TAM still exhibit estrogen receptor expression upon disease progression. While various cancers may initially respond to chemotherapy, they can gradually acquire resistance through a spectrum of mechanisms. These include genetic and epigenetic shifts, changes in drug targets or DNA repair mechanisms, inducing drug detoxifying mechanisms, multi-drug efflux pumps, inhibition of cell death pathways, and the heterogeneity of cancer cells, which fosters metabolic alterations favoring drug resistance and degradation (Guney Eskiler et al. 2016). The induction of chemoresistance across various mechanisms involves the participation of three distinct branches of the ER stress signaling pathways (Khaled et al. 2022). ER stress is a phenomenon when misfolded/unfolded proteins are aggregated in the lumen of ER, it

triggers the unfolded protein response (UPR). The misfolded proteins may accumulate if ER's folding capacity is surpassed by cellular demand or if there is insufficient cellular energy to properly fold synthesized proteins entering the ER (Haeri et al. 2012). The UPR aids in restoring cellular balance through various mechanisms: reducing protein synthesis, enhancing ER's ability to fold and eliminate unfolded/misfolded proteins, and activating chaperones/heat shock proteins to address the accumulation of misfolded proteins and induce cell cycle arrest. The UPR induces alterations in the activities of pivotal regulators, balancing pro-death and pro-survival signals and functions, ultimately dictating the fate of the cells (Senft and Ronai 2015). This process is orchestrated by signals that communicate across the plasma membrane, ER, cytosol, mitochondria, and nucleus. These signals prompt alterations in cellular metabolism, facilitating the activation or suppression of apoptosis and/or autophagy (Sisinni et al. 2019). This stress can be stimulated by factors such as hypoxia, nutrient deprivation, high translation rate, low folding capacity, chemotherapeutic drugs so on. When ER stress is triggered, the three sensors in the mammalian cells which are PERK, IRE1α, and ATF6 get activated by dissociation of BiP. Normally, BiP keeps all these transmembrane receptors in inactive form, and its expression is increased in many types of cancer such as breast, prostate, colorectal, etc (Andruska et al. 2015; Drake et al. 2015; Mhaidat et al. 2015). The stress due to hypoxia and nutrient deprivation is resulted from cytotoxic and endocrine therapeutic interventions in the BC. The studies showed that prolonged activation of UPR correlates with resistance to therapy and the recurrence of the disease. The upregulation of BiP and XBP1 are observed in BC which is resistant to both endocrine and chemotherapy treatments. Epibrassinolide (EBR) which is a member of brassinosteroids (BR), regulates growth in plants, but its apoptotic and autophagic activities have been shown in different cancer types (Adacan and Obakan Yerlikaya 2020; Coskun et al. 2015; Steigerová et al. 2010, 2012). BRs govern gene expression by interacting with metabolic pathways, thereby stimulating cell division and differentiation processes in plants. Their roles are extensively described in plants. Additionally, the signaling mechanism is well-understood in plants, involving a transmembrane heterodimer BR receptor comprising brassinosteroids insensitive 1 (BRI1) and its associated receptor kinase (BAK1). However, the precise mechanism of EBR in mammalian cells remained elusive. EBR,

a derivative of BRs, bears structural resemblances to mammalian steroids. It has been observed to induce cell cycle arrest at the G1/M phase, resulting in apoptosis in hormone-dependent breast and prostate cancer cell lines (Steigerová et al. 2010, 2012a). Previous studies showed that EBR caused ER stress-mediated apoptosis in a hormone-independent manner (Obakan et al. 2014a). In this study, we aimed to evaluate the potential therapeutic effect of ER stress and apoptotic mechanism stimulated by the combination of EBR and TAM in both MCF-7 and MDA-MB-231 cell lines. For this purpose, the first step was to check the viability of both cell lines after treatment with these two drugs alone and in combination for 24 hours. When we look at the results we have obtained, the cell viability of MCF-7 which is hormone-sensitive, and MDA-MB-231 which is hormone-insensitive was reduced by 30 µM EBR at 24 hours. The decrease is seen more in hormone-sensitive BC cells than in non-sensitive ones. It has been shown that hormone-insensitive MDA-MB-468 was more resistant to the brassinosteroids (BRs) than sensitive MCF-7 cells (Malíková et al. 2008). The reason behind this difference could be that BRs might bind to steroid receptors based on their structural motifs (Steigerová et al. 2012). As expected, 20µM TAM caused a moderate decrease in cell viability of hormone-sensitive but a slight effect on hormone-insensitive cells. This small decrease effect might have resulted from the off-target effect of TAM. When cells were treated with 20 µM TAM and 30 µM EBR, the viability was drastically reduced in both cell lines. As stated before, 20 µM TAM cannot kill MDA-MB-231 cells unlike in MCF-7 since it has no target. However, when combined with 30 µM EBR, the cell viability was significantly decreased under 50%. Therefore, we thought there might be a synergistic effect of EBR on the TAM. To understand the presence of synergistic effect, we plotted each drug's dose-response curve and the dose-response matrix. The closer the fall on the line, the dose is better thereby 20 µM TAM and 30 µM EBR were the best fits for these two drugs. After 25% inhibition, they are accepted as synergistic. In our result, 30 µM EBR and 20 µM TAM ended with 15% which was the closest to 25%, EBR synergistically increases the effect of TAM when combined. Wang *et al*. demonstrated that the combination of Celastrol, plant root extract, with TAM, had synergistically inhibited the proliferation of MCF-7 breast cancer cell line (Lijun Wang et al. 2021). Therefore, our results obtained are consistent with the literature thereby our drug

combination has a synergistic effect. When we look at the effect of EBR on the survival of MCF-10A, MCF-7, and MDA-MB-231 cells, we can see that 30 μM EBR in combination with 20 μM TAM has a significant cytotoxic effect on both hormone-sensitive and insensitive in time-dependently. After 24 hours, the cytostatic effect continues when compared with their controls. The important thing is that EBR has no significant effect on the survival of MCF-10A breast epithelial cells. Our findings were similar in the literature that Malikova *et al.* (2008) found out that BRs did not reduce the cell viability in BJ fibroblast cells, implying that BRs had different effects on normal and malign cell types. Our data suggested that 30 μM EBR in combination with 20 μM TAM lowered cell viability and survival time-dependently, and inhibited colony formation potential of both hormone-sensitive MCF-7 and insensitive MDA-MB-231 in 2D and 3D. Similar results have been obtained also in HCT116, and HT-29 colon cancer cells. In addition, previous studies demonstrated that hormone-insensitive MDA-MB-468 breast, DU 145, and PC3 prostate cells reduced cell viability and survival after EBR treatment which is consistent with our findings (Coskun et al. 2015; Obakan et al. 2014b; Steigerová et al. 2010). Moreover, colony formation capacity significantly decreased following 30 μM EBR and 20 μM TAM treatment in both cell lines, the similar effect of EBR on the colony formation capacity was also shown in pancreatic cancer cells (Obakan Yerlikaya et al. 2022). In addition to this, the inhibitory effect of the combination of TAM with Celastrol on the colony-forming capacity was shown in the BC cell line (Wang et al. 2021). Besides, to see how the colony-forming potency changed in the aspect of 3D, the hanging drop assay was performed. We expected to see shrinkage in the diameter of the sphere, and we obtained both the formation of cavities and significantly shrank spheres after treatment with TAM and EBR. Therefore, the combined treatment TAM and EBR significantly decreased the diameter of the sphere. A comparable outcome was achieved when pancreatic cancer cells were treated with EBR and gemcitabine, resulting in a significant reduction in the diameter of the spherical formation (Obakan Yerlikaya et al. 2022). In addition, the combined treatment may disrupt the cell-cell connections thereby forming cavities. In the previous study, transmission electron microscopy showed that MCF-7 and HepG2 cells formed densely packed spheroids, characterized by the abundant secretion of extracellular matrix (ECM) on the surface (Kelm et al.

2003). Therefore, the combination of TAM and EBR may affect the ECM. This could be searched in the upcoming studies.

We further conducted fluorescence staining. When we look at the results of fluorescence staining, PI-positive cell numbers that indicate dead cells were remarkably enhanced with co-treatment of EBR and TAM at 24 hours in both MCF-7 and MDA-MB-231 cell lines when compared to the control and drugs alone. The EBR elevates the TAM response, and the same effect was observed in the Gemcitabine response in pancreatic cell lines (Obakan Yerlikaya et al. 2022). According to the results of DAPI and DiOC6, the combinational therapy of TAM and EBR significantly increased the DNA fragmentation and dramatically decreased the mitochondrial membrane potential (MMP) in both MCF-7 and MDA-MB-231. In the previous study, Mandal et al. demonstrated that the combination of TAM with D-limonene, which is a natural bioactive nutritional compound, boosted DNA fragmentation and condensation compared to the treatment of these two drugs alone (Mandal et al. 2023). Additionally, co-treatment with EBR lowered the MMP in neuroblastoma cancer cells (Yerlikaya et al. 2022). Malikova et al. (2008) showed the EBR-induced cell cycle arrest in MCF-7, MDA-MB-468, and LNCaP cells thereby reducing the cells in the S phase. In addition to this study, Steigerova et al. (2010) also showed that cell cycle arrest at the G1 phase in BC cells resulted in apoptosis. However, we did not obtain such an arrest in our results. When we compare the numbers of subG1phase that indicate dead cells to the controls and EBR alone and TAM alone, there is a significant increase in both cell lines. In concomitant with our findings, a similar result was obtained in prostate cancer and BC (Obakan et al. 2014; To et al. 2022). At that time, EBR induces apoptosis but through which mechanisms were unknown. To decipher which mechanism plays a role in EBR-induced apoptosis, stable isotope labeling amino acids in cell culture (SILAC) based mass spectrometry was performed to analyze the changes in proteome in the LNCaP cells (Obakan et al. 2015). The result showed that the expression of 160 proteins which are responsible for cellular growth, proliferation, cell death, survival, cellular function, maintenance, nucleic acid metabolism, DNA replication, protein synthesis, and folding changed after 12 hours of EBR treatment. Calreticulin (CALR) was one of the most dramatically changed proteins after EBR treatment. This change could be related to ER stress since it is a

chaperone protein responsible for protein folding residing in the ER lumen. Besides, they found that EBR altered CALR expression in a time-dependent manner by inducing caspase-dependent apoptotic cell death in androgen receptor (AR) positive and negative prostate cancer cells (Obakan et al. 2015). Our immunoblotting result showed that the expression of CALR, CALNX, and PDI which are chaperone proteins were increased after cotreatment of EBR and TAM for 24 hours in both MCF-7 and MDA-MB-231. Moreover, we have obtained such results that the expression of BiP, ATF6, PERK, and IRE1α were elevated when exposed to the treatment of EBR and TAM in both cell lines. All these findings were matched with the literature (Obakan-Yerlikaya et al. 2017). Tunicamycin was used as a positive control to induce ER stress and increase the expression of BiP and CHOP indicating that ER stress was activated (You et al. 2021). We expected to see a rise in the expression of CHOP, which is the downstream target of PERK, but we could not obtain such a huge increase as expected only a small change was obtained in MDA-MB-231, not in MCF-7. Up to now, cells were treated with EBR and TAM for 24 hours, and ER stress was induced which was proven by the increase in the expression profiles of ER stress biomarkers. Apoptotic biomarkers that are c-PARP, Caspase 9, and caspase 3 expression were checked. We have obtained that after cells were treated with EBR and TAM, PARP and Caspase 9 cleavages augmented in both cell lines. For the cleavage of PARP, in a study, the combination of TAM with BreastDefend, which is a dietary supplement containing extract from mushrooms, increased the cleavage of PARP in BC cell lines (Cheng et al. 2017). In addition, in another study, the combined treatment of TAM with Isothiocyanates found in cruciferous further increased the cleavage of PARP in BC cell lines (Pawlik et al. 2016). Moreover, To et al. showed that the combination of TAM with pentadecanoic acid, an odd-chain fatty acid, further increased the cleavage of Caspase 9 in the BC cell line (To et al. 2022). Since MCF-7 Caspase 3-deficient cell line, Caspase 3 expression was decreased in only MDA-MB-231. We have obtained what we expected since the EBR treatment increased apoptotic markers in prostate and BC cells (Obakan, et al. 2014; Steigerová et al. 2010, 2012). Morover, a similar finding was observed that the combination of TAM with Curcumin enhanced the cleavage of Caspase 3 in MDA-MB-231 (Geng et al. 2016). Our results and these findings demonstrated that the combination of TAM and EBR increased the sensitivity to TAM

in BC cell lines and boosted the intrinsic apoptosis in both hormone-sensitive and insensitive BC cell lines. The main purpose was to overcome the natural drug resistance of MDA-MB-231 to TAM since there is no target in it. Therefore, we also checked the multi-drug resistance biomarkers (MRP1 and P-glycoprotein/P-gp) to see whether the resistance was eliminated. For MCF-7, only MRP1 expression was observed since P-gp is not expressed. When we look at the expression of MRP1 in EBR alone and TAM alone, the expression was not too much, yet when these two drugs were combined, the expression was fully inhibited. A similar scenario was obtained in MDA-MB-231. Since it is naturally resistant to TAM, the expression was high; however, it was downregulated when TAM was combined with EBR. In addition, the P-gp expression of MDA-MB-231 was significantly decreased. All the results aligned with the study that measured the expression levels of MDR proteins. High levels of MDR expression indicated a resistant profile, and lowering their expression resulted in the elimination of resistance (Guney Eskiler et al. 2016). These results indicated that the resistance that naturally occurred to TAM in MDA-MB-231 was overcome. To prove all these things were achieved through ER stress-mediated apoptosis, TUDCA which is an ER stress inhibitor was utilized. When we checked the literature, we saw different doses such as 100 µM, 200 µM, and 250 µM so on were used (Yoon et al. 2016). After many tries of MTT assay for TUDCA, we decided on 5µM TUDCA pretreatment for 30 min. When the cells were pretreated with 5 µM and 10 µM TUDCA for 30 min, then EBR, TAM and the combination of these drugs; the decrease resulted from the EBR alone, TAM alone, and their combination was prevented which means that the cellular viability was lost through ER stress, and the inhibitor was given, the loss was revented. We have obtained a similar recovery scenario after TUDCA administration; therefore, we continued to use 5 µM TUDCA. Moreover, to prove this in the aspect of protein profiles, we again detected the same ER stress, apoptosis, and drug resistance biomarkers in the presence of TUDCA. We can see that when cells were treated with TAM and EBR, the expression levels of CALR, CALNX, PDI, BiP, ATF6, were all increased, and when cells were pretreated with 5 µM TUDCA for 30 min, the increase was decreased in both cell lines as expected. Since TUDCA alleviates the ER stress, the similar scenario was observed that the ER stress, stimulated by Fusaric acid, was reduced by TUDCA thereby

decreasing the expression levels of ER stress-associated biomarkers in the BC cell line (J. Zhang et al. 2023). Since we proposed that the apoptosis was triggered through ER stress, the expression of apoptotic biomarkers such as PARP, Caspase 9, and Caspase 3 were analyzed in the presence of TUDCA. Upon examining the results, we observed that the expression of c-PARP increased following EBR and TAM combined treatment. However, the increase was reversed in the presence of TUDCA in MCF-7. We have observed that the expression of PARP was declined upon combined treatment in MDA-MB-231. However, TUDCA pretreatment inhibited the decrease in PARP. In addition to these, the expression of Caspase 9 was diminished; however, in the case of TUDCA, the decrease was recovered in both cell lines. Moreover, Caspase 3 expression was diminished by the combined treatment of EBR and TAM, and the decline was recovered in the presence of TUDCA. TUDCA, a bile acid with chaperone proteins, has been proposed as an effective ER stress inhibitor in a number of studies. For example, TUDCA administration in the preventive setting, reduced carcinogen-induced apoptosis in hepatocytes and tumor model of hepatocellular carcinoma (Vandewynckel et al. 2015). The same study also indicated that TUDCA reduced eukaryotic initiation factor 2 α (eIF2α) phosphorylation, CHOP expression and Caspase 12 processing, suggesting it was an inhibitor of UPR (Vandewynckel et al. 2015). More specifically, the TUDCA administration was able to reduce MDA-MB-231 cell proliferation and invasion by modulating matrix metalloproteinases, suggesting that TUDCA was able to block cell growth and division in an ER stress-dependent manner (Park et al. 2016). Drug resistance related to ER stress induction was also evaluated in the presence of TUDCA. Thapsigargin and methylseleninic acid-resistant prostate cancer cells and Adriamycin-resistant MCF-7 cells exhibited reduced apoptosis rates in the presence of TUDCA (Zhu et al. 2019). Taken together, similar to our study, the inhibition of ER stress was able to recover drug resistance in several cell lines.

Therefore, we can say that the combined treatment of EBR and TAM caused the cells to undergo apoptosis through the ER stress mechanism. Our main purpose was to combat drug resistance by combining TAM with EBR and proposing a different treatment approach for both hormone-sensitive and insensitive BC. Therefore, the drug resistance markers, which were checked before, MRP1, and P-gp were analyzed in the

presence of TUDCA. P-gp expression was decreased by EBR in the presence of TAM, and the decrease was prevented by TUDCA in MDA-MB-231. For both cell lines, we have obtained the same result that the decline in expression of MRP1 caused by combined treatment of EBR and TAM was inhibited by TUDCA. In short, all these findings say that EBR treatment in the presence of TAM stimulates ER stress-mediated apoptosis, and the natural drug resistance in hormone-insensitive BC could be eliminated by cotreatment of TAM with EBR.

5. REFERENCES

Adacan, Kaan, and Pınar Obakan Yerlikaya. 2020. "Epibrassinolide Activates Akt to Trigger Autophagy with Polyamine Metabolism in Sw480 and Dld-1 Colon Cancer Cell Lines." *Turkish Journal of Biology* 44(6): 417–26. doi:10.3906/biy-2005-37.

Adachi, Yusuke, Keisuke Yamamoto, Tetsuya Okada, Hiderou Yoshida, Akihiro Harada, and Kazutoshi Mori. 2008. 33 CELL STRUCTURE AND FUNCTION *ATF6 Is a Transcription Factor Specializing in the Regulation of Quality Control Proteins in the Endoplasmic Reticulum*.

Adams, Christopher J., Megan C. Kopp, Natacha Larburu, Piotr R. Nowak, and Maruf M.U. Ali. 2019. "Structure and Molecular Mechanism of ER Stress Signaling by the Unfolded Protein Response Signal Activator IRE1." *Frontiers in Molecular Biosciences* 6(MAR). doi:10.3389/fmolb.2019.00011.

Akram, Muhammad, Mehwish Iqbal, Muhammad Daniyal, and Asmat Ullah Khan. 2017. "Awareness and Current Knowledge of Breast Cancer." *Biological Research* 50(1). doi:10.1186/s40659-017-0140-9.

Al-Shami, Khayry, Sajeda Awadi, Almu'atasim Khamees, Ahmad Malek Alsheikh, Sumaiya Al-Sharif, Raneem Ala' Bereshy, Sharaf F. Al-Eitan, et al. 2023a. "Estrogens and the Risk of Breast Cancer: A Narrative Review of Literature." *Heliyon*: e20224. doi:10.1016/j.heliyon.2023.e20224.

Al-Shami, Khayry, Sajeda Awadi, Almu'atasim Khamees, Ahmad Malek Alsheikh, Sumaiya Al-Sharif, Raneem Ala' Bereshy, Sharaf F. Al-Eitan, et al. 2023b. "Estrogens and the Risk of Breast Cancer: A Narrative Review of Literature." *Heliyon*: e20224. doi:10.1016/j.heliyon.2023.e20224.

Amin-Wetzel, Niko, Reuben A. Saunders, Maarten J. Kamphuis, Claudia Rato, Steffen Preissler, Heather P. Harding, and David Ron. 2017.

"A J-Protein Co-Chaperone Recruits BiP to Monomerize IRE1 and Repress the Unfolded Protein Response." *Cell* 171(7): 1625-1637.e13. doi:10.1016/j.cell.2017.10.040.

An, Ki Chan. 2016. "Selective Estrogen Receptor Modulators." *Asian Spine Journal* 10(4): 787–91. doi:10.4184/asj.2016.10.4.787.

Andruska, N., X. Zheng, X. Yang, W. G. Helferich, and D. J. Shapiro. 2015. "Anticipatory Estrogen Activation of the Unfolded Protein Response Is Linked to Cell Proliferation and Poor Survival in Estrogen Receptor α-Positive Breast Cancer." *Oncogene* 34(29): 3760–69. doi:10.1038/onc.2014.292.

Aragón, Tomás, Eelco Van Anken, David Pincus, Iana M. Serafimova, Alexei V. Korennykh, Claudia A. Rubio, and Peter Walter. 2009. "Messenger RNA Targeting to Endoplasmic Reticulum Stress Signalling Sites." *Nature* 457(7230): 736–40. doi:10.1038/nature07641.

Asadi, Marzieh, Saeed Taghizadeh, Elina Kaviani, Omid Vakili, Mortaza Taheri-Anganeh, Mahshid Tahamtan, and Amir Savardashtaki. 2022. "Caspase-3: Structure, Function, and Biotechnological Aspects." *Biotechnology and Applied Biochemistry* 69(4): 1633–45. doi:10.1002/bab.2233.

Bánhegyi, Gábor, Peter Baumeister, Angelo Benedetti, Dezheng Dong, Yong Fu, Amy S. Lee, Jianze Li, et al. 2007. "Endoplasmic Reticulum Stress." In *Annals of the New York Academy of Sciences*, Blackwell Publishing Inc., 58–71. doi:10.1196/annals.1391.007.

Barnard, Mollie E., Caroline E. Boeke, and Rulla M. Tamimi. 2015. "Established Breast Cancer Risk Factors and Risk of Intrinsic Tumor Subtypes." *Biochimica et Biophysica Acta - Reviews on Cancer* 1856(1): 73–85. doi:10.1016/j.bbcan.2015.06.002.

Barzaman, Khadijeh, Jafar Karami, Zeinab Zarei, Aysooda Hosseinzadeh, Mohammad Hossein Kazemi, Shima Moradi-Kalbolandi, Elahe Safari, and Leila Farahmand. 2020. "Breast Cancer: Biology, Biomarkers, and Treatments." *International Immunopharmacology* 84. doi:10.1016/j.intimp.2020.106535.

Bashir, Samirul, Mariam Banday, Ozaira Qadri, Arif Bashir, Nazia Hilal, Nida-i-Fatima, Stephen Rader, and Khalid Majid Fazili. 2021. "The

Molecular Mechanism and Functional Diversity of UPR Signaling Sensor IRE1." *Life Sciences* 265. doi:10.1016/j.lfs.2020.118740.

Beral, Valerie, D. Bull, R. Doll, R. Peto, and G. Reeves. 2002. "Breast Cancer and Breastfeeding: Collaborative Reanalysis of Individual Data from 47 Epidemiological Studies in 30 Countries, Including 50 302 Women with Breast Cancer and 96 973 Women without the Disease." *Lancet* 360(9328): 187–95. doi:10.1016/S0140-6736(02)09454-0.

Berridge, Michael J. 2002. "The Endoplasmic Reticulum: A Multifunctional Signaling Organelle." *Cell Calcium* 32: 235–49. doi:10.1016/S0143-4160(02)00182-3.

Bhattarai, Kashi Raj, Manoj Chaudhary, Hyung Ryong Kim, and Han Jung Chae. 2020. "Endoplasmic Reticulum (ER) Stress Response Failure in Diseases." *Trends in Cell Biology* 30(9): 672–75. doi:10.1016/j.tcb.2020.05.004.

Bukowski, Karol, Mateusz Kciuk, and Renata Kontek. 2020. "Mechanisms of Multidrug Resistance in Cancer Chemotherapy." *International Journal of Molecular Sciences* 21(9). doi:10.3390/ijms21093233.

"Calfon2002."

Carneiro, Benedito A., and Wafik S. El-Deiry. 2020. "Targeting Apoptosis in Cancer Therapy." *Nature Reviews Clinical Oncology* 17(7): 395–417. doi:10.1038/s41571-020-0341-y.

Carrara, Marta, Filippo Prischi, Piotr R Nowak, Megan C Kopp, and Maruf MU Ali. "Noncanonical Binding of BiP ATPase Domain to Ire1 and Perk Is Dissociated by Unfolded Protein C H 1 to Initiate ER Stress Signaling." doi:10.7554/eLife.03522.001.

Cavalcante, Giovanna C., Ana Paula Schaan, Gleyce Fonseca Cabral, Mayara Natália Santana-Da-Silva, Pablo Pinto, Amanda F. Vidal, and Ândrea Ribeiro-Dos-Santos. 2019. "A Cell's Fate: An Overview of the Molecular Biology and Genetics of Apoptosis." *International Journal of Molecular Sciences* 20(17). doi:10.3390/ijms20174133.

Chen, Fangyi, Zhe Ge, Nan Li, Zuochong Yu, Rongbo Wu, Yan Zhao, Xianwei He, and Guoping Cai. 2022. "TUDCA Protects against

Tunicamycin-induced Apoptosis of Dorsal Root Ganglion Neurons by Suppressing Activation of ER Stress." *Experimental and Therapeutic Medicine* 24(2). doi:10.3892/etm.2022.11436.

Chen, Xi, and Juan R. Cubillos-Ruiz. 2021a. "Endoplasmic Reticulum Stress Signals in the Tumour and Its Microenvironment." *Nature Reviews Cancer* 21(2): 71–88. doi:10.1038/s41568-020-00312-2.

Chen, Xi, and Juan R. Cubillos-Ruiz. 2021b. "Endoplasmic Reticulum Stress Signals in the Tumour and Its Microenvironment." *Nature Reviews Cancer* 21(2): 71–88. doi:10.1038/s41568-020-00312-2.

Cheng, Shujie, Victor Castillo, Matt Welty, Mark Alvarado, Isaac Eliaz, Constance J. Temm, George E. Sandusky, and Daniel Sliva. 2017. "BreastDefend Enhances Effect of Tamoxifen in Estrogen Receptor-Positive Human Breast Cancer in Vitro and in Vivo." *BMC Complementary and Alternative Medicine* 17(1). doi:10.1186/s12906-017-1621-7.

De Cicco, Paola, Maria Valeria Catani, Valeria Gasperi, Matteo Sibilano, Maria Quaglietta, and Isabella Savini. 2019. "Nutrition and Breast Cancer: A Literature Review on Prevention, Treatment and Recurrence." *Nutrients* 11(7). doi:10.3390/nu11071514.

Clarke, Robert, Katherine L. Cook, Rong Hu, Caroline O.B. Facey, Iman Tavassoly, Jessica L. Schwartz, William T. Baumann, et al. 2012. "Endoplasmic Reticulum Stress, the Unfolded Protein Response, Autophagy, and the Integrated Regulation of Breast Cancer Cell Fate." *Cancer Research* 72(6): 1321–31. doi:10.1158/0008-5472.CAN-11-3213.

Clusan, Léa, François Ferrière, Gilles Flouriot, and Farzad Pakdel. 2023a. "A Basic Review on Estrogen Receptor Signaling Pathways in Breast Cancer." *International Journal of Molecular Sciences* 24(7). doi:10.3390/ijms24076834.

Clusan, Léa, François Ferrière, Gilles Flouriot, and Farzad Pakdel. 2023b. "A Basic Review on Estrogen Receptor Signaling Pathways in Breast Cancer." *International Journal of Molecular Sciences* 24(7). doi:10.3390/ijms24076834.

Clusan, Léa, François Ferrière, Gilles Flouriot, and Farzad Pakdel. 2023c. "A Basic Review on Estrogen Receptor Signaling Pathways

in Breast Cancer." *International Journal of Molecular Sciences* 24(7). doi:10.3390/ijms24076834.

Coe, Helen, and Marek Michalak. 2009. 28 F96 Gen. Physiol. Biophys *R e v i e w Calcium Binding Chaperones of the Endoplasmic Reticulum*.

Corazzari, Marco, Mara Gagliardi, Gian M. Fimia, and Mauro Piacentini. 2017. "Endoplasmic Reticulum Stress, Unfolded Protein Response, and Cancer Cell Fate." *Frontiers in Oncology* 7(APR). doi:10.3389/fonc.2017.00078.

Coskun, Deniz, Pinar Obakan, Elif Damla Arisan, Ajda Çoker-Gürkan, and Narçin Palavan-Ünsal. 2015a. "Epibrassinolide Alters PI3K/MAPK Signaling Axis via Activating Foxo3a-Induced Mitochondria-Mediated Apoptosis in Colon Cancer Cells." *Experimental Cell Research* 338(1): 10–21. doi:10.1016/j.yexcr.2015.08.015.

Coskun, Deniz, Pinar Obakan, Elif Damla Arisan, Ajda Çoker-Gürkan, and Narçin Palavan-Ünsal. 2015b. "Epibrassinolide Alters PI3K/MAPK Signaling Axis via Activating Foxo3a-Induced Mitochondria-Mediated Apoptosis in Colon Cancer Cells." *Experimental Cell Research* 338(1): 10–21. doi:10.1016/j.yexcr.2015.08.015.

Credle, Joel J, Janet S Finer-Moore, Feroz R Papa, Robert M Stroud, and Peter Walter. 2005. *On the Mechanism of Sensing Unfolded Protein in the Endoplasmic Reticulum*. https://www.pnas.org.

Crusio, Wim E, Haidong Dong, and Heinfried H Radeke. Advances in Experimental Medicine and Biology *Volume 1187 Series Editors*. http://www.springer.com/series/5584.

D'Arcy, Mark S. 2019. "Cell Death: A Review of the Major Forms of Apoptosis, Necrosis and Autophagy." *Cell Biology International* 43(6): 582–92. doi:10.1002/cbin.11137.

David, Gloria L., Srinivasan Yegnasubramanian, Arunima Kumar, Valerie L. Marchi, Angela M. De Marzo, Xiaohui Lin, and William G. Nelson. 2004. "MDR1 Promoter Hypermethylation in MCF-7 Human Breast Cancer Cells: Changes in Chromatin Structure

Induced by Treatment with 5-Aza-Cytidine." *Cancer Biology and Therapy* 3(6): 540–48. doi:10.4161/cbt.3.6.845.

Drake, T. M., J. E. Ritchie, C. Kanthou, J. J. Staves, R. Narramore, and L. Wyld. 2015. "Targeting the Endoplasmic Reticulum Mediates Radiation Sensitivity in Colorectal Cancer." *Experimental and Molecular Pathology* 98(3): 532–39. doi:10.1016/j.yexmp.2015.03.032.

Elrod, Heath A., and Shi Yong Sun. 2008. "Modulation of Death Receptors by Cancer Therapeutic Agents." *Cancer Biology and Therapy* 7(2): 163–73. doi:10.4161/cbt.7.2.5335.

English, Amber R., and Gia K. Voeltz. 2013. "Endoplasmic Reticulum Structure and Interconnections with Other Organelles." *Cold Spring Harbor Perspectives in Biology* 5(4): 1–16. doi:10.1101/cshperspect.a013227.

Erzurumlu, Yalçın, and Hatice Kübra Doğan. 2023. "Breast Cancer and the Molecular Mechanism of Estrogen Signaling." *Interdisciplinary Medical Journal* 14(48): 57–68. doi:10.17944/interdiscip.1285662.

Feng, Yixiao, Mia Spezia, Shifeng Huang, Chengfu Yuan, Zongyue Zeng, Linghuan Zhang, Xiaojuan Ji, et al. 2018a. "Breast Cancer Development and Progression: Risk Factors, Cancer Stem Cells, Signaling Pathways, Genomics, and Molecular Pathogenesis." *Genes and Diseases* 5(2): 77–106. doi:10.1016/j.gendis.2018.05.001.

Feng, Yixiao, Mia Spezia, Shifeng Huang, Chengfu Yuan, Zongyue Zeng, Linghuan Zhang, Xiaojuan Ji, et al. 2018b. "Breast Cancer Development and Progression: Risk Factors, Cancer Stem Cells, Signaling Pathways, Genomics, and Molecular Pathogenesis." *Genes and Diseases* 5(2): 77–106. doi:10.1016/j.gendis.2018.05.001.

Feng, Yixiao, Mia Spezia, Shifeng Huang, Chengfu Yuan, Zongyue Zeng, Linghuan Zhang, Xiaojuan Ji, et al. 2018c. "Breast Cancer Development and Progression: Risk Factors, Cancer Stem Cells, Signaling Pathways, Genomics, and Molecular Pathogenesis." *Genes and Diseases* 5(2): 77–106. doi:10.1016/j.gendis.2018.05.001.

Fortner, Renée T., Julia Sisti, Boyang Chai, Laura C. Collins, Bernard Rosner, Susan E. Hankinson, Rulla M. Tamimi, and A. Heather Eliassen. 2019. "Parity, Breastfeeding, and Breast Cancer Risk by Hormone Receptor Status and Molecular Phenotype: Results from the Nurses' Health Studies." *Breast Cancer Research* 21(1). doi:10.1186/s13058-019-1119-y.

Fuentes, Nathalie, and Patricia Silveyra. 2019. "Estrogen Receptor Signaling Mechanisms." In *Advances in Protein Chemistry and Structural Biology*, Academic Press Inc., 135–70. doi:10.1016/bs.apcsb.2019.01.001.

Galiè, Mirco. 2019. "RAS as Supporting Actor in Breast Cancer." *Frontiers in Oncology* 9. doi:10.3389/fonc.2019.01199.

Galluzzi, Lorenzo, Ilio Vitale, Stuart A. Aaronson, John M. Abrams, Dieter Adam, Patrizia Agostinis, Emad S. Alnemri, et al. 2018. "Molecular Mechanisms of Cell Death: Recommendations of the Nomenclature Committee on Cell Death 2018." *Cell Death and Differentiation* 25(3): 486–541. doi:10.1038/s41418-017-0012-4.

Geng, Chong, Jiyu Li, Feng Ding, Guojun Wu, Qing Yang, Yongjie Sun, Zhun Zhang, Tianyi Dong, and Xingsong Tian. 2016. "Curcumin Suppresses 4-Hydroxytamoxifen Resistance in Breast Cancer Cells by Targeting SLUG/Hexokinase 2 Pathway." *Biochemical and Biophysical Research Communications* 473(1): 147–53. doi:10.1016/j.bbrc.2016.03.067.

Gershuni, Victoria M., Rexford S. Ahima, and Julia Tchou. 2016. "Obesity and Breast Cancer: A Complex Relationship." *Current Surgery Reports* 4(4). doi:10.1007/s40137-016-0134-5.

Gimple, Ryan C., and Xiuxing Wang. 2019. "RAS: Striking at the Core of the Oncogenic Circuitry." *Frontiers in Oncology* 9. doi:10.3389/fonc.2019.00965.

Girgert, Rainer, Günter Emons, and Carsten Gründker. 2019. "Estrogen Signaling in ERα-Negative Breast Cancer: ERβ and GPER." *Frontiers in Endocrinology* 10(JAN). doi:10.3389/fendo.2018.00781.

Gonzalez, Tania N, Carmela Sidrauski, Silke Dö, and Peter Walter. 1999. 18 The EMBO Journal *Mechanism of Non-Spliceosomal*

MRNA Splicing in the Unfolded Protein Response Pathway. https://www.embopress.org.

Gordon, Ryan R., and Peter S. Nelson. 2012. "Cellular Senescence and Cancer Chemotherapy Resistance." *Drug Resistance Updates* 15(1–2): 123–31. doi:10.1016/j.drup.2012.01.002.

Guan, Bo Jhih, Vincent van Hoef, Raul Jobava, Orna Elroy-Stein, Leos S. Valasek, Marie Cargnello, Xing Huang Gao, et al. 2017. "A Unique ISR Program Determines Cellular Responses to Chronic Stress." *Molecular Cell* 68(5): 885-900.e6. doi:10.1016/j.molcel.2017.11.007.

Guney Eskiler, Gamze, Gulsah Cecener, Berrin Tunca, and Unal Egeli. 2016. "An in Vitro Model for the Development of Acquired Tamoxifen Resistance." *Cell Biology and Toxicology* 32(6): 563–81. doi:10.1007/s10565-016-9355-8.

Haeri, Mohammad, ; Barry, and E Knox. 2012. 7 Translational Eye Research JOURNAL OF OPHTHALMIC AND VISION RESEARCH *Endoplasmic Reticulum Stress and Unfolded Protein Response Pathways: Potential for Treating Age-Related Retinal Degeneration EnDoPlASMiC RETiCUlUM STRESS AnD PRoTEin FolDing*.

Hampton, Randolph Y. 2000. 10 Current Biology *ER Stress Response: Getting the UPR Hand on Misfolded Proteins*. http://www.cell.com/cgi/content/full/101/3/249/DC1.

Hanson, Sweata, Aiswarya Dharan, P. V. Jinsha, Sanjay Pal, Bipin G. Nair, Rekha Kar, and Nandita Mishra. 2023. "Paraptosis: A Unique Cell Death Mode for Targeting Cancer." *Frontiers in Pharmacology* 14. doi:10.3389/fphar.2023.1159409.

Hartl, Franz-Ulrich, Megan C Kopp, Piotr R Nowak, Natacha Larburu, Christopher J Adams, and Maruf MU Ali. "In Vitro FRET Analysis of IRE1 and BiP Association and Dissociation upon Endoplasmic Reticulum Stress." doi:10.7554/eLife.30257.001.

Haze, Kyosuke, Hiderou Yoshida, Hideki Yanagi, Takashi Yura, and Kazutoshi Mori. 1999. 10 Molecular Biology of the Cell *Mammalian Transcription Factor ATF6 Is Synthesized as a*

Transmembrane Protein and Activated by Proteolysis in Response to Endoplasmic Reticulum Stress.

He, Ji, Erika Fortunati, Dong Xu Liu, and Yan Li. 2021. "Pleiotropic Roles of Abc Transporters in Breast Cancer." *International Journal of Molecular Sciences* 22(6): 1–24. doi:10.3390/ijms22063199.

Hetz, Claudio. 2012. "The Unfolded Protein Response: Controlling Cell Fate Decisions under ER Stress and Beyond." *Nature Reviews Molecular Cell Biology* 13(2): 89–102. doi:10.1038/nrm3270.

Hillary, Robert F., and Una Fitzgerald. 2018a. "A Lifetime of Stress: ATF6 in Development and Homeostasis." *Journal of Biomedical Science* 25(1). doi:10.1186/s12929-018-0453-1.

Hillary, Robert F., and Una Fitzgerald. 2018b. "A Lifetime of Stress: ATF6 in Development and Homeostasis." *Journal of Biomedical Science* 25(1). doi:10.1186/s12929-018-0453-1.

Hoekstra, Hopi E., Rachel J. Hirschmann, Richard A. Bundey, Paul A. Insel, and Janet P. Crossland. 2006. "A Single Amino Acid Mutation Contributes to Adaptive Beach Mouse Color Pattern." *Science* 313(5783): 101–4. doi:10.1126/science.1126121.

Hong, Ruoxi, and Binghe Xu. 2022. "Breast Cancer: An up-to-Date Review and Future Perspectives." *Cancer Communications* 42(10): 913–36. doi:10.1002/cac2.12358.

Houghton, Serena C., and Susan E. Hankinson. 2021. "Cancer Progress and Priorities: Breast Cancer." *Cancer Epidemiology Biomarkers and Prevention* 30(5): 822–44. doi:10.1158/1055-9965.EPI-20-1193.

Howell, A., and S. J. Howell. 2023. "Tamoxifen Evolution." *British Journal of Cancer* 128(3): 421–25. doi:10.1038/s41416-023-02158-5.

Hu, Hai, Mingxing Tian, Chan Ding, and Shengqing Yu. 2019. "The C/EBP Homologous Protein (CHOP) Transcription Factor Functions in Endoplasmic Reticulum Stress-Induced Apoptosis and Microbial Infection." *Frontiers in Immunology* 10(JAN). doi:10.3389/fimmu.2018.03083.

Hu, Ye, Jiyue Gao, Meiling Wang, and Man Li. 2021. “Potential Prospect of CDK4/6 Inhibitors in Triple-Negative Breast Cancer.” *Cancer Management and Research* 13: 5223–37. doi:10.2147/CMAR.S310649.

Huang, Shijia, Yuying Xing, and Yong Liu. 2019. “Emerging Roles for the ER Stress Sensor IRE1 in Metabolic Regulation and Disease.” *Journal of Biological Chemistry* 294(49): 18726–41. doi:10.1074/jbc.REV119.007036.

Igney, Frederik H., and Peter H. Krammer. 2002. “Death and Anti-Death: Tumour Resistance to Apoptosis.” *Nature Reviews Cancer* 2(4): 277–88. doi:10.1038/nrc776.

Imagawa, Yusuke, Akira Hosoda, Shin ichi Sasaka, Akio Tsuru, and Kenji Kohno. 2008. “RNase Domains Determine the Functional Difference between IRE1α and IRE1β.” *FEBS Letters* 582(5): 656–60. doi:10.1016/j.febslet.2008.01.038.

International Variation, Effects of Migration, and Time Trends.

Jänicke, Reiner U., Michael L. Sprengart, Mas R. Wati, and Alan G. Porter. 1998. “Caspase-3 Is Required for DNA Fragmentation and Morphological Changes Associated with Apoptosis.” *Journal of Biological Chemistry* 273(16): 9357–60. doi:10.1074/jbc.273.16.9357.

Kaufman, Randal J. 2002. “Orchestrating the Unfolded Protein Response in Health and Disease.” *Journal of Clinical Investigation* 110(10): 1389–98. doi:10.1172/jci200216886.

Kay, Lewis E, G Elif Karagö, Diego Acosta-Alvear, Hieu T Nguyen, Crystal P Lee, Feixia Chu, and Peter Walter. 2017. “An Unfolded Protein-Induced Conformational Switch Activates Mammalian IRE1.” doi:10.7554/eLife.30700.001.

Kciuk, Mateusz, Adrianna Gielecińska, Somdutt Mujwar, Damian Kołat, Żaneta Kałuzińska-Kołat, Ismail Celik, and Renata Kontek. 2023. “Doxorubicin—An Agent with Multiple Mechanisms of Anticancer Activity.” *Cells* 12(4). doi:10.3390/cells12040659.

Kelm, Jens M., Nicholas E. Timmins, Catherine J. Brown, Martin Fussenegger, and Lars K. Nielsen. 2003. “Method for Generation of

Homogeneous Multicellular Tumor Spheroids Applicable to a Wide Variety of Cell Types." *Biotechnology and Bioengineering* 83(2): 173–80. doi:10.1002/bit.10655.

Khaled, Jaafar, Maria Kopsida, Hans Lennernäs, and Femke Heindryckx. 2022. "Drug Resistance and Endoplasmic Reticulum Stress in Hepatocellular Carcinoma." *Cells* 11(4). doi:10.3390/cells11040632.

Kim, Ji Hye, Su Yeon Lee, Su Young Oh, Song Iy Han, Hye Gyeong Park, Mi-Ae Yoo, and Ho Sunh Kang. 2004. *Methyl Jasmonate Induces Apoptosis through Induction of Bax/Bcl-X s and Activation of Caspase-3 via ROS Production in A549 Cells*.

Kinnel, Briana, Santosh Kumar Singh, Gabriela Oprea-Ilies, and Rajesh Singh. 2023a. "Targeted Therapy and Mechanisms of Drug Resistance in Breast Cancer." *Cancers* 15(4). doi:10.3390/cancers15041320.

Kinnel, Briana, Santosh Kumar Singh, Gabriela Oprea-Ilies, and Rajesh Singh. 2023b. "Targeted Therapy and Mechanisms of Drug Resistance in Breast Cancer." *Cancers* 15(4). doi:10.3390/cancers15041320.

Le, Quynh Giang, and Yukio Kimata. 2021. 46 CELL STRUCTURE AND FUNCTION *Multiple Ways for Stress Sensing and Regulation of the Endoplasmic Reticulum-Stress Sensors*.

LeBlanc, H. N., and A. Ashkenazi. 2003. "Apo2L/TRAIL and Its Death and Decoy Receptors." *Cell Death and Differentiation* 10(1): 66–75. doi:10.1038/sj.cdd.4401187.

Lee, Kenneth P.K., Madhusudan Dey, Dante Neculai, Chune Cao, Thomas E. Dever, and Frank Sicheri. 2008. "Structure of the Dual Enzyme Ire1 Reveals the Basis for Catalysis and Regulation in Nonconventional RNA Splicing." *Cell* 132(1): 89–100. doi:10.1016/j.cell.2007.10.057.

Li, J., and J. Yuan. 2008. "Caspases in Apoptosis and Beyond." *Oncogene* 27(48): 6194–6206. doi:10.1038/onc.2008.297.

Lima, Joema Felipe, Sharon Nofech-Mozes, Jane Bayani, and John M.S. Bartlett. 2016. "EMT in Breast Carcinoma—A Review." *Journal of Clinical Medicine* 5(7). doi:10.3390/jcm5070065.

Lin, Yuning, Mei Jiang, Wanjun Chen, Tiejian Zhao, and Yanfei Wei. 2019. “Cancer and ER Stress: Mutual Crosstalk between Autophagy, Oxidative Stress and Inflammatory Response.” *Biomedicine and Pharmacotherapy* 118. doi:10.1016/j.biopha.2019.109249.

Liu, J., H. Gao, X. Wang, Q. Zheng, C. Wang, X. Wang, and Q. Wang. 2014. “Effects of 24-Epibrassinolide on Plant Growth, Osmotic Regulation and Ion Homeostasis of Salt-Stressed Canola.” *Plant Biology* 16(2): 440–50. doi:10.1111/plb.12052.

Łukasik, Paweł, Irena Baranowska-bosiacka, Katarzyna Kulczycka, and Izabela Gutowska. 2021. “Inhibitors of Cyclin-dependent Kinases: Types and Their Mechanism of Action.” *International Journal of Molecular Sciences* 22(6): 1–23. doi:10.3390/ijms22062806.

Malíková, Jana, Jana Swaczynová, Zdeněk Kolář, and Miroslav Strnad. 2008. “Anticancer and Antiproliferative Activity of Natural Brassinosteroids.” *Phytochemistry* 69(2): 418–26. doi:10.1016/j.phytochem.2007.07.028.

Mandal, Deepa, Bikash Ranjan Sahu, and Tithi Parija. 2023. “Combination of Tamoxifen and D-Limonene Enhances Therapeutic Efficacy in Breast Cancer Cells.” *Medical Oncology* 40(8). doi:10.1007/s12032-023-02081-y.

Marie Hardwick, J., and Lucian Soane. 2013. “Multiple Functions of BCL-2 Family Proteins.” *Cold Spring Harbor Perspectives in Biology* 5(2). doi:10.1101/cshperspect.a008722.

Martin, Heather L., Laura Smith, and Darren C. Tomlinson. 2014. “Multidrug-Resistant Breast Cancer: Current Perspectives.” *Breast Cancer: Targets and Therapy* 6(0): 1–13. doi:10.2147/BCTT.S37638.

Mayrovitz, Harvey N. *Breast Cancer*.

Mayrovitz, Harvey N. *Breast Cancer*.

McGrath, Eoghan P., Susan E. Logue, Katarzyna Mnich, Shane Deegan, Richard Jäger, Adrienne M. Gorman, and Afshin Samali. 2018a. “The Unfolded Protein Response in Breast Cancer.” *Cancers* 10(10). doi:10.3390/cancers10100344.

McGrath, Eoghan P., Susan E. Logue, Katarzyna Mnich, Shane Deegan, Richard Jäger, Adrienne M. Gorman, and Afshin Samali. 2018b. "The Unfolded Protein Response in Breast Cancer." *Cancers* 10(10). doi:10.3390/cancers10100344.

Mhaidat, Nizar M., Karem H. Alzoubi, Nabeela Almomani, and Omar F. Khabour. 2015. "Expression of Glucose Regulated Protein 78 (GRP78) Determines Colorectal Cancer Response to Chemotherapy." *Cancer Biomarkers* 15(2): 203–9. doi:10.3233/CBM-140454.

Momenimovahed, Zohre, and Hamid Salehiniya. 2019a. "Epidemiological Characteristics of and Risk Factors for Breast Cancer in the World." *Breast Cancer: Targets and Therapy* 11: 151–64. doi:10.2147/BCTT.S176070.

Momenimovahed, Zohre, and Hamid Salehiniya. 2019b. "Epidemiological Characteristics of and Risk Factors for Breast Cancer in the World." *Breast Cancer: Targets and Therapy* 11: 151–64. doi:10.2147/BCTT.S176070.

Mounir, Zineb, Jothi Latha Krishnamoorthy, Shuo Wang, Barbara Papadopoulou, Shirley Campbell, William J. Muller, Maria Hatzoglou, and Antonis E. Koromilas. 2011. "Akt Determines Cell Fate through Inhibition of the PERK-EIF2α Phosphorylation Pathway." *Science Signaling* 4(192). doi:10.1126/scisignal.2001630.

Nagarajan, Divya, and Stephanie E.B. McArdle. 2018. "Immune Landscape of Breast Cancers." *Biomedicines* 6(1). doi:10.3390/biomedicines6010020.

Nedeljković, Milica, and Ana Damjanović. 2019. "Mechanisms of Chemotherapy Resistance in Triple-Negative Breast Cancer-How We Can Rise to the Challenge." *Cells* 8(9). doi:10.3390/cells8090957.

Oakes, Scott A. 2020. "Endoplasmic Reticulum Stress Signaling in Cancer Cells." *American Journal of Pathology* 190(5): 934–46. doi:10.1016/j.ajpath.2020.01.010.

Oakes, Scott A., and Feroz R. Papa. 2015. "The Role of Endoplasmic Reticulum Stress in Human Pathology." *Annual Review of*

Pathology: Mechanisms of Disease 10: 173–94. doi:10.1146/annurev-pathol-012513-104649.

Obakan, Pinar, Elif Damla Arisan, Annarica Calcabrini, Enzo Agostinelli, Şehnaz Bolkent, and Narçin Palavan-Unsal. 2014a. "Activation of Polyamine Catabolic Enzymes Involved in Diverse Responses against Epibrassinolide-Induced Apoptosis in LNCaP and DU145 Prostate Cancer Cell Lines." *Amino Acids* 46(3): 553–64. doi:10.1007/s00726-013-1574-1.

Obakan, Pinar, Elif Damla Arisan, Annarica Calcabrini, Enzo Agostinelli, Şehnaz Bolkent, and Narçin Palavan-Unsal. 2014b. "Activation of Polyamine Catabolic Enzymes Involved in Diverse Responses against Epibrassinolide-Induced Apoptosis in LNCaP and DU145 Prostate Cancer Cell Lines." *Amino Acids* 46(3): 553–64. doi:10.1007/s00726-013-1574-1.

Obakan, Pinar, Elif Damla Arisan, Ajda Coker-Gurkan, and Narcin Palavan-Unsal. 2014a. "Epibrassinolide-Induced Apoptosis Regardless of P53 Expression via Activating Polyamine Catabolic Machinery, a Common Target for Androgen Sensitive and Insensitive Prostate Cancer Cells." *Prostate* 74(16): 1622–33. doi:10.1002/pros.22879.

Obakan, Pinar, Elif Damla Arisan, Ajda Coker-Gurkan, and Narcin Palavan-Unsal. 2014b. "Epibrassinolide-Induced Apoptosis Regardless of P53 Expression via Activating Polyamine Catabolic Machinery, a Common Target for Androgen Sensitive and Insensitive Prostate Cancer Cells." *Prostate* 74(16): 1622–33. doi:10.1002/pros.22879.

Obakan, Pinar, Carlos Barrero, Ajda Coker-Gurkan, Elif Damla Arisan, Salim Merali, and Narcin Palavan-Unsal. 2015a. "SILAC-Based Mass Spectrometry Analysis Reveals That Epibrassinolide Induces Apoptosis via Activating Endoplasmic Reticulum Stress in Prostate Cancer Cells." *PLoS ONE* 10(9). doi:10.1371/journal.pone.0135788.

Obakan, Pinar, Carlos Barrero, Ajda Coker-Gurkan, Elif Damla Arisan, Salim Merali, and Narcin Palavan-Unsal. 2015b. "SILAC-Based Mass Spectrometry Analysis Reveals That Epibrassinolide Induces

Apoptosis via Activating Endoplasmic Reticulum Stress in Prostate Cancer Cells." *PLoS ONE* 10(9). doi:10.1371/journal.pone.0135788.

Obakan Yerlikaya, Pınar, Leila Mehdizadehtapeh, Özge Rencüzoğullari, Fadina Kuryayeva, Sena Sedef Çevikli, Şevval Özağar, Sibel Pınar Odabaş, et al. 2022a. "Gemcitabine in Combination with Epibrassinolide Enhanced the Apoptotic Response in an ER Stress-Dependent Manner and Reduced the Epithelial-Mesenchymal Transition in Pancreatic Cancer Cells." *Turkish Journal of Biology* 46(6). doi:10.55730/1300-0152.2630.

Obakan Yerlikaya, Pınar, Leila Mehdizadehtapeh, Özge Rencüzoğullari, Fadina Kuryayeva, Sena Sedef Çevikli, Şevval Özağar, Sibel Pınar Odabaş, et al. 2022b. "Gemcitabine in Combination with Epibrassinolide Enhanced the Apoptotic Response in an ER Stress-Dependent Manner and Reduced the Epithelial-Mesenchymal Transition in Pancreatic Cancer Cells." *Turkish Journal of Biology* 46(6). doi:10.55730/1300-0152.2630.

Obakan-Yerlikaya, Pinar, Elif Damla Arisan, Ajda Coker-Gurkan, Kaan Adacan, Utku Ozbey, Berna Somuncu, Didem Baran, and Narcin Palavan-Unsal. 2017a. "Calreticulin Is a Fine Tuning Molecule in Epibrassinolide-Induced Apoptosis through Activating Endoplasmic Reticulum Stress in Colon Cancer Cells." *Molecular Carcinogenesis* 56(6): 1603–19. doi:10.1002/mc.22616.

Obakan-Yerlikaya, Pinar, Elif Damla Arisan, Ajda Coker-Gurkan, Kaan Adacan, Utku Ozbey, Berna Somuncu, Didem Baran, and Narcin Palavan-Unsal. 2017b. "Calreticulin Is a Fine Tuning Molecule in Epibrassinolide-Induced Apoptosis through Activating Endoplasmic Reticulum Stress in Colon Cancer Cells." *Molecular Carcinogenesis* 56(6): 1603–19. doi:10.1002/mc.22616.

Park, Ga Young, Yu Kyeong Han, Jeong Yoon Han, and Chang Geun Lee. 2016. "Tauroursodeoxycholic Acid Reduces the Invasion of MDA-MB-231 Cells by Modulating Matrix Metalloproteinases 7 and 13." *Oncology Letters* 12(3): 2227–31. doi:10.3892/ol.2016.4842.

Patel, Hitisha K., and Teeru Bihani. 2018. "Selective Estrogen Receptor Modulators (SERMs) and Selective Estrogen Receptor Degraders

(SERDs) in Cancer Treatment." *Pharmacology and Therapeutics* 186: 1–24. doi:10.1016/j.pharmthera.2017.12.012.

Patra, Arunita, Arghya Adhikary, and Swatilekha Ghosh. 2023. "The Unfolded Protein Response (UPR) Pathway: The Unsung Hero in Breast Cancer Management." *Apoptosis* 28(3–4): 263–76. doi:10.1007/s10495-022-01803-3.

Pawlik, Anna, Monika Słomińska-Wojewódzka, and Anna Herman-Antosiewicz. 2016. "Sensitization of Estrogen Receptor-Positive Breast Cancer Cell Lines to 4-Hydroxytamoxifen by Isothiocyanates Present in Cruciferous Plants." *European Journal of Nutrition* 55(3): 1165–80. doi:10.1007/s00394-015-0930-1.

Perkins, Meghan S., Renate Louw Du Toit, and Donita Africander. 2018. "Hormone Therapy and Breast Cancer: Emerging Steroid Receptor Mechanisms." *Journal of Molecular Endocrinology* 61(4): R133–60. doi:10.1530/JME-18-0094.

Preissler, Steffen, and David Ron. 2019. "Early Events in the Endoplasmic Reticulum Unfolded Protein Response." *Cold Spring Harbor Perspectives in Biology* 11(4). doi:10.1101/cshperspect.a033894.

Promlek, Thanyarat, Yuki Ishiwata-Kimata, Masahiro Shido, Mitsuru Sakuramoto, Kenji Kohno, and Yukio Kimata. 2011. "Membrane Aberrancy and Unfolded Proteins Activate the Endoplasmic Reticulum Stress Sensor Ire1 in Different Ways." *Molecular Biology of the Cell* 22(18): 3520–32. doi:10.1091/mbc.E11-04-0295.

Read, Adam, and Martin Schröder. 2021. "The Unfolded Protein Response: An Overview." *Biology* 10(5). doi:10.3390/biology10050384.

Rondón-Lagos, Milena, Victoria E. Villegas, Nelson Rangel, Magda Carolina Sánchez, and Peter G. Zaphiropoulos. 2016. "Tamoxifen Resistance: Emerging Molecular Targets." *International Journal of Molecular Sciences* 17(8). doi:10.3390/ijms17081357.

Sarcinelli, Carmen, Helena Dragic, Marie Piecyk, Virginie Barbet, Cédric Duret, Audrey Barthelaix, Carole Ferraro-Peyret, et al. 2020. "ATF4-Dependent NRF2 Transcriptional Regulation Promotes Antioxidant Protection during Endoplasmic Reticulum Stress ATF4-

Dependent NRF2 Transcriptional Regulation Promotes Antioxidant Protection during Endoplasmic Reticulum Stress ATF4-Dependent NRF2 Transcriptional Regulation Promotes Antioxidant Protection during Endoplasmic Reticulum Stress." *Cancers* 12(3). doi:10.3390/cancers12030569ï.

Sarhangi, Negar, Shahrzad Hajjari, Seyede Fatemeh Heydari, Maryam Ganjizadeh, Fatemeh Rouhollah, and Mandana Hasanzad. 2022. "Breast Cancer in the Era of Precision Medicine." *Molecular Biology Reports* 49(10): 10023–37. doi:10.1007/s11033-022-07571-2.

Savitskaya, M. A., and G. E. Onishchenko. 2015. "Mechanisms of Apoptosis." *Biochemistry (Moscow)* 80(11): 1393–1405. doi:10.1134/S0006297915110012.

Schuur, Eric R., and James P. DeAndrade. 2015. "Breast Cancer: Molecular Mechanisms, Diagnosis, and Treatment." In *International Manual of Oncology Practice*, Springer International Publishing, 155–200. doi:10.1007/978-3-319-21683-6_9.

Schwarz, Dianne S., and Michael D. Blower. 2016. "The Endoplasmic Reticulum: Structure, Function and Response to Cellular Signaling." *Cellular and Molecular Life Sciences* 73(1): 79–94. doi:10.1007/s00018-015-2052-6.

Senft, Daniela, and Ze'ev A. Ronai. 2015. "UPR, Autophagy, and Mitochondria Crosstalk Underlies the ER Stress Response." *Trends in Biochemical Sciences* 40(3): 141–48. doi:10.1016/j.tibs.2015.01.002.

Shamu1, Caroline E, and Peter Walter. 1996. 15 The EMBO Journal *Oligomerization and Phosphorylation of the Irelp Kinase during Intracellular Signaling from the Endoplasmic Reticulum to the Nucleus*.

Sharma, Ganesh N, Rahul Dave, Jyotsana Sanadya, Piush Sharma, and K K Sharma. "VARIOUS TYPES AND MANAGEMENT OF BREAST CANCER: AN OVERVIEW." *J. Adv. Pharm. Tech. Res* 1(2). www.japtr.org.

Shim, Joong Sup, and Jun O. Liu. 2014. "Recent Advances in Drug Repositioning for the Discovery of New Anticancer Drugs."

International Journal of Biological Sciences 10(7): 654–63. doi:10.7150/ijbs.9224.

Siegel, Rebecca L., Kimberly D. Miller, Nikita Sandeep Wagle, and Ahmedin Jemal. 2023. "Cancer Statistics, 2023." *CA: A Cancer Journal for Clinicians* 73(1): 17–48. doi:10.3322/caac.21763.

Sisinni, Lorenza, Michele Pietrafesa, Silvia Lepore, Francesca Maddalena, Valentina Condelli, Franca Esposito, and Matteo Landriscina. 2019a. "Endoplasmic Reticulum Stress and Unfolded Protein Response in Breast Cancer: The Balance between Apoptosis and Autophagy and Its Role in Drug Resistance." *International Journal of Molecular Sciences* 20(4). doi:10.3390/ijms20040857.

Sisinni, Lorenza, Michele Pietrafesa, Silvia Lepore, Francesca Maddalena, Valentina Condelli, Franca Esposito, and Matteo Landriscina. 2019b. "Endoplasmic Reticulum Stress and Unfolded Protein Response in Breast Cancer: The Balance between Apoptosis and Autophagy and Its Role in Drug Resistance." *International Journal of Molecular Sciences* 20(4). doi:10.3390/ijms20040857.

Slee, Elizabeth A., Colin Adrain, and Seamus J. Martin. 2001. "Executioner Caspase-3, -6, and -7 Perform Distinct, Non-Redundant Roles during the Demolition Phase of Apoptosis." *Journal of Biological Chemistry* 276(10): 7320–26. doi:10.1074/jbc.M008363200.

So, Jae Seon. 2018. "Roles of Endoplasmic Reticulum Stress in Immune Responses." *Molecules and Cells* 41(8): 705–16. doi:10.14348/molcells.2018.0241.

Song, Yanlin, Zhenfei Bi, Yu Liu, Furong Qin, Yuquan Wei, and Xiawei Wei. 2023. "Targeting RAS–RAF–MEK–ERK Signaling Pathway in Human Cancer: Current Status in Clinical Trials." *Genes and Diseases* 10(1): 76–88. doi:10.1016/j.gendis.2022.05.006.

Steigerová, Jana, Jana Oklestkova, Monika Levková, Lucie Rárová, Zdeněk Kolář, and Miroslav Strnad. 2010a. "Brassinosteroids Cause Cell Cycle Arrest and Apoptosis of Human Breast Cancer Cells." *Chemico-Biological Interactions* 188(3): 487–96. doi:10.1016/j.cbi.2010.09.006.

Steigerová, Jana, Jana Oklestkova, Monika Levková, Lucie Rárová, Zdeněk Kolář, and Miroslav Strnad. 2010b. "Brassinosteroids Cause Cell Cycle Arrest and Apoptosis of Human Breast Cancer Cells." *Chemico-Biological Interactions* 188(3): 487–96. doi:10.1016/j.cbi.2010.09.006.

Steigerová, Jana, Lucie Rárová, Jana Oklešťková, Kateřina Křížová, Monika Levková, Michaela Šváchová, Zdeněk Kolář, and Miroslav Strnad. 2012a. "Mechanisms of Natural Brassinosteroid-Induced Apoptosis of Prostate Cancer Cells." *Food and Chemical Toxicology* 50(11): 4068–76. doi:10.1016/j.fct.2012.08.031.

Steigerová, Jana, Lucie Rárová, Jana Oklešťková, Kateřina Křížová, Monika Levková, Michaela Šváchová, Zdeněk Kolář, and Miroslav Strnad. 2012b. "Mechanisms of Natural Brassinosteroid-Induced Apoptosis of Prostate Cancer Cells." *Food and Chemical Toxicology* 50(11): 4068–76. doi:10.1016/j.fct.2012.08.031.

Sun, Yi Sheng, Zhao Zhao, Zhang Nv Yang, Fang Xu, Hang Jing Lu, Zhi Yong Zhu, Wen Shi, et al. 2017a. "Risk Factors and Preventions of Breast Cancer." *International Journal of Biological Sciences* 13(11): 1387–97. doi:10.7150/ijbs.21635.

Sun, Yi Sheng, Zhao Zhao, Zhang Nv Yang, Fang Xu, Hang Jing Lu, Zhi Yong Zhu, Wen Shi, et al. 2017b. "Risk Factors and Preventions of Breast Cancer." *International Journal of Biological Sciences* 13(11): 1387–97. doi:10.7150/ijbs.21635.

Sung, Hyuna, Jacques Ferlay, Rebecca L. Siegel, Mathieu Laversanne, Isabelle Soerjomataram, Ahmedin Jemal, and Freddie Bray. 2021. "Global Cancer Statistics 2020: GLOBOCAN Estimates of Incidence and Mortality Worldwide for 36 Cancers in 185 Countries." *CA: A Cancer Journal for Clinicians* 71(3): 209–49. doi:10.3322/caac.21660.

Szegezdi, Eva, Susan E. Logue, Adrienne M. Gorman, and Afshin Samali. 2006. "Mediators of Endoplasmic Reticulum Stress-Induced Apoptosis." *EMBO Reports* 7(9): 880–85. doi:10.1038/sj.embor.7400779.

Tait, Stephen W.G., and Douglas R. Green. 2010. "Mitochondria and Cell Death: Outer Membrane Permeabilization and Beyond." *Nature*

Reviews Molecular Cell Biology 11(9): 621–32. doi:10.1038/nrm2952.

Thorn, Caroline F., Connie Oshiro, Sharon Marsh, Tina Hernandez-Boussard, Howard McLeod, Teri E. Klein, and Russ B. Altman. 2011. "Doxorubicin Pathways: Pharmacodynamics and Adverse Effects." *Pharmacogenetics and Genomics* 21(7): 440–46. doi:10.1097/FPC.0b013e32833ffb56.

To, Ngoc Bao, Vi Nguyen Phuong Truong, Meran Keshawa Ediriweera, and Somi Kim Cho. 2022. "Effects of Combined Pentadecanoic Acid and Tamoxifen Treatment on Tamoxifen Resistance in MCF−7/SC Breast Cancer Cells." *International Journal of Molecular Sciences* 23(19). doi:10.3390/ijms231911340.

Tower, John. 2015. "Programmed Cell Death in Aging." *Ageing Research Reviews* 23(PA): 90–100. doi:10.1016/j.arr.2015.04.002.

Ubeda, Mariano, Xiao-Zhong Wang, Helene Zinszner, Irene Wu, Joel F Habener, and David Ron. 1996. 16 MOLECULAR AND CELLULAR BIOLOGY *Stress-Induced Binding of the Transcription Factor CHOP to a Novel DNA Control Element*.

Upton, John Paul, Likun Wang, Dan Han, Eric S. Wang, Noelle E. Huskey, Lionel Lim, Morgan Truitt, et al. 2012. "IRE1α Cleaves Select MicroRNAs during ER Stress to Derepress Translation of Proapoptotic Caspase-2." *Science* 338(6108): 818–22. doi:10.1126/science.1226191.

Vandewynckel, Yves-Paul, Debby Laukens, Lindsey Devisscher, Annelies Paridaens, Eliene Bogaerts, Xavier Verhelst, Anja Van Den Bussche, et al. 6 Oncotarget *Tauroursodeoxycholic Acid Dampens Oncogenic Apoptosis Induced by Endoplasmic Reticulum Stress during Hepatocarcinogen Exposure*. www.impactjournals.com/oncotarget/.

Wang, Lei, Yun Yuan Xu, Qi Bin Ma, Dan Li, Zhi Hong Xu, and Kang Chong. 2006. "Heterotrimeric G Protein α Subunit Is Involved in Rice Brassinosteroid Response." *Cell Research* 16(12): 916–22. doi:10.1038/sj.cr.7310111.

Wang, Lijun, Luqun Tang, Chengyun Yao, Chunyan Liu, and Yongqian Shu. 2021. "The Synergistic Effects of Celastrol in Combination

with Tamoxifen on Apoptosis and Autophagy in MCF-7 Cells." *Journal of Immunology Research* 2021. doi:10.1155/2021/5532269.

Wang, Xuan, Haiyun Zhang, and Xiaozhuo Chen. 2019. "Drug Resistance and Combating Drug Resistance in Cancer." *Cancer Drug Resistance* 2(2): 141–60. doi:10.20517/cdr.2019.10.

Weaver, Beth A. 2014. "How Taxol/Paclitaxel Kills Cancer Cells." *Molecular Biology of the Cell* 25(18): 2677–81. doi:10.1091/mbc.E14-04-0916.

Wilkinson, Louise, and Toral Gathani. 2022. "Understanding Breast Cancer as a Global Health Concern." *British Journal of Radiology* 95(1130). doi:10.1259/BJR.20211033.

Winters, Stella, Charmaine Martin, Daniel Murphy, and Navkiran K. Shokar. 2017. "Breast Cancer Epidemiology, Prevention, and Screening." *Progress in molecular biology and translational science* 151: 1–32. doi:10.1016/BS.PMBTS.2017.07.002.

Yamamoto, Keisuke, Takashi Sato, Toshie Matsui, Masanori Sato, Tetsuya Okada, Hiderou Yoshida, Akihiro Harada, and Kazutoshi Mori. 2007. "Transcriptional Induction of Mammalian ER Quality Control Proteins Is Mediated by Single or Combined Action of ATF6α and XBP1." *Developmental Cell* 13(3): 365–76. doi:10.1016/j.devcel.2007.07.018.

Ye, Feng, Saikat Dewanjee, Yuehua Li, Niraj Kumar Jha, Zhe Sheng Chen, Ankush Kumar, Vishakha, et al. 2023. "Advancements in Clinical Aspects of Targeted Therapy and Immunotherapy in Breast Cancer." *Molecular Cancer* 22(1). doi:10.1186/s12943-023-01805-y.

Ye, Jin, Robert B Rawson, Ryutaro Komuro, Xi Chen, Utpal P Davé, Ron Prywes, Michael S Brown, and Joseph L Goldstein. 2000. 6 Molecular Cell *ER Stress Induces Cleavage of Membrane-Bound ATF6 by the Same Proteases That Process SREBPs*.

Yerlikaya, Pinar Obakan, and Shafaq Naxmedova. 2022. "Epibrassinolide Triggers Apoptotic Cell Death in SK-N-AS Neuroblastoma Cells by Targeting GSK3β in a ROS Generation-Dependent Way." *European Journal of Biology* 81(2): 240–50. doi:10.26650/EurJBiol.2022.1191701.

Yoon, Yeo Min, Jun Hee Lee, Seung Pil Yun, Yong Seok Han, Chul Won Yun, Hyun Jik Lee, Hyunjin Noh, et al. 2016. "Tauroursodeoxycholic Acid Reduces ER Stress by Regulating of Akt-Dependent Cellular Prion Protein." *Scientific Reports* 6. doi:10.1038/srep39838.

You, Zhongsheng, Linkang He, and Nianlong Yan. 2021. "Tunicamycin-Induced Endoplasmic Reticulum Stress Promotes Breast Cancer Cell MDA-MB-231 Apoptosis through Inhibiting Wnt/ β -Catenin Signaling Pathway." *Journal of Healthcare Engineering* 2021. doi:10.1155/2021/6394514.

Youle, Richard J., and Andreas Strasser. 2008. "The BCL-2 Protein Family: Opposing Activities That Mediate Cell Death." *Nature Reviews Molecular Cell Biology* 9(1): 47–59. doi:10.1038/nrm2308.

Yuan, Shujun, and Christopher W. Akey. 2013. "Apoptosome Structure, Assembly, and Procaspase Activation." *Structure* 21(4): 501–15. doi:10.1016/j.str.2013.02.024.

Yuan, Shujun, Xinchao Yu, John M. Asara, John E. Heuser, Steven J. Ludtke, and Christopher W. Akey. 2011. "The Holo-Apoptosome: Activation of Procaspase-9 and Interactions with Caspase-3." *Structure* 19(8): 1084–96. doi:10.1016/j.str.2011.07.001.

Zhang, Jun, Huikai Yuan, Wei Li, Shuo Chen, Siwen Liu, Chunyu Li, and Xiaoqiang Yao. 2023. "Fusaric Acid Inhibits Proliferation and Induces Apoptosis through Triggering Endoplasmic Reticulum Stress in MCF-7 Human Breast Cancer Cells." *Mycotoxin Research* 39(4): 347–64. doi:10.1007/s12550-023-00497-z.

Zhang, Mengna, Lingxian Zhang, Ruoxuan Hei, Xiao Li, Haonan Cai, Xuan Wu, Qiping Zheng, and Cheguo Cai. 2021. 11 Am J Cancer Res *CDK Inhibitors in Cancer Therapy, an Overview of Recent Development*. www.ajcr.us/.

Zhu, Yifei, Mingxu Xie, Zhaoyue Meng, Lai Kwok Leung, Franky Leung Chan, Xin Hu, Kaiwen Chi, Cuiling Liu, and Xiaoqiang Yao. 2019. "Knockdown of TM9SF4 Boosts ER Stress to Trigger Cell Death of Chemoresistant Breast Cancer Cells." *Oncogene* 38(29): 5778–91. doi:10.1038/s41388-019-0846-y.

6. SUPPLEMENTARY

Supplementary Table 1. The recipe of 10X transfer buffer.

10X Transfer Buffer
30.3 g Tris base
144 g Glycine
1L dH20 pH 8.3

Supplementary Table 2. The recipe of SDS gel.

	THERMO	
Gel Percentage (%)	**12 (Separating)**	**5 (Stacking)**
H_2O	2.3	1.7
30% polyacrylamide (mL)	2.8	0.425
Tris (mL)	1.75 (1.5M pH 8.8)	0.313 (0.5M pH 6.8)
10% SDS (µL)	70	25
10% APS (µL)	47	18.5
TEMED (µL)	14	4.1
Total volume (mL)	7	2.5

Supplementary Table 3. The solution A and B recipes for ECL are shown.

ECL			
Solution A		**Solution B**	
dH_2O	9 mL	dH_2O	9 mL
1M Tris-HCl pH 8.5	1 mL	1M Tris-HCl pH 8.5	1 mL
p-Coumaric acid	45 µL	30% H_2O_2	6 µL
Luminol	100 µL		
Total volume	10 mL	Total volume	10 mL
Luminol 250 mM		**Caumaric Acid 90 mM**	
0.44 g Luminol		0.148 g p-Coumaric acid	
DMSO to 10 mL		Absolute ethanol to 10 mL	

Store in dark at -20C	Store in dark +4C

Tris-HCl 1M pH 8.5
8.74 g Tris base
4.42 g Tris HCl
dH2O to 100 mL

Supplementary Table 4. The chemicals used are demonstrated.

Chemicals	Brand	Cat No.
(E/Z)-4-hydroxy Tamoxifen	CAYMAN CHEMICAL	17308
0.25% Trypsin-EDTA(1X)	Gibco	25200-056
10X PBS	Serox	SRD-807-500
10X TBS	EcoTech	PBS10x-10
4X Laemmli	EcoTech	LSB-4X
Acrylamide/Bis-acrylamide (37.5:1)	EcoTech	AB3751100
Ammonium persulfate (APS)	Sigma-Aldrich	01709-500ML
Asetic asit	Bio-Rad	BL0250001
ATF6 polyclonal antibody	Invitrogen	PA5-20215
Bradford Assay kit	Thermo Scientific	1856209
Bradford Reagent	Sigma-Aldrich	B6916-500ML
BSA	Sigma-Aldrich	A2153-10GR
Calnexin	CST	#2433
Calreticulin	CST	#12238
Caspase 3	CST	#9662
Caspase 9	CST	#9502
CHOP monoclonal antibody	CST	#L63F7
Coomassie Brilliant Blue-G250	MERCK	D273
Crystal Violet	KimyaLAB	V21166.100
DAPI	Thermo	PI62247
DiOC6	Thermo	D273
DMEM	Gibco	11965092

DMSO	Riedel-De-Haën	41640
ECL (Solution A/B)	EcoTech	ECL50
Epibrassinolide	ApolloScientific	BIE0244
Ethanol Pure	ISOlab	920.026.2500
Fetal Bovine Serum (FBS)	Gibco	10270-106
Formaldehyde solution 37%	Sigma	15512-5L-R
GAPDH polyclonal antibody	Boster	A00227-1
Glycine	Bio-Rad	BL-01400202
GRP78 polyclonal antibody	Invitrogen	PA1-014A
Hydrochloric acid %30	KİMYALAB	V00318.905
Hydrogen peroxide	TEKKİM	TK.0880220.01001
IRE1α	ABclonal	A21021
Luminol	Sigma-Aldrich	123072
Methanol	Riedel-de-Haën	24229-2.5L
M-PER	Thermo Scientific	78501
MDR1	CST	#12683
MRP1 polyclonal antibody	Invitrogen	PA5-30594
MTT reagent	Bio Basic	NC461720
PARP1 polyclonal antibody	St John's Laboratory	STJ193190-50
p-Coumaric acid	Sigma-Aldrich	501-984
Penicillin/Streptomycin Solution (100X)	Capricorn Scientific	PS-B
Penicillin/Streptomycin Solution (100X)	SEROX	SLP-508-100
PERK monoclonal antibody	ABclonal	A21255
PDI	CST	#80797
P-glycoprotein monoclonal antibody	ABclonal	/A19093
Ponceau S	Sigma-Aldrich	P3504-10G
Propidium iodide	Sigma-Aldrich	P-4170-100MG
Protease inhibitor	Roche	4693116001
Protein Marker (Pre-stained)	EcoTech	PM12

Protein Marker (Pre-stained)	Abbkine	BMM3001
RNase	EcoTech	EZRA1, EZRA5
SDS	Scharlau	SD0010
Secondary antibody (anti-mouse)	BOSTER	BA1050-0.5
Secondary antibody (anti-rabbit)	CST	#7074
Skim milk powder	Bioshop	SKI400.250
Sodium Chloride (NaCl)	MERCK	1.06404.1000
Sodium Hydroxide (NaOH)	Biosince (SentezLab)	000322
Sodium Hydroxyde Extra Pure	KimyaLab	1310-73-2
TEMED	MERCK	1107320100
Tris base	Sigma-Aldrich	T1503-1KG
Tris HCl	Scharlau	TR0425
Triton X-100	Sigma-Aldrich	T8787-10ML
Trypan Blue (0.4% solution)	EcoTech	TRY-B100
TUDCA	Sigma Aldrich	35807-85-3
Tunicamycin	Sigma-Aldrich	T7765-1MG
Tunicamycin	CAYMAN CHEMICAL	11445
Tween-20	Sigma-Aldrich	P1379-500ML
β- actin monoclonal antibody	Boster	M01263

Supplementary Table 5. The devices used are shown.

Device	Brand
Axio Observer 5 Colibri7	Carl Zeiss Microscopy
Azure 300 Chemiluminescent Western Blot Imager	Azure Biosystems
Biometra Fastblot	Analytic Jena
C6 Plus Personal Flow Cytometer	BD Accuri
Centrifuge 5418 R - Microcentrifuge	Eppendorf
Centrifuge 5424 R	Eppendorf
Centrifuge Z 206 A	Hermle

CO_2 incubators (C150)(9040-0078)	BINDER
Digital Orbital Shaker (sk-0180-s)	DLAB
ECLIPSE TS100 (Inverted microscope)	Nikon
FLV1090 Mini Refrigerator	Flavel
Heat blocker	Thermo Scientific
Invitrogen™ Mini Gel Tank	Thermo Scientific
Invitrogen™ Western Blot Wet Transfer Device | Mini Blot Module	Thermo Scientific
Lab Benchtop Mini Centrifuge	ONiLAB's Scientific
Laminar Flow Cabinet /Hood	Labconco
MicroCL 17 Microcentrifuge	Thermo scientific
Milli Q Ultrapure Water Purification System	Merck
Mini Vortex	Isolab
mPAGE® Mini Gel Tank (MGT-4 Millipore)	Merck
Multiskan FC 357 Microplate Photometer	Thermo Scientific
MW151 MAX pH Meter	Milwaukee
Power Supply	VWR
PowerPac™ Basic Power Supply	Bio-Rad
Roller	DLAB
Self-Contained Ice Machine	Scotsman AF 80
Ultra-low Temperature Freezer	Haier
Vertical Laboratory Steam Sterilizers	Nuve
Water Bath VWB 18	VWR